

CONTENTS  
(Section 13)

	Page
13. POWER PLANT ACCIDENTS.....	13-1
13.1. Introduction.....	13-1
13.1.1 Heat Flux.....	13-1
13.1.2 Fuel Temperature.....	13-2
13.1.3 Primary System Insurge Rate.....	13-2
13.2. Reactivity Accidents.....	13-2
13.2.1 Startup Accident.....	13-2
13.2.2 Rod Withdrawal.....	13-8
13.2.3 Cold Loop Start.....	13-13
13.2.4 Secondary System Rupture.....	13-17
13.2.5 Xenon Burnout Transient.....	13-20
13.3. Mechanical Failures.....	13-22
13.3.1 Control Rod Drive Failures.....	13-22
13.3.2 Sudden Reduction of Steam Flow.....	13-26
13.3.3 Loss of Primary Pumping Power.....	13-27
13.3.4 Fuel Element Failures.....	13-30
13.3.5 Primary Water Leak.....	13-32
13.3.6 Loss of Air Supply for Instruments and Controls.....	13-35
13.3.7 False Containment High-Pressure Signal.....	13-38
13.3.8 Loss of ac Power.....	13-40
13.4. Reactor Systems Fire Hazards.....	13-42
13.4.1 Oil Fire Hazard.....	13-42
13.4.2 Hydrogen Fire Hazard.....	13-44
13.4.3 Conclusions.....	13-45
13.5. Maximum Credible Accident.....	13-45
13.5.1 Maximum Credible Operating Accident (Core I).....	13-45
13.5.2 Effect of Shuffled Core on Loss-of-Coolant Accident.....	13-73

### List of Tables

<b>Table</b>		<b>Page</b>
13-1.	Maximum Control Rod Misalignment.....	13-24
13-2.	Safety Margins for Flow Coastdown Power Levels Required for DNB.....	13-29
13-3.	Limiting Concentrations of Radioactive Gases in Primary Coolant.....	13-32
13-4.	Summary of Hydraulic Analysis.....	13-50
13-5.	Fraction of Radial Shell Slumped at 3995 Seconds.....	13-53
13-6.	Summary of Potential Pressure Suppression Effects.....	13-64
13-7.	Summary of Environmental Analysis.....	13-74
13-8.	Peak Fuel Node Conditions.....	13-75

## 13. REACTOR OPERATING ACCIDENTS

### 13.1. Introduction

Throughout the design, construction, and operation of the N. S. SAVANNAH, the predicted performance of the power plant has been analyzed for abnormal operation conditions. The purpose of these analyses is to demonstrate that the power of plant design has adequate safety margins to ensure the safety of the crew and the public in the event of power plant misoperation. The accidents which have been analyzed are divided into four categories: reactivity accidents, mechanical accidents, fire hazards, and the maximum credible accident (MCA). The criteria for plant damage used in the accident analyses are defined below.

#### 13.1.1. Heat Flux

The local heat flux in the hottest primary coolant channel is used as a damage criterion. When the heat flux exceeds the burnout heat flux for steady-state power operations, the damage criterion is assumed to be exceeded. The third-pass average heat flux is used as a measure of burnout power even though burnout occurs in the hot channel. The average heat flux in the third-pass is  $198,000 \text{ Btu/hr-ft}^2$  when the hot channel heat flux is at the burnout level. Thus, it is assumed that the limit of safety is reached when the thrid-pass heat flux reaches  $198,000 \text{ Btu/hr-ft}^2$ .

### 13.1.2 Fuel Temperature

No fuel melting is permitted in the core. Thus, the damage criterion is a maximum fuel temperature of 5000 F.

### 13.1.3 Primary System Insurge Rate

The criterion for damage to the Primary System is that the volume rate of insurge into the pressurizer shall not exceed the steam volume discharge rate of the code relief valves. This criterion can be met if the rate of primary system heatup does not exceed 0.7 F/sec. If the primary system heatup rate exceeds this value, overpressurization of the Primary System may occur.

## 13.2 Reactivity Accidents

### 13.2.1 Startup Accident

#### 13.2.1.1 Nature of the Accident

The objective of a reactor startup is to bring a relatively cold, subcritical reactor to the critical or slightly supercritical condition, thereafter increasing the power level in a controlled manner until the desired power level and system temperature are attained. This is accomplished by the withdrawal of control rods. If, as the result of some malfunction, a rod withdrawal should continue through the prompt-critical stage, the rate of change of power would rapidly exceed the normally desired value. This situation might conceivably develop as a result of operator error, nuclear instrumentation failure, or control rod circuitry malfunction. Operating procedures as well as instrumentation and circuitry are designed

to prevent such an occurrence.

#### 13.2.1.2 Safety Circuitry

Protection of the core from damage during this transient is provided by two independent features of the Safety System. As the rods are withdrawn, the rate of reactor power increase becomes larger. If the rate of reactor power increase reaches 2.8 decades per minute, the Safety System initiates a scram. A second safety feature scrams the control rods if the reactor power reaches the overpower trip level. With the START-RUN switch in the START position, and the primary system temperature below 325 F, the trip level is at an indicated level of about MWt. When the primary system temperature is above 325 F, the trip level is at an indicated level of 16 MWt. In the RUN position, the over-power trip level is 96 MWt.

#### 13.2.1.3 Method of Analysis

The startup accident has been analyzed by use of an analog computer. The analysis evaluates the reactivity addition rate required to approach the limit of plant safety. The maximum potential reactivity addition rate is then compared with the limiting safe rate in order to demonstrate the safety margin of the actual rod trip system. The effect of abnormal scram conditions is evaluated by analyzing the effect of a wide range of scram times. A large variation in the Doppler coefficient is studied since the Doppler is a parameter that significantly affects the characteristics of the accident. The moderator coefficient is assumed to be zero although it has been measured as negative throughout the range of this accident. The only safety action considered is a scram beginning 240 milliseconds after reactor power reaches the 96 MWt trip point.

## Maximum Potential Reactivity Addition Rate

The rate at which reactivity can be added to the reactor by withdrawing control rods is dependent upon the inherent neutron-absorbing potential of the rod material, the temperature and vertical position of the rods in the core, the withdrawal sequence, the number of rods withdrawn simultaneously, and the rod withdrawal velocity. Circuitry is so designed that it is not possible to withdraw more than five rods simultaneously.

The worth of the five most active rods (X rod and A rod group) in the shuffled core at 68 F is 0.0893. The average reactivity addition rate was calculated using this measured rod worth, a 58-inch rod stroke, and a maximum rod speed of 17 inches per minute. To account for the increased addition rate at the middle of the rod stroke, the average reactivity addition rate was doubled. Thus, the maximum potential reactivity addition rate for the five rods is  $9 \times 10^{-4}$   $\Delta k/\text{sec}$ .

## Reactor Condition

The analysis is based on the physical case of a cold reactor startup with the primary temperature at 240 F and the beginning-of-life core characteristics. The reactor is 2% subcritical with all control rods inserted, and the neutron flux level is 10 decades below full power. Investigation indicated that increasing the subcritical margin has only a minor effect on the final results of the transient. The assumptions of beginning-of-life characteristics for the delayed neutron fractions, the power split between core passes, and the fuel pin thermal characteristics combine to give the most conservative analysis. The total delayed neutron fraction for the shuffled core is less than that for the original

core. Calculations were performed to verify that this small change has essentially no effect on the reactor period at 1 Mwt. Thus, it does not affect the results of the analysis. The relative importance of the Doppler coefficient of the third-pass is three to four times greater than the importance of the second-pass Doppler coefficient. The fraction of power generated in the third-pass in the shuffled core is greater than that for the original core. Use of the power split at the beginning of life for the original core results in minimum power generation where the Doppler coefficient has its greatest worth; therefore, this is a conservative assumption.

#### 13.2.1.4 Results

The integrated heat generation below 1 Mwt is so small that fuel and water temperature changes are insignificant. In this range the only reactivity change in the core is due to the motion of the control rods. The total reactivity in the core (in excess of the initial subcritical margin) at the time the power level reaches 1 Mwt depends on the rate at which reactivity is added (Figure 13-1). Reactivity rates of  $5 \times 10^{-4} \Delta k/\text{sec}$  or greater, result in a reactor that is prompt-critical at 1 Mwt.

The important characteristics of the power transient resulting from a startup accident are shown in Figure 13-2 for a typical case. The power reaches a very high peak for only a very short period of time. The power increase stops when the fuel temperature has increased to a point where the Doppler coefficient compensates for reactivity in excess of the delayed neutron fraction. The delayed neutrons are ineffective until some time after peak power is reached because the average period between 1 Mwt and the power peak is approximately 10 milliseconds. Further fuel heating causes a very rapid decrease in power level. The fuel temperature coefficient is far more effective than the Safety System in limiting

the peak power of this accident. The power level decreases from a peak of 7500 MWt to about 600 MWt before control rods begin to become effective. The peak heat flux in the fuel pin lags the peak power by 0.7 second because of the heat transfer time delay at the fuel pin. Also, owing to the time delay, the peak heat flux corresponds to a steady-state power level of about 82 MWt rather than to the peak power of 7500 MWt. The change in water temperature is very small, so that the moderator temperature coefficient has no effect on the short-time transient characteristics of this accident.

The maximum value of heat flux in the third-pass is shown for various reactivity addition rates in Figure 13-3. A control rod insertion time of 1 second at a linear rate is assumed. A nominal Doppler coefficient of  $-1.14 \times 10^{-5} \Delta k/MW$ . The measured power coefficient of approximately 1.1 cents per MW is equivalent to  $7.7 \times 10^{-5} \Delta k/MW$ . Therefore, for accident hazards which are reduced by the Doppler effect, it is conservative to base conclusions on the nominal Doppler coefficient of  $-1.14 \times 10^{-5} \Delta k/F$ .

Extrapolation of the results for the nominal Doppler coefficient of  $-1.14 \times 10^{-5} \Delta k/F$  predicts that the reactivity addition rate must be on the order of  $1 \times 10^{-2} \Delta k/sec$  in order to approach the heat flux safety limit. The maximum potential reactivity addition rate of the present Control Rod Drive System,  $9 \times 10^{-4} \Delta k/sec$ , is a factor of 11 smaller than this limiting addition rate. The maximum heat flux for a reactivity addition rate of  $1 \times 10^{-3} \Delta k/sec$  is approximately 50,000 Btu/hr-ft<sup>2</sup>, far below the 198,000 Btu/hr-ft<sup>2</sup> safety limit. A reactivity addition rate of  $4.0 \times 10^{-3} \Delta k/sec$  is necessary to reach the heat flux safety limit when the Doppler coefficient is one-half its nominal value. Thus, even with a Doppler coefficient of one-half the nominal value, the permissible reactivity rate for the startup

accident is approximately 4.5 times the maximum potential rate that can be obtained with the present Control Rod Drive System. The maximum fuel temperature in the core is less than 4300 F for the reactivity addition rate that just causes burnout. This is below the 5000 F melting temperature, so that fuel melting is not involved in the startup accident.

It has been shown that the inherent shutdown characteristics of the reactor, and not a scram, provide initial protection from a startup accident. After the power excursion, however, some control rod insertion must be provided to effect a complete shutdown. The ability of the core to protect itself from damage with abnormally slow rod scram rates is demonstrated by Figure 13-4, in which maximum heat flux is plotted as a function of control rod insertion time. Even if the control rods just stop, and do not insert when the high-power scram trip is actuated, the maximum heat flux is 177,000 Btu/hr-ft<sup>2</sup>, below the 198,000 Btu/hr-ft<sup>2</sup> heat flux required for burnout. The assumed reactivity addition rate of  $4 \times 10^{-3} \Delta k/\text{sec}$  (Figure 13-4) is approximately 4.5 times the maximum potential rate with the present rod drive system. Furthermore, no credit is taken for the moderator temperature coefficient, which will reduce the peak heat flux for the slower shutdown times. Note that the peak heat flux, as shown in the cross plotted data of Figure 13-4, actually occurs in the order of 1 to 4 seconds after the power first reaches 1 Mwt. Four seconds is less than one loop time.

The number of primary pumps operating has no effect on the peak reactor power and has negligible effect on the peak heat flux because of the relatively short duration of the power excursion.

### 13.2.1.5 Conclusions

If no safety action is assumed in connection with a short reactor period in the subpower range, the Doppler temperature coefficient is effective in protecting the reactor from damage due to a startup accident. Reactivity addition rates on the order of 11 times faster than the maximum accidental rate will not cause core damage under normal scram conditions. Even under abnormal scram conditions, reactivity addition rates 4.5 times faster than the maximum accidental rate will not cause a maximum heat flux approach a burnout condition.

### 13.2.2 Rod Withdrawal

#### 13.2.2.1 Nature of the Accident

This accident, which is similar to the startup accident, occurs during the continuous withdrawal of control rods in violation of normal reactor control procedure. For all cases the reactor is assumed to be critical at a steady-state power level greater than 1 MWt, and the assumed primary temperature is 508F prior to the accident.

#### 13.2.2.2 Safety Circuitry

The reactor plant is protected against a rod withdrawal accident by the following scram set points on the safety system:

1. Scram on startup rate of 2.8 decades per minute in the startup range.
2. Scram on overpower at an indicated level of about 16 MWt in the startup range and at 96 MWt in the power range.

3. Scram on high reactor outlet temperature of 535 F.
4. Scram on high Primary System pressure of 1950 psig.

In the analysis of this accident, a scram is assumed to occur on overpower of 104 MWt, high reactor outlet temperature of 540 F, or high primary system pressure of 2000 psig. The high scram set points used in the accident analysis add conservatism to the analysis.

#### 13.2.2.3 Method of Analysis

The rod withdrawal accident was analyzed by analog simulation of the accident. The philosophy used in the analysis of the startup accident and in the investigation of ultimate safety limits and parameter variations was used in the analysis of the rod withdrawal accident. The analog studies were first made before the reactor was authorized for 69 MWt full power. In the present study, a wide range of reactivity addition rates were used. The plant was upgraded to 80 MWt, the earlier results for relatively high reactivity addition rates were extrapolated. For relatively slow reactivity addition rates, it was necessary to perform new analyses.

#### 13.2.2.4 Results

Analysis of rod withdrawal accidents at relatively high reactivity addition rates results in a power history which is similar to that of the startup accident. Figure 13-5 shows peak reactor power versus reactivity addition rate for 10.35 MWt initial power, four pumps running, nominal temperature coefficients, and a 1-second scram time after initiation at

90 Mwt. This condition is taken from previous analysis and is based on starting the accident after startup rate protection is disconnected. The peak power is high, but the heat flux, which lags reactor power, does not exceed safe margins. For a reactivity ramp rate of  $7.5 \times 10^{-3} \Delta k/\text{sec}$ , the peak power is about 900 Mwt, but the maximum third-pass heat flux is only 19,000 Btu/hr-ft<sup>2</sup>. Since this ramp rate is approximately 7 times the maximum potential reactivity addition rate, the core is considered safe with an overpower trip point of 96 Mwt.

For relatively slow reactivity addition rates, the peak flux approaches, but never exceeds, the full-power value. Figure 13-6 shows maximum heat flux versus initial power level for two reactivity addition rates. The parameters (except initial power) are the same as for Figure 13-5. Figure 13-6 indicates that maximum heat flux does not significantly exceed the steady-state, full-power value, and therefore data for 80 Mwt full power may be extrapolated with confidence.

The effect of changes in the moderator temperature coefficient or Doppler coefficient is shown in Figure 13-7 for the case where rods are not inserted. Reducing either of these coefficients to one-half value causes increased peak heat flux by about 5%.

The results of analog studies indicate that over-pressure in the primary system is the most important consideration from the standpoint of potential damage. Rod withdrawal accidents with slow rates of reactivity addition beginning at low power cause the highest pressures. The analysis for 80 Mwt operation concentrated on slow reactivity addition rates.

Power transients for several reactivity addition rates without a high-pressure scram are shown

in Figure 13-8. For slow reactivity addition rates, the moderator temperature coefficient limits the power rise. Ultimate shutdown results from a high reactor outlet temperature scram. The reactivity addition rate that produces the maximum rate of primary-coolant temperature rise occurs when the overpower scram set point and the high-temperature scram set point are reached at approximately the same time after initiation of the rod withdrawal.

A number of rod withdrawal accidents were analyzed without a high primary system pressure scram. These cases are shown in Figures 13-8 and 13-9. Of the cases shown in Figure 13-8, the  $2.25 \times 10^{-10}$   $\Delta k/\text{sec}$  reactivity addition rate produces the highest primary system pressure, which is 220 psia based on the capacity of one code relief valve and no spray action. Figure 13-9 shows the potential primary system pressure for various adverse combinations of parameters. The high pressurizer level case assumes that the accident begins with the level just below the high alarm point. Figure 13-10 shows the effect of a high pressure scram at 2000 psia.

#### 13.2.2.5 Experimental Verification of Model and Results

The SPERT-1 oxide core was made up of fuel rods used in the critical assembly tests conducted for the N. S. SAVANNAH at B&W CEL in Lynchburg, Virginia. Fuel spacing was the same as that used in the N. S. SAVANNAH core (0.663 inch). Thus, with the exception of total core volume, the characteristics of the SPERT-1 core were similar to those of the N. S. SAVANNAH core.

The ratio of prompt neutron lifetime to total delayed neutron fraction ( $\lambda^*/\beta$ ) for the SPERT-1 assembly as determined by  $1/v$  poison perturbation and from

excursion data is  $3.7 \times 10^{-3}$  second. For the analog study ( $\lambda^*/B$ ) was between  $3.6 \times 10^{-3}$  and  $3.85 \times 10^{-3}$  second. The latest calculated ( $\lambda^*/B$ ) value for the N.S. SAVANNAH is  $3.9 \times 10^{-3}$  second.

The experimental core originally had an excess reactivity of \$3.3 and had the ability to initiate essentially a maximum step change in reactivity of +\$2.10 by the sudden ejection of one control rod. All transients were initiated at approximately 68F with the reactor critical at a power level of a few watts. The initial critical condition of the experimental reactor corresponds to the initial condition for the analysis of rod withdrawal in the power range. However, the experiment of stepping in reactivity in excess of B is very similar to introducing reactivity in a more modest ramp fashion beginning from the subcritical state, as in the analytical startup accident.

A comparison of the experimental and analytical results in terms of MW per liter of core volume is shown in Figures 13-11 and 13-12. Figure 13-12 is similar to Figure 13-11 except that a wider range is covered, illustrating ten times the power densities reached in the analog work. The minimum reactor period was  $3.2 \times 10^{-3}$  second and  $10 \times 10^{-3}$  second for the SPERT 1961 experiment and the analog work respectively. The peak power reached in the SPERT-1 test was 7500 MWt. No fuel pin damage resulted from the aforementioned tests.

The analog results compared well with the test results, thus substantiating the validity of the analytical model for the reactor kinetics and fuel pins. Since no fuel pin damage occurred in the SPERT-1 tests, it may be concluded that the analog results with regard to pin damage are highly conservative.

In order to duplicate the step reactivity addition of \$2.10, a ramp reactivity addition of approximately \$8/sec would be required. For the N.S. SAVANNAH shuffled core this is roughly equivalent to all control rods moving out of the core simultaneously at a speed of 465 inches per minute with a worth of twice the average value. At this speed, rods would be ejected halfway out of the core in approximately 4 seconds.

#### 13.2.2.6 Conclusions

The overpower trip at 96 MWt protects the core from excessive heat flux even with reactivity addition rates approximately 8 times the maximum potential rate. For relatively slow reactivity addition rates, where excessive primary system pressure is the important damage criterion, the plant is protected by the high-pressure scram at approximately 1950 psia.

From the results of the SPERT-1 experiments it may be concluded that, barring sudden ejection of all rods due to destruction of the rod drive mechanisms, a rod withdrawal accident on the N.S. SAVANNAH will not result in damage to the fuel pins.

#### 13.2.3. Cold Loop Startup

##### 13.2.3.1. Nature of the Accident

This accident consists of positive reactivity addition resulting from cold water addition to the core. When an idle loop is started up, the negative moderator coefficient of the core in combination with water at a temperature lower than the water previously occupying the core will result in this reactivity addition. In the analysis, it is

assumed that one of the two primary coolant loops is inoperative and has been isolated from the operating loop by closing appropriate isolation valves. The water in this loop is assumed to become cooler than the operating loop by heat loss to the containment atmosphere. There are two cases of interest. In the first case, it is assumed that both pumps in the idle loop have been started before the isolation valves are opened. In the second case, it is assumed that the isolation valves are opened first and then the pumps are started.

There is no normal operating condition in which a primary loop would be isolated. It may be necessary to isolate a loop due to a leak or an equipment malfunction, but the loop would be inoperative until the equipment was repaired. Maintenance within the containment vessel is restricted to periods of reactor shutdown, so that an idle loop in which equipment has been repaired would be reactivated with the reactor subcritical. The postulated accident is one in which an isolated loop has been deliberately activated by an operator while the reactor is critical. This cold water accident has led to the determination of the interlocks required to protect the reactor.

#### 13.2.3.2 Safety Interlocks

There are three interlocks which limit the temperature and rate of cold water introduction to the core. The reactor inlet valve is a slow-opening valve requiring approximately 4 minutes for full stroke. An interlock controls the sequence of inlet valve and pump operations so that the pumps in the idle loop cannot be started with the reactor inlet valve open. A second interlock prohibits starting the pump unless the temperature difference of the coolant between the idle loop and the reactor is less than 75 F. In addition to minimizing the power excursion following activation of an idle loop, this interlock also protects the primary

pipng and boilers from severe temperature gradients due to the sudden introduction of hot water to a cold loop. An additional interlock prevents idle loop startup unless all 21 control rods are fully inserted in the core. Should the cooler water be introduced into the reactor by intentionally defeating the interlocks, the resulting power excursion would be halted by the combined effects of the negative fuel temperature reactivity coefficient and the overpower scram.

Any cold water addition to the core as a result of an idle loop startup must be preceded by a complete failure or deliberate bypassing of the three interlocks mentioned above. In the accident analysis it is assumed that none of these interlocks functioned. It is further assumed that the control rods are withdrawn so as to make the core exactly critical.

#### 13.2.3.3 Method of Analysis

It is assumed that the reactor was operating at a power level of 37.3 MWt with one loop shut down. The cold water from the idle loop was mixed homogeneously with the hot water returning from the active loop. The resulting reactor inlet temperature transient was introduced to the simulator, which then computed the resultant reactor power excursion. The assumption that there is perfect mixing of the flow from the two loops before entering the active portion of the core is not an accurate representation of the actual conditions within the thermal shield area, where the mixing is assumed to occur. However, nuclear calculations show that this approach is conservative. A calculation using slab geometry indicates that perfect mixing of the water would yield a  $k^{eff}$  slightly higher than that obtained if the cold water were to remain on one side of the core separated from the hotter water entering the other side. The assumption of perfect mixing is, therefore, conservative in the sense that it predicts a greater reactivity addition as a result of a cold water accident.

#### 13.2.3.4 Results

The idle loop cold water accident was analyzed for both valve-limiting and pump-limiting cases. Since the isolation valve between the pumps and the reactor inlet cannot be opened fully in less than 4 minutes, the valve-limiting case is not as severe as the pump-limiting case. This can be seen by comparison of Figures 13-13 and 13-14. In the valve-limiting case, the combined flow reaches 90% of full flow in about 60 seconds. In the pump-limiting case, the combined flow reaches 90% of full flow in about 0.6 second.

The power excursion resulting from the pump-limiting flow transient was investigated with and without overpower scram. In these analyses the temperature of the loop was assumed to be 130 F. At this temperature the flow transient introduces 2% excess reactivity in the first second. The combined effects of the negative Doppler coefficient and the overpower scram limit the power excursion to approximately 500 MWt. The power rises and falls sharply within one second so that the integrated heat generation is not appreciable. For the case of no safety action, the extent and duration of the excursion are increased, and damage to the core will result. The pump-valve interlocks are incorporated to prevent this rapid reactivity addition by allowing the slow-opening valve to limit the flow rate from the idle loop. In addition, the rod bottom interlock prevents starting of pumps in an idle loop with the reactor critical.

The accidental activation of the idle loop in the valve-limiting case was investigated for several values of idle loop temperature and for two valve-opening times. The results of this study are presented in Figure 13-15 for the cases in which there is no scram. With a rapid power increase, the heat generated in the pin has less time to diffuse to the coolant, resulting in higher fuel temperature.

### 13.2.3.5 Conclusions

The reactor is protected by three safety interlocks that prevent the introduction of cold water into the reactor. In addition, the operating manual specifies that the reactor must be shut down prior to starting the pumps in an isolated loop. The manual also specifies that the temperature of the idle loop must be within 75 F of the active loop temperature prior to starting pumps in the isolated loop. In the unlikely event that the interlocks are disabled and the operating procedures are violated, a reactor scram will terminate the excursion.

### 13.2.4. Secondary System Rupture

#### 13.2.4.1 Nature of the Accident

A rupture in the steam system between the steam generators and the turbines will release excessive amounts of steam from the boiler drums, resulting in a rapid reduction in pressure and temperature of the secondary water. This temperature decrease on the secondary side will cool the primary water passing through the steam generators, thereby resulting in a reduced primary coolant temperature at the reactor inlet. Thus, a cold water accident is the potential result.

#### 13.2.4.2 Method of Analysis

For the purpose of defining the maximum leak, it is assumed that the 10-inch header, which carries the combined flow of both steam generators, is completely severed so that steam discharges directly to atmospheric pressure. A larger break might be postulated in the form of a complete axial rupture of a steam drum, but this accident would not be as severe because:

1. The accident occurs in only one drum, rather than in an area where both steam generators are affected.

2. Although the primary coolant in this generator might be cooled somewhat more quickly, the rate of heat transfer is strongly dependent upon boiler tube and primary coolant film resistances.

3. The cooling effect can occur only while water remains in the heat exchanger. Rapid flashing in the drum would produce a cooling effect of limited duration.

It was calculated that the postulated rupture of a 10-inch pipe (leakage area of 78 sq. in.) results in total steam flow equivalent to 380 MWt, at normal full-load steam pressure. The steam pressure and thus the leak rate immediately drop as the excess demand causes flashing of steam and cooling of the primary and secondary water masses.

The effects of varying the primary flow, initial power, temperature coefficients, high-power trip point, and reactivity removal rate were analyzed in order to determine the most adverse combination of parameters. The size of the steam leak rate was also varied from the maximum pipe break (leakage area of 78 sq. in.) down to one-third maximum (leakage area of 26 sq. in.).

#### 3.2.4.3 Results

For operation with one pump and nominal temperature coefficients, the maximum steam leak does not result in primary pressure dropping below 1500 psia, or in central fuel melting, even without any control rod motion. For operation with more than one primary pump the accident results are potentially more severe. With higher primary flow, the heat

transferred across the boiler tubes is increased, which causes steam temperature and pressure to drop less drastically, which in turn results in a higher steam leak rate (the limitations of feedwater flow were not considered).

Figures 13-16 and 13-17 illustrate the typical system response to a relatively small steam leak with nominal plant conditions and no control rod motion. Figure 13-18 is a cross plot of maximum reactor power versus leak rate and summarizes significant results for four-pump operation over a range of parameter values.

Based on measured shipboard values and calculations, the actual variation of moderator and Doppler reactivity effects is covered by the range analyzed in the analog study. Figure 13-18 indicates that without safety action central fuel melting commences with leak rates between 20 and 30% maximum of the 10 inch steam line break, and that burnout occurs with leak rates greater than 60% of the maximum.

Figure 13-19 which displays maximum reactor power versus the high-power scram trip point, indicates that with a trip point at 96 MWt the power overshoot is less than 3 MWt. Conclusions drawn from Figure 13-19 are conservative because:

1. The moderator and Doppler reactivity coefficient used in the analyses are pessimistic.
2. The calculated transient is terminated by fast rod insertion instead of a scram.
3. The heat flux slightly lags the maximum power.

#### 13.2.4.4 Conclusions

It is concluded that a rupture of the Secondary System would cause some central melting of the fuel, but would not cause a DNB. Any other abnormal steam demands would be less severe than the postulated maximum steam leak.

#### 13.2.5. Xenon Burnout Transient

##### 13.2.5.1 Nature of the Accident

In this accident it is postulated that the reactor has been shutdown after an extensive period at full power. The Xe-135 concentration begins to increase upon shutdown because it is being produced by the decay of its precursor, I-135, but is no longer being destroyed by the mechanism of neutron absorption. The Xe-135 concentration reaches a maximum value and then decreased as decay of the xenon begins to exceed its production from a decaying I-135 supply.

If the reactor were brought back to full power at the time when the Xe-135 concentration was a maximum, the xenon would burn out at a rate which would introduce reactivity into the reactor. This possibility has been examined to determine the rate of reactivity addition as a function of time and its implications in terms of reactor safety.

##### 13.2.5.2 Reactivity Effects

The poisoning effect of xenon as the events above take place is shown in Figure 13-20. The portion of the curve labeled A to B represents the steady-state poisoning effect of xenon in terms of reactivity. At point B the reactor is shutdown to zero power. The curve B-C represents the buildup of xenon to its maximum value. Thereafter, it would

decay according to the dotted line if the reactor were not brought back to full power at point C, some 4 hours after shutdown. Curve C-D illustrates the more rapid xenon depletion resulting from this power increase. The initial slope of this part of the curve is shown as C-C<sup>1</sup> and is about  $1.5 \times 10^{-5} \Delta k/\text{min}$ . This addition of positive reactivity results in an increase in reactor power. The rate of reactivity addition is assumed to continue throughout the period of interest at  $1.5 \times 10^{-5} \Delta k/\text{min}$ .

Since there has been no additional power demand, any extra power increase can only tend to add energy to the primary and the steam system coolants and result in a temperature increase in these coolants.

By virtue of the inherent negative temperature coefficient of reactivity, this temperature increase tends to compensate for the reactivity being added. The power level increases to a point where the excess energy addition to the system increases primary water temperature at a rate which exactly corresponds to the reactivity addition rate. This power increase has been calculated to be less than 0.5 MW. This power increase is so small that it causes little concern regarding burnout. Figure 13-21 illustrates this power increase as a function of core life for the most probable combination of reactor parameters and for the worst possible combination.

#### 13.2.5.3 Conclusions

The most extreme reactivity addition rate due to xenon burnout was postulated in this analysis. The resulting power increase is small in comparison with normal power. No rapid power transient results. If the operator ignores the immediate condition, the plant will operate normally for approximately 1 hour before alarms bring the condition to the operator's attention. Adequate time is available to accomplish the required minor adjustment in control rod position to compensate for the positive effect of xenon burnout.

## 13.3. Mechanical Failures

### 13.3.1 Control Rod Drive Failures

#### 13.3.1.1. Nature of the Problem

The malfunction or disability of reactor control rods or control rod drives is of concern because of the potential hazards involved in the inability to place the reactor in the subcritical condition. This problem has been studied to determine the probability of rod malfunctions of various degrees of severity. There are three reactivity conditions which must be considered in the analysis of these failures.

These reactivity conditions are:

1. Shutdown. At full power the average fuel temperature is considerably higher than the moderator temperature. This results in a broadening of the fuel resonances and a reduction in reactivity. A loss of power (100% to zero power) would result in a cooling down of the fuel and an associated addition of positive reactivity. A certain degree of control is necessary to compensate for this reactivity addition. The reactivity associated with a reduction in power from 100% to zero power is defined as the power (Doppler) deficit.

2. Cooldown The reactor coolant exhibits a negative temperature coefficient of reactivity for the temperature range of practical operation. The loss of reactivity associated with the heating up of the moderator from approximately 100 F to the operating temperature of 508 F is defined as the temperature deficit. As the reactor is heated, control rods may be withdrawn to compensate for this reactivity loss. Likewise, control rods equivalent in reactivity to the temperature deficit must be inserted before the reactor may be cooled down.

3. Holddown. If the reactor is shut down for several days after a power run, the Xe-135 will

decay, and since the xenon thermal neutron absorption cross section is quite high, this results in the need for additional control compensation. With the shuffled core, the reactivity effect of xenon between zero and 80 MWt is 1.75%  $\Delta k$ .

#### 13.3.1.2 Shutdown Requirements

The reactivity required for hot shutdown is 1.2%  $\Delta k$ , and the reactivity required for cold hold-down is 4.3%  $\Delta k$ , including steady-state xenon poisoning. The cold worth of all control rods is 13.9%  $\Delta k$ , and the hot worth is 19.4%  $\Delta k$ .

#### 13.3.1.3 CRD System Failures

A study of 65 possible component failures within the CRD System determined the effect of each potential failure. Failures of interest in this study are those resulting in the loss of ability to scram one or more rods. The conclusions drawn from the analysis of these failures are summarized below:

1. In all cases a CRD system failure does not result in the disability of more than one rod.
2. During normal operation, the loss of ability to hydraulically scram any rod does not preclude the ability to accomplish a fast insertion using the electric motor drive. Only a complete failure of both electromechanical and hydraulic systems would prevent an insertion of the rod.

In similar fashion, the electronic scram circuitry is designed so that a power failure of any part of it does not prevent a rod scram. Each individual monitoring channel has its own power supply, and duplication or multiplicity

of each of the important safety channels is used. The scram signal bus is fed by all these voltage signals, and the bus in turn feeds the safety amplifier circuit. Interruption of bus power automatically initiates a scram.

#### 13.3.1.4 Misalignment Study

Assurance of a rod scram depends upon proper alignment of the control rod. The reactor internals are designed and supported to prevent binding of the control rod when the reactor is under the worst gravitational deflective forces--that is, when the ship is on its side so that the reactor is in a horizontal position. Table 13-1 gives the minimum control rod side clearance at each section of the reactor assembly with the estimated maximum misalignment and displacement at that point.

Table 13-1. Maximum Control Rod Misalignment

<u>Location</u>	<u>Minimum side clearance, in.</u>	<u>Maximum misalignment and displacement, in. (a)</u>
<u>Upper flow baffle</u>		
Top	0.247	+0.032
Bottom	0.247	+0.017
<u>Upper grid plate</u>		
Top	0.370	+0.007
Bottom	0.370	+0.009
<u>Fuel Container assembly</u>		
Top	0.179	-0.275
Bottom	0.179	-0.067
<u>Lower flow baffle</u>		
Top	0.307	-0.043
Bottom	0.425	-0.085

(a) + indicates upward direction with ship on its side.  
 - indicates downward direction with ship on its side.

The control rod is pivoted at its connection with a flexible extension rod. In the horizontal position the control rod rests on some surface or surfaces of the control rod channel. The misalignment and displacement caused by both the fuel container assembly and the lower flow baffle are in the downward direction, but the upper flow baffle and the upper grid plate could, in the worst case, cause misalignment and displacement in the upward direction. Clearances that are specified in Table 13-1 cause the rod to rest at the bottom ends of the fuel container assembly and the upper flow baffle. The top of the fuel container assembly has the maximum misalignment and displacement in the downward direction, and the control rod channel at this point is nearest the top surface of the control rod. Since the control rod rests on the upper flow baffle assembly when in the horizontal position, its total downward displacement from the normal position is the difference between the minimum rod side clearance, 0.247 inch, and the upward misalignment of the upper flow baffle, 0.032 inch. This motion, 0.215 inch, plus the minimum fuel container assembly clearance of 0.179 inch is larger than the downward misalignment plus displacement (0.275 inch) of the fuel container assembly at this point. Therefore, no bending of the rod results from the above described worst conceivable condition.

The manufacturer has indicated that the drives function properly while in a horizontal position. This statement is based on tests at a 30-degree list, tests under imposed misalignment, drive deflection measurements, and calculated support structure deflections. There is no reason to believe that the drive would not properly scram, even if the ship should capsize completely. The lateral deflective forces on the core assembly would again be less than those in the horizontal position. The safety latch mechanisms are spring loaded and therefore do not rely on gravity.

The mechanical and structural integrity and the alignment features of both the CRD System and the core assembly permit a successful scram even when the ship is in the worst possible attitude.

#### 13.3.1.5. Conclusions

It is concluded that safe reactor shutdown is ensured under any credible assumption of control rod system malfunction. It is further concluded that the CRD System design features, the analytical failure analysis, and the continued program of surveillance, tests, and administrative control, ensure that a rod drive malfunction of other than a minor nature is highly improbable.

#### 13.3.2 Sudden Reduction of Steam Flow

##### 13.3.2.1. Nature of the Accident Analysis

This accident, though highly improbable, could be caused by the simultaneous closing of both steam stop valves. Potential plant damage would be caused by excess pressure as a result of primary coolant heatup and expansion if control action is not initiated.

The analog analysis was based on the conservative assumption of 80 MWt initial power, one-half nominal moderator coefficient, no pressurizer spray action, no high-pressure scram, and no operator control action. The effect of an adverse Doppler coefficient (twice nominal) and the effect of only two primary pumps operating were also investigated. It was not considered credible to assume an abnormally adverse moderator coefficient together with an adverse Doppler coefficient.

Figure 13-22 shows the reactor power versus time for the worst assumed conditions, with and without scram action. Figure 13-23 shows the primary and secondary temperatures versus time for the same conditions. Without a scram, the primary system average temperature reaches a peak of 538 F, which does not result in exceeding the relief valve steam capacity or in filling the pressurizer, even if the level were initially just below the high alarm point. The secondary effects of containment overpressure (because of boiler relief action) and possible electrical failures were not considered.

#### 13.3.2.2. Conclusions

It is concluded that an excessive ratio of reactor power to steam flow due to sudden closing of steam stop valves is not a safety hazard, even without control rod motion. The moderator coefficient is effective in shutting down the reactor. The relief valves prevent overpressurization of the primary and secondary systems.

#### 13.3.3. Loss of Primary Pumping Power

The accident examined here results from a sudden partial reduction or complete loss of coolant flow through the reactor core when the reactor is operating at an appreciable power level. A reduction of flow within the primary system may be caused by an electrical failure of the power supply to the pumps, or it may be caused by mechanical failure of a single pump. The reduction of flow below that required to cool the reactor at the particular power level in question will naturally increase in the temperature of the coolant as well as the reactor internals. Furthermore, there is the danger that a combination of low coolant flow and excessive reactor power for the flow might result in burnout of some of the hotter fuel pins.

In order to establish the region of safe operation, the potential consequences of single or multiple pump failures were

analyzed by determining the steady-state reactor power at which coolant heat transfer burnout, DNB, or pellet central melting occurs in the hot channel, under various combinations of pump operation - Figure 13-24.

The pellet central melting limit line is based on the maximum hot channel peaking factor in the shuffled core lifetime computed to occur at 2000 EFPH. The limit line is independent of the coolant flow because the fuel rod clad surface temperature has been conservatively taken to be the wall superheat temperature derived from the Jens-Lottes correlation.

A curve of the reactor power to reach the hot channel DNB as a function of reactor core coolant flow is shown on Figure 13-24 for the case of the lowest margin which occurs at 8500 EFPH.

Also shown on Figure 13-24 are the SAVANNAH normal steady-state reactor power operating limits. This figure therefore shows that under all partial loss of flow accidents to one pump operating, DNB would not occur even if the reactor power remained at the steady-state power limit for the initial number of operating pumps.

During complete loss of flow accidents, an automatic power scram is initiated. The complete loss of flow accident has also been analyzed for four, three, and two pump initial operation. Results of these calculations are shown on Figures 13-25, 26, and 27 for four, three, and two pump operation respectively. The power level for safe natural circulation heat removal is also shown on each of the figures. The internal circulation flow path is up through the fuel elements and down through the control rod channels during natural circulation.

The DNB safety margins are shown in Table 13-2 for the initial conditions of the flow coastdown transients. It should be noted that these steady state power levels include a 1.2 safety factor on the fundamental burnout correlation as reported in WAPD-188.

Table 13-2 Safety Margins for Flow Coastdown  
Power Levels Required for DNB

<u>Pumps at Full Speed</u>	<u>Third Pass Average Heat Transfer, BTU/Hr Ft<sup>2</sup> @ 1750 psi</u>	<u>Steady-State Reactor Power</u>
4	165,000	155 MWt
3	150,000	139 MWt
2	123,000	120 MWt
1	104,000	88 MWt

Although these results lead to the conclusion that, with appropriate safety action, the fuel element cladding in the hot channel does not melt following the loss of coolant flow, cooling might be required to prohibit the formation and collection of steam at the top of the reactor vessel. With either auxiliary diesel generator operating, the primary coolant pumps can operate on the low speed windings to circulate primary coolant through the reactor, cooling it over a long period following the accident. Thus, decay heat can be removed through the boilers, and auxiliary condenser. If primary pumps cannot be used to circulate the coolant, two additional methods are available depending upon the source of emergency electrical power. With either of the auxiliary diesel generators operating, decay heat can be removed through the let-down coolers and the intermediate coolers by operation of the buffer change pump and one set of intermediate cooling water pumps. With the emergency diesel generator operating decay heat can be removed by the emergency cooling system. Thus, at least two methods are available for removing decay heat in

case of a loss of turbine generator power. Since the auxiliary diesel generators and the emergency diesel generator are independent sources of electric power, a simultaneous failure of both sources is not likely to occur.

It should be emphasized that the calculations of cladding temperatures in the hot channel were based on very conservative assumptions. The temperature of the hottest fuel pins will very likely fall considerably below the values reported for film boiling. It may be concluded that partial or complete loss of flow will not result in fuel melting or DNB.

#### 13.3.4 Fuel Element Failures

##### 13.3.4.1. Nature of the Problem

Failure of the fuel cladding can result in dispersal of fission products throughout the Primary and Auxiliary systems, causing increased radiation levels.

##### 13.3.4.2. Analysis

Although pin failure is considered improbable, the potential effects of fission product leakage into the primary water have been analyzed. The fission product leakage was predicted by theoretical means with empirical constants for the composition and quantity of fission products which can be released as a function of the amount of oxide fuel exposed to the coolant. The analyses assumed 300 days of operation at 69 MWt prior to pin failure and 100 days of operation following pin failure. Failure of up to 5% of the total core fuel pins was assumed in the analyses.

Compared with the N-16 activity, the radiation due to fission products leaking from the fuel pins is negligible during high-power operation. Increased

radiation from fission products within primary system components becomes significant only after shutdown. Approximately 1 week is required to reduce radiation levels near primary system components to 100 mrem/hr. This imposes a maintenance inconvenience rather than an accident hazard. The shielding on the demineralizers is conservatively sized to reduce the radiation dose at the surface to 200 mr/hr with approximately 5% failed fuel pins.

#### 13.3.4.3. Operating Experience

##### N.S. SAVANNAH Experience

During the entire lifetime of Core I, no evidence of fuel pin failure based on the analysis of primary water samples has developed. From early power operation at Yorktown until August 1968, a period of approximately 6 years, the samples taken during medium- and high-power operation have yielded essentially constant results. Representative values are  $5 \times 10^{-2}$   $\mu\text{ci/ml}$  and  $3 \times 10^{-4}$   $\mu\text{ci/ml}$  for the gross 15-minute degassed sample and the gross 1-hour iodine activity, respectively, from samples taken upstream of the the purification ion exchangers and filters. Approximately 90% of the measured primary water activity at medium- and high-power is due to activation of corrosion products and other impurities in the primary water.

#### 13.3.4.4. Conclusions

The favorable operating record to date, the results of accident analysis, the results of related fuel pin tests, the results of calculations predicting fuel pin life, and the inherent safeguards, provide the basis for the conclusion that fuel pin failure is highly unlikely. The results of analytical investigation indicate that ship operations could be continued with a small percentage of failed

fuel pins without undue hazard. Radiation monitoring, the results of periodic sampling, and administrative control based on hazards analysis will dictate the conditions that might prevent operating with failed fuel pins.

### 13.3.5 Primary Water Leak

#### 13.3.5.1. Nature of the Accident

Of concern here are small continuous leaks or small pipe ruptures outside of the containment vessel. Rupture of the large reactor coolant piping and the gross release of water within the containment is analyzed later.

The potential radiation hazard from gases is the controlling factor in leak analysis. With normal ventilation, these gases could exceed maximum permissible concentration (MPC) for the crew in the manned spaces. All gases are assumed to evolve from the leaking water without delay or decay. Argon-41 is controlling if there are no failed fuel pins, in the core. If there are failed fuel pins, krypton, xenon, and iodine isotopes must be considered in addition to the argon. From a consideration of normal shipboard functions, the theoretical limit of fuel pin failure (before shutdown is required) is approximately 28 pins (0.5% of the core). The analysis is therefore based on this condition.

The limiting concentrations of radioactive gases in the primary coolant are shown in Table 13-3.

Table 13-3 Limiting Concentrations of Radioactive Gases in Primary Coolant

<u>Gas</u>	<u>Concentration</u> <u>μci/ml</u>
Argon-41	0.031
Noble gases	2.3
Iodine	0.53

### 13.3.5.2 Continuous Leakage Between the Containment Vessel and the Demineralizer

A water leak upstream of the demineralizer is assumed because of the greater potential iodine hazard. Since the temperature of the leaking water would be approximately 100 F, no flashing is assumed. The leakage discussed below is liquid water. All gases which are evolved into the lower reactor void space from the leaking water are eventually discharged via the emergency prefilters, absolute filters, and iodine filters in a fresh air carrier stream of 1000 cubic feet per minute. Based on the data of Table 13-3 and an iodine filter efficiency of 99%, the following continuous leak rates are permissible without exceeding the MPC for occupational exposure, ignoring any credit for dispersion from the stack:

<u>Gas considered</u>	<u>Permissible leak rate, cc/min</u>
Argon	1810
Noble gases	98
Iodine	130

### 13.3.5.3. Continuous Leakage Outside the Reactor Compartment

After passing through the PP system ion exchangers and filters, primary-grade water is circulated through the SL System, part of which is located in equipment spaces outside the reactor compartment. Gases evolving from any water which leaks into these spaces mix with uncontaminated air in a ventilation system having an exhaust air flow 15 to 60 times greater than that of the RSV System. Although there are no iodine filters in the ventilation system, the water necessarily passes through the purification filters, which have an iodine decontamination factor equal to or greater than that of the iodine filters. Therefore, the allowable leakage rates are

greater than those given in section 13.3.5.2. In case of ventilation system failure, radiation monitoring procedures and administrative control would dictate when operation should be suspended.

#### 13.3.5.4 Gross Leakage Outside the Containment Vessel

The buffer seal surge tank, located in the secondary shield area, is assumed to discharge 1330 liters within 3.5 minutes. The gases in the water (Table 13-3) are assumed to be released and distributed to the volume of the smallest room occupied by the SL system equipment. The maximum dosage to any person was calculated in two ways: (1) the stationary cloud concept and (2) the moving cloud concept.

With the stationary cloud the 1-hour dosage for a person enveloped in the cloud, which is confined to a finite volume, is 154 mr whole body and 4.6 mr thyroid. With the moving cloud, which is assumed to be at ground elevation with a velocity of 1 meter per second, the total dosage is 0.14 mr whole body and 4.1 mr thyroid.

#### 13.3.5.5. Conclusions

With approximately 0.5% of the total fuel pins failed, continuous primary water leakage of 5900 cc/hr outside the containment vessel will result in gaseous concentrations less than occupational MPC with normal ventilation. In the event of a complete ventilation system failure simultaneous with leakage of 1330 liters from either the PP or SL System into the smallest room outside the containment, the 1-hour dosage for a person immersed in the static finite cloud would be 154 mr whole body and 4.6 mr thyroid. With the 1330 liter leak and the assumption of a concentrated finite cloud that moves 1 meter

per second (due to partial ventilation or natural dispersion) the maximum total dosage to a person is 0.14 mr whole body and 4.1 mr thyroid. It is therefore concluded that small continuous operational leaks outside the containment do not present any undue radiation hazard and that the probable dosage from a gross water leak outside the containment would not constitute a serious hazard. The maximum credible dosage from a gross water leak would not approach the once-in-a-lifetime accident limits of 25 r whole body and 300 r thyroid.

### 13.3.6 Loss of Air Supply for Instruments and Controls

#### 13.3.6.1. Nature of the Accident

Loss of the instrumentation and control air supply will result in pneumatically operated valves automatically assuming the deactivated position except where the flow of bleed air is retarded by the closing of isolation valves. Air operated instruments and indicators may operate improperly or not at all; thus false indications and annunciated conditions may result. For example, annunciator alarms will indicate low pressure in the CW System, low pressure and low level in the pressurizer, and low steam flow even though these conditions may not actually exist.

#### 13.3.6.2. Analysis of Accident

The failure of one air compressor will not disable the system since there are two compressors in parallel, each one capable of handling the entire air demand without continuous operation. In the event of failure of the normal automatic compressor control, the operator can exercise complete manual control from the console. Instrument air pressure is displayed on the console, and an annunciator is actuated if air pressure approaches an abnormally low value.

An adequate number of manual isolation valves are provided so that operation can be continued if a leak in a critical area can be isolated.

Following loss of instrument air, most of the indicator gages do not function. Therefore, the operator is forced to shut down the reactor because he cannot determine actual conditions within the plant. This action automatically closes the main propulsion turbine throttle and causes a startup of the two 750 kw auxiliary diesel generators. Steam is used by the turbine generators until they are taken off the line by the operator when the electrical load is picked up by the diesel generators. Sufficient steam supply is available for at least 16 minutes of turbine generator operation.

#### 13.3.6.3. Operator Action

After shutting down the reactor on loss of air supply, the operator is instructed to take definite stops, including the following:

1. Shutdown the buffer seal charge and booster pumps. The loss of air causes isolation of all flow paths within the Buffer Seal System with the exception of the flow path through the buffer seals into the reactor. The return line, bypass line, and letdown system are closed automatically. Failure to shut off the buffer seal charge pumps could result in draining the buffer seal surge tank in the Primary System in approximately 6 to 12 minutes, depending on the number of pumps operating.

2. Start the DK System. This is done to remove the reactor decay heat following rod scram. The feedwater valves close automatically on loss of air so that no makeup water is available to the steam generators.

3. Check auxiliary diesel generator operation. These generators should have started automatically on reactor scram. Otherwise, they may be started manually.

4. Close the main steam stop valves. This may be done if the auxiliary generators have been started. Closing these valves shuts off steam supply to the turbine generators.

Failure of the operator to take any action will result in a depletion of the available water in the boilers and subsequent loss of steam supply to the turbine generators, thereby causing a loss of electrical power to the main bus. The automatic scram resulting from this loss of power will shut the reactor down. The primary pumps will lose power and thereby will shut off. The DK System will be activated automatically on loss of power to the main bus. The only possible damage that might result from no operator action would be to the buffer seal booster and the charge pumps. Also, the boilers may run dry.

#### 13.3.6.4. Conclusions

The air supply system is designed to provide reliable service, and the likelihood of a failure of this system is quite small. In case of a failure, the loss of control air results in the need for a plant shutdown until the leak can be repaired. No damage to the Primary System will result, and adequate time is provided for the operator to take appropriate action to prevent damage to the buffer seal booster pumps, the charge pumps, and the boilers.

### 13.3.7. False Containment High-Pressure Signal

#### 13.3.7.1 Nature of the Accident

High-range and low-range instruments are provided to measure and indicate pressure within the containment vessel. The high-range instrument covers a pressure range from 0 to 200 psig. The low-range instrument is more sensitive and indicates pressures from 0 to 15 psig. The low-range pressure transmitter actuates an annunciator when the containment pressure exceeds 3 psig. It also actuates a pressure controller, which in turn isolates the containment when the containment pressure reaches 5 psig. This feature is provided so that all containment vessel penetrations will close if a steam leak within the containment vessel creates a pressure of 5 psig. The problem examined is a false high-pressure indication that results in the automatic closing of these valves.

#### 13.3.7.2. Immediate Effects

The immediate effect of a false high-pressure signal is the isolation of reactor auxiliary systems due to the automatic closing of the containment isolation valves. Two of the most vital functions interrupted are the PP system flow and the CW system flow to the primary pumps, reactor shield tank, CC System, and purification coolers. It is still possible to supply water to the Primary System via the buffer seal leakage. Since there is no water flowing from the Primary System to the buffer seal surge tank, the reserve water is emptied into the Primary System in 6 to 12 minutes, without external makeup. Boiler blowdown capability is also lost. The ability of the control rod hydraulic system to accomplish a scram is not impeded.

### 13.3.7.3. Operator Action

The accident is immediately brought to the attention of the operator by the following annunciator alarms:

HIGH PRESSURE CONTAINMENT - LOW RANGE  
LOW FLOW PRIMARY LETDOWN  
LOW FLOW COOLING WATER PRIMARY PUMP PS-P4  
LOW FLOW COOLING WATER PRIMARY PUMP PS-P3  
LOW FLOW COOLING WATER PRIMARY PUMP PS-P2  
LOW FLOW COOLING WATER PRIMARY PUMP PS-P1

Immediately upon acknowledging these alarms, the operator must determine whether abnormal pressure actually exists in the containment vessel. He can do this by checking both pressure gauges mentioned previously. In addition to checking these gauges, he can check the pressure within the Primary System and its auxiliaries to verify that a rupture has not occurred within the containment. If it is found that a false pressure is the cause of the situation, normal functions may be reestablished by overriding the pressure controller by pushing a button on the main console. This will open the valves that had previously been shut and will permit the auxiliary systems to resume their normal operation.

The operator should take several steps to prevent damage to equipment if he cannot override the air pressure controller. The turbine generators may be taken off the line as soon as the auxiliary diesels have picked up the load following the scram. Since the primary pumps are without cooling water flow, they should be cut back to one in each loop at half speed. Each pump can operate in this condition for one-half hour, thus allowing a full hour of pump operation by switching pumps. This will permit dumping of reactor decay heat to the steam generators.

The DK System is also operable, has not been isolated by the false pressure indication, and may be used to cool the reactor at the operator's discretion. If the situation cannot be corrected in a few minutes, the buffer seal charge pumps should be shut off to prevent excessive makeup to the Primary System and to prevent damage to the pumps if the surge tanks are drained.

If the operator takes no action, automatic reactor scram, auxiliary diesel generator startup, and DK System startup will prevent reactor damage.

#### 13.3.7.4 Conclusions

Improper functioning of the low-range containment pressure system could result in automatic shut-down of auxiliary systems. Normal operator action will restore these systems to the original operating condition. Failure of the operator to take any action will result in minor plant damage and no undue hazard to shipboard personnel.

#### 13.3.8. Loss of ac Power

##### 13.3.8.1. Nature of the Accident

Much of the normally functioning equipment within the N.S. SAVANNAH power plant depends on electrical power. This equipment includes pumps, compressors, pressurizer heaters, electrical control rod drive motors, and instrumentation. The loss of electrical power to some of this equipment could result in abnormal conditions described in this section.

##### 13.3.8.2. Loss of Turbine Generators

The first condition considered is the loss of one 1500 kw turbine generator during normal operation.

Loss of one turbine generator results in an automatic startup of the two 750 kw auxiliary diesel generators as well as an automatic tripping of the nonvital loads. Prior to auxiliary diesel generator startup, the turbine generator load requirement is less than 1800 kw. Each turbine generator is capable of delivering a 25% overload (1875 kw) for 2 hours. Although the remaining turbine generator is momentarily overloaded, the first diesel generator parallels with the turbine generator in less than 10 seconds and is soon followed by the second auxiliary diesel generator. The generating capacity of the two auxiliary diesels equals that of the lost turbine generator; thus continued nuclear plant operation is possible.

A rapid loss of power from both turbine generators results in a momentary complete loss of power before the auxiliary diesel generators start up. This loss of power to the main bus results in an automatic scram of the reactor and automatic startup of the emergency diesel generator and the DK System. Although the loss of one or both turbine generators normally results in a startup of the diesel generators, the scram signal causes an independent signal for automatic startup of the auxiliary diesel generators and automatically trips nonvital loads. The main propulsion turbine throttle is also closed automatically upon scram. The first diesel generator starts up in less than 10 seconds after the scram signal is initiated. This diesel generator is soon followed by the second unit.

#### 13.3.8.3. Loss of Auxiliary Generators

Another consideration is the highly improbable event that neither diesel generator would start following loss of one turbine generator. As mentioned above,

this would result in a period of overload on the remaining turbine generator, but could be corrected by reducing power to a point where only two primary coolant pumps are required, thus reducing the total load on the turbine generator to 1373 kw, well within its normal rating. The diesel generators would then be started manually.

A still more remote possibility is that neither diesel generator would start upon loss of both turbine generators. It is not likely that both diesel generators will fail unless the main engine room was flooded. In this case, the 300 kw emergency diesel generator (located on the navigation bridge deck) and the DK System would start automatically.

#### 13.3.8.4 Conclusions

Provision of two independent turbine generators and two independent auxiliary diesel generators results in an extremely low probability of loss of electrical power to the main bus. Even in the very unlikely event that both the normal and the auxiliary sources of electrical power become inoperable, the emergency diesel generator can provide the necessary power for reactor cooling.

#### 13.4. Reactor Systems Fire Hazards

##### 13.4.1. Oil Fire Hazard

The control drive hydraulic system uses a petroleum base oil (150 gallons, total). This hydraulic oil has a flash point of 420 F. The vapors will support continuous combustion if the oil is above 470 F. The auto-ignition temperature of the oil is 755 F. The potential hazards associated with an oil fire are affected by these temperatures.

#### 13.4.1.1. Oil Fire Hazard Outside of Containment

The pumps and associated equipment for the hydraulic system are located in a normally closed and locked room, which is force ventilated. The reactor operators on watch maintain administrative control over this hydraulic room, and only qualified crew members or other authorized personnel have access to the hydraulic system. The CW System maintains the oil temperature below 120 F. The flash point of the oil is approximately 300 F above the normal operating temperature of the oil or any other object in the room. The auto-ignition temperature is at least 600 F above the maximum expected ambient temperature. Therefore, the oil does not present a fire hazard.

The oil piping, which runs to and from the containment vessel, passes through a narrow portion of the upper reactor compartment which, similar to the hydraulic pump room, is free from fire hazard.

#### 13.4.1.2. Fire Hazard Within Containment

In order to eliminate any potential fire hazard within the containment when the reactor is operating, the containment free volume is made inert with nitrogen so that the oxygen content is maintained below 10% whenever the reactor temperature is above 400 F. A supply of nitrogen is carried aboard to make up any losses and to reinert the containment should purging for maintenance access become necessary. In the unlikely event that the inert containment atmosphere cannot be maintained at the same time that the primary system components are at normal operating temperature, the reactor is shut down.

The only solid material within the containment that warrants discussion from the standpoint of fire hazard is the thermal insulation. Insulation, covering, and sealer are all rated fireproof and therefore would not initiate or support combustion. The auto-ignition temperature of the oil is more than 200 F higher than any metal temperature within the containment.

#### 13.4.2. Hydrogen Fire Hazard

The use of the Hydrogen Addition System raises some question regarding a hydrogen fire or explosion. The hydrogen is supplied from a single line connected to a supply header, which in turn is connected to two hydrogen supply cylinders. This single line adds hydrogen to the buffer seal surge tank, which is located outside the containment vessel.

A relief valve is provided in the supply line to prevent excessive pressure should the pressure regulator fail. In the event of a fire in the area of this system, two check valves are provided on the discharge side of the hydrogen supply header to prevent flames from reaching the hydrogen supply cylinders through the piping. An excess-flow shutoff valve isolates the supply header if the hydrogen supply line is severed. As an additional precaution, hydrogen detectors are located so that leakage from the system can be detected. The piping from the hydrogen bottles to the buffer seal surge tank is completely enclosed, and the air in the surrounding annulus is monitored for the presence of excess hydrogen. Detectors also monitor the air inside the containment vessel and secondary shielding.

Operating experience has demonstrated that the normal requirements for hydrogen addition are small. Thus, hydrogen requirements are met by periodic manual additions to the buffer seal surge tank. At all other time, the hydrogen is shut off at the bottles in the A-deck storage room.

### 13.4.3. Conclusions

In view of the location of the hydrogen supply room, the operating precautions, and the engineered piping, equipment, and detection safeguards, fire caused by the Hydrogen Addition System is considered most unlikely.

An oil fire outside the containment vessel is virtually incredible since oil outside the containment is maintained at temperatures of 120 F or less. The possibility of oil fires inside the containment is drastically reduced by the operating procedure of maintaining an inert atmosphere in the containment, when the primary system temperature is in excess of 400 F. The system for injection of CO<sub>2</sub> into the containment through the CO<sub>2</sub> injection nozzles assures prompt control of any fire in the containment.

### 13.5 Maximum Credible Accident

The maximum credible accident that is associated with reactor startup and operation is considered and analyzed in two parts. The accident was first analyzed for Core I, with the results set forth in Section 13.5.1. The analysis was then modified to meet the characteristics of the shuffled core (Core Ia) and presented in Section 13.5.2.

#### 13.5.1. Maximum Credible Operating Accident (Core I)

##### 13.5.1.1. Nature of the Maximum Credible Accident

The maximum credible operating accident (MCA) is a major loss-of-coolant (LOC) from the Primary System. The specific LOC accident was assumed to be instantaneous, complete, transverse shear of primary system pipe. Various primary

system pipe breaks were analyzed in order to maximize effects as post accident core temperatures and core hydraulic loading. The range of pipe breaks studies was:

1. 1-1/2-in. purification line
2. 4-in. pressurizer surge line
3. 12-9/16 in. reactor inlet and outlet lines

#### 13.5.1.2. Blowdown

##### 13.5.1.2.1 Description of Analytical Method

Blowdown of the Primary System of the N.S. SAVANNAH nuclear power plant is analyzed by FLASH, a digital computer program. The variations with time during blow-down of primary system flows, vapor and liquid inventories, pressures, and coolant and fuel temperatures are calculated by this code. Calculations are made to determine the coolant flow rate through the leak, water inventory above and below the core, pressure drop across the core, flow through the core and loops, neutron and gamma heating in the fuel temperatures in both the average fuel channel and in the hot channel. The heat transfer calculation includes the determination of Departure from Nucleate Boiling (DNB) and the subsequent decrease in heat transfer due to film boiling.

##### 13.5.1.2.2 Assumptions and Conditions

The following assumptions are made in analyzing the blowdown of the N.S. SAVANNAH reactor Primary System:

1. The reactor is operating at full power of 80 MWT and has been operating at this power level for two years. The initial system pressure is 1750 psia and the initial water inventory is 1357 ft<sup>3</sup> - normal operating conditions.

2. The leak is an instantaneous, complete, transverse shear of the selected size pipe.
3. For breaks in pipes greater than 4 in. in diameter, the control rods are not inserted into the core. In these cases, reactor shutdown results from void coefficient effects. Control rod insertion at the design scram rate initiated by the pressure sensing system at 1445 psia is assumed for pipe breaks of 4-in. diameter or less.
4. The radial peaking factor is 1.95 and the axial peaking factor is 1.66 (maximum-to-average power). The factors are based on a worst case assumption that all control rods are fully withdrawn - a condition which could exist during operation at end-of-life.
5. There is no post-accident core spray or injection of cooling water in the pressure vessel.
6. The primary system pumps continue operating throughout the blowdown period since there are no pump shutdown interlocks. Sufficient electrical power to the pumps will be maintained during the period without depending on alternate or emergency power supplies.
7. The containment pressure during blowdown is 173 psig which is the expected equilibrium pressure immediately following blowdown:
8. One steam generation ruptures and its contents are released to the containment.
9. Heat removal from the primary coolant by the operating steam generator decreases linearly from full power to zero within 5 sec after the break.
10. Geometry of the Primary System is simulated in the program by dividing the primary coolant inventory into the following three volumes:

- Volume 1 Upper half of core, exit plenum, hot leg, and half of steam generator.
- Volume 2 Lower half of core, inlet plenum, cold leg, and half of steam generator
- Volume 3 Pressurizer

This idealized geometry was utilized for the FLASH analysis of the N. S. SAVANNAH blowdown for the three types of failure considered:

1. Top break - flow baffle remains intact
2. Bottom break - flow baffle fails
3. Bottom break - flow baffle remains intact

Seven cases, covering a range of break sizes from 1-1/2 to 1-9/16 in., occurring from the top to the bottom of the primary system geometry and with the new flow baffle both failed and intact, were analyzed.

#### 13.5.1.2.3. Results

Figure 13-28 is a graph correlating the fuel temperatures in the average channels and hot channels of each pass of the core, and the fractional power of the core relative to full power for the double ended pipe break with the flow baffle intact. Table 13-4 summarizes the salient results of these analyses.

The following conclusions are evident from these data:

1. The blowdown time ranges from 8.5 sec for the 12-9/16-in. diameter line, with double-ended break, to 150 sec for the 4-in., double-ended break.
2. The blowdown time for the 12-9/16-in. double-ended, bottom break is increased from 8.5 sec to 10 sec if the flow baffle remains intact during the blowdown.

3. The fuel temperatures are substantially reduced during blowdown by heat transfer to the fluid whose temperature is decreasing during this period. The fuel temperatures reach a minimum near the end of blowdown and then start to increase due to the change in mode of heat transfer. In Figure 13-28, representing Case G, the double-ended bottom break is marked to indicate the times at which the heat transfer mode changes from convection to nucleat boiling to film boiling.
4. The reactor is effectively shut down by the void coefficient.
5. The break in the smooth  $P/P_0$  curves occur in the transition period between subcooled and two-phase flow through the core channels. Variations in core flow during this period cause a momentary change from two-phase to subcooled flow resulting in the  $P/P_0$  variations.
6. Case G, the double-ended 12-9/16 in. bottom break, with intact flow baffle, is selected as the worst case upon which to base subsequent core heatup and slumping. This case was chosen in preference to Case D, which yielded a slightly shorter blowdown time and higher fuel temperatures, because of stress analysis showed that the flow baffle remained intact at the maximum pressure differential calculated during the transient.

### 13.5.1.3 Hydraulic Effects on Core Structures

#### 13.5.1.3.1. Analytical Method, Assumptions, and Conditions

The accident re-analysis included investigation of the hydraulic loads imposed on the pressure vessel internal structures during the blowdown period.

Three structures were analyzed for stress conditions:

1. The conical support ring from which the core and thermal shields are suspended and which prevents mixing of reactor inlet flow with reactor outlet flow

2. The lower flow baffle which directs inlet flow across the thermal shields and into the core first pass
3. The fuel elements.

The highest pressure differentials and flow conditions from the FLASH results were used in the stress analyses.

#### 13.5.1.3.2 Results

Table 13-4 summarizes the results of the analyses.

The following conclusions are made as to the integrity of the components studies.<sup>1</sup>

##### 1. Lower Flow Baffle

The maximum membrane stress of 37,125 psi occurs in the center and knuckle regions of the ellipsoidal section. The ellipsoidal head would distort under these stresses in such a manner as to assume a more spherical shape and therefore reduce the stress levels. No failure, in terms of separation of parts or leakage, would occur. Analysis of the welds between the ellipsoidal head and the cylindrical section indicates no excessive stresses.

##### 2. Conical Support Ring

The loading configuration of the conical support ring makes it susceptible to failure when the membrane stress exceeds the yield stress. The maximum calculated membrane stress is 73,851 psi and occurs in the conical section approximately 2 in. below the top flange. Since this greatly exceeds the material yield stress, it is expected that the conical section will fail. It is not possible to predict the exact mode of failure or the final config-

Table 13-4 Summary of Hydraulic Analysis

<u>Component</u>	<u>Location of Maximum Stress</u>	<u>Maximum Stress, * psi</u>	<u>Minimum Yield Stress, psi</u>	<u>Minimum Ultimate Stress, psi</u>
Lower flow baffle	Center of ellipsoidal head	$P_m = 37,125$	20,000	54,000
	Knuckle region of ellipsoidal head	$P_b = 49,593$		
Conical sup - port ring	2 in. below the top flange	$P_m = 73,851$	20,000	54,000
	Just below the top flange	$P_b = 251,000$		
Fuel element	Lower support tabs	$P_m = 1000$	20,000	54,000
	Upper nozzle	$P_m = 1240$		

\* $P_m$  = membrane stress;  $P_b$  = fiber stress

uration of the ring. Failure of the conical support ring would result in very little movement of the core structure due to the proximity of the flow baffle to the pressure vessel. The failure would not affect subsequent flow through the core or the core reactivity.

### 3. Fuel Element

The stresses in the upper nozzle area resulting from upward loading forces are approximately 1200 psi. The element cannot move in an upward direction since it is held down by the upper grid plate. The tabs in the lower support frame are subjected to a compressive stress of approximately 1000 psi and therefore will not fail.

#### 13.5.1.4 Core Heating and Slumping

##### 13.5.1.4.1 Description of Analytical Method

Core heating and slumping is analyzed by NURLOC, a digital computer program that performs the heat and mass transfer computations simulating the core behavior following the blowdown phase of the loss-of-coolant accident. The processes included are: conduction, convection, thermal radiation, fission-product decay heating, delayed neutron heating, metal-water reaction, boil-off of residual water remaining after blowdown, and core slumping.

##### 13.5.1.4.2 Assumptions and Conditions

The following assumptions and conditions are provided for the NURLOC analysis of the N.S. SAVANNAH loss-of-coolant accident:

1. The accident analyzed in FLASH Case G, the double-ended inlet pipe break. This case resulted in the highest fuel temperatures at the end of blowdown with the flow baffle intact. Input data included power level at the end of the blowdown, initial temperatures, heat generation rate, and containment vessel pressure.

2. The residual water remaining in the flow baffle after blowdown is 1250 lb. This is the weight of residual water predicted by FLASH less the amount of water calculated to be in the annulus outside the flow baffle, and less the amount of water that will flow through the 3/4 in. diameter hole in the bottom of the flow baffle. The amount of water in the annulus outside of the flow baffle was deducted from the total amount since it is not available for core cooling or metal-water reaction.
3. The core slumping model is:
  - (a) All material in a fuel and cladding node slumps down to the flow baffle when the failure temperature is reached.
  - (b) If water is present in the flow baffle, the slumped material is quenched to water temperature (370 F). Steam is generated from the water by both the heat of quenching and the subsequent decay heat.
  - (c) When the water has been completely evaporated, slumped fuel is discarded from the model. Also, the metal-water reaction ceases when the water has been evaporated.
  - (d) The slumping temperature is 2780 F, the temperature at which type 304 stainless steel in contact with  $UO_2$  starts to soften.

The slumping model is conservative for the following reasons. The low slumping temperature provides for earlier transfer of the fuel to the flow baffle which ultimately puts fuel at a higher heat generation rate in contact with the pressure vessel. Direct slumping eliminates any hold-up time between melting and transport to the flow baffle and also results in fuel of a higher heat generation rate in contact with the pressure vessel.

### 13.5.1.4.3. Results

The fraction of core slumped is plotted in Figure 13-29 as a function of time to 3995 sec after the start of the loss-of-coolant accident. Slumping, which occurs at cladding temperatures of 2780 F, begins at 1180 sec and is approximately linear with time over the range analyzed. At 3995 sec, the last time increment of the NURLOC analysis, the fraction of the core slumped is 0.246.

At 3995 sec, slumping is confined to the central five radial shells in the core model. Table 13-6 summarizes the fraction of each radial shell slumped at 3995 sec.

Slumping is concentrated in the central portion of the core because decay heat generation peaks at the center with the control rods out and heat transfer to the thermal shield is greater at the outer part of the core.

Table 13- 5 Fraction of Radial Shell  
Slumped at 3995 Seconds

	<u>Shell 1</u>	<u>Shell 2</u>	<u>Shell 3</u>	<u>Shell 4</u>	<u>Shell 5</u>
Fraction Slumped	0.615	0.615	0.538	0.462	0.308

Although the slumping rate will decrease at longer times, as the decay heat generation falls and the thermal radiation from the outer fuel shells rises, the slumping rate is extrapolated linearly in Figure 13-30 to 100% core slumping. The entire core will slump according to this extrapolation in 12,200 sec. Actually a thermal equilibrium will be reached prior to slumping of the entire core. This equilibrium will be reached when the heat transfer by thermal radiation from the unslumped fuel is equal to the decay heating of that fuel. The NURLOC analysis was

terminated before this equilibrium was reached since this information was not necessary for purposes of determining the integrity of the reactor vessel.

Water remaining in the flow baffle as a function of time is shown in Figure 13-31. About 50 lb. of water are vaporized during the initial 200 sec by conduction of heat from the flow baffle. Between 200 and 1180 sec, the water boil-off is negligible because the flow baffle, which is only 1-in. thick, has cooled to the water saturation temperature. At 1180 sec, the water remaining decreases in an approximately linear relationship with time as the core slumps. The boil-off approaches linearity because the fuel slumping rate is nearly linear. At 2780 sec, all the water has been evaporated and the metal-water reaction ends, with 9.36% of the cladding reacted.

Oxidation of the cladding by the steam generated by boil-off from the water in the flow baffle is correlated with time in Figure 13-32. The oxidation rate is very low until 1180 sec because of the limited steam flow. The oxidation rate increases sharply at 1180 sec since the steam generation increases at this time because of fuel slumping.

Material temperatures of the lowest ferrule spacer were monitored throughout the NURLOC analysis. The maximum temperature reached was 736 F which is considerably lower than the melting point of the ferrule braze (approximately 1900 F).

#### 13.5.5.1.5 Hydrogen Generation, Combustion and Detonation

##### 13.5.1.5.1. Description of Analytical Method

Molar fractions of hydrogen, steam and oxygen are calculated from the integrated hydrogen generation results of NURLOC. These fractions are compared to published

flammability and detonation limits of hydrogen, steam and air mixtures. Since the concentrations of the constituents will be determined by the steam pressure, the gas molar fractions are computed at the lowest steam pressure in the containment volume. The hydrogen molar fraction will be highest when the steam pressure (and hence steam concentration) is the least.

#### 13.5.1.5.2 Assumptions and Conditions

The following assumptions and conditions are made for the hydrogen analysis:

1. The total production of hydrogen from the metal-water reaction is 15.1 lb-moles. This is the quantity of hydrogen calculated by NURLOC.
2. Hydrogen, oxygen, nitrogen, and steam will form a mass containing the stoichiometric amount of oxygen to react completely with all the hydrogen.
3. The containment atmosphere is 10 percent by volume oxygen and 90 percent nitrogen prior to the accident.
4. The minimum containment vessel pressure after the accident is 65.8 psia.
5. Since the flammability correlation is based on air, the sum of the molar fractions of oxygen and nitrogen is assumed to be the molar fraction of air. This is a conservative assumption since the same mole fraction of air contains more oxygen than the depleted oxygen atmosphere actually present in the N.S. SAVANNAH containment.

#### 13.5.1.5.3 Results

Cumulative hydrogen generation from the metal-water reaction is shown in Figure 13-33. Hydrogen is generated at a slow rate until 1180 sec, when fuel slumping begins and steam formation is accelerated. Hydrogen formation increases rapidly until the residual water held up in the flow baffle is completely evaporated at 2780 sec. After the water is

depleted, no further hydrogen is generated. The total hydrogen resulting from the metal-water reaction is 15.1 lb-moles.

The molar fractions of the containment vessel constituents at the lowest steam pressure after the accident are:

<u>Gas</u>	<u>Molar Fraction</u>
Hydrogen	0.053
Oxygen	0.026
Nitrogen	0.238
Steam	0.684

The point representing these fractions (assuming the sum of nitrogen and oxygen equal to the molar fraction of air) is shown on Figure 13-34, a triangular correlation of the flammability and detonation limits for hydrogen, air, and steam. Since the point lies outside the flammability envelope, the hydrogen generated during the loss-of-coolant accident will not combust in the containment vessel.

#### 13.5.1.6 Effect on Reactor Vessel

##### 13.5.1.6.1 Description of Analytical Method

Integrity of the pressure vessel is determined by analyzing the temperature distribution in the bottom head of the vessel resulting from the slumped fuel. Temperatures above at the level at which the creep rupture time decreases sharply would cause failure of the vessel. Decay heat from the slumped fuel must be conducted through the pressure vessel wall to the primary coolant water, resulting from the blowdown, in the bottom of the containment vessel. Primary coolant will circulate by natural convection along the outside surface of the reactor bottom head through the 3/4 in. channel provided between the thermal insulation and the reactor vessel in this region, as shown in Figure 13-35.

Temperature distribution in the vessel wall is calculated using the TIGER digital computer program. For this analysis, TIGER calculates time-dependent temperatures of a two-dimensional configuration simulating the slumped fuel with internal heat generation, pressure vessel lower head, water heat sink with nucleate boiling heat transfer coefficient, and heat sinks representing the structures that act as thermal radiation heat sinks. The Laplace heat conduction equation, with the appropriate boundary conditions and internal heat generation term, is numerically solved by the computer using the finite difference method.

#### 13.5.1.6.2. Assumptions and Conditions

The following assumptions and conditions apply to the pressure vessel integrity analysis.

1. The entire core slumps to the bottom of the reactor vessel 3800 seconds (approximately 63 minutes) after initiation of the accident. This time is calculated assuming the fuel is retained by the flow baffle until the flow baffle reaches its failure temperature. Until the water is completely evaporated at 2780 sec, the fuel and flow baffle remain at the saturation temperature of water at a containment pressure of 173 psia. The decay heat from the fuel already slumped plus decay heat and sensible heat of further slumped fuel (slumping occurs at 2780 F) raise the flow baffle temperature to its failure temperature, which is 1800 F, at 3800 sec.
2. Decay heating in the fuel is based on an 80 MWt operating history for two years.
3. Temperatures are evaluated for the case of no ship's list and the maximum design list of 15 degrees.
4. The initial temperature of the vessel is assumed to be the inlet temperature of primary coolant at full power, 508 F.

5. The thermal radiation heat sinks are assumed to be at 508 F, the reactor vessel temperature prior to the accident.
6. The heat transfer coefficient between the vessel surface and the cooling water is 1000 Btu/hr-ft<sup>2</sup>-F in all cases (0 and 15° list). The value is well below the heat transfer coefficients found in the literature for heat fluxes of the order of 30,000 Btu/hr-ft<sup>2</sup> under conditions of nucleate pool boiling and water moving at low velocities. The heat flux and the 5% exit quality of the coolant are sufficiently low to prevent DNB at any point along the vessel surface.
7. The simulation model for TIGER is shown in Figure 13-36.
8. Physical properties of the slumped fuel are the same as the data for the NURLOC analysis.

#### 13.5.1.6.3 Results

Four cases were investigated to determine the effects of list, time of slumping, and fuel temperature at the time of initial contact with the reactor vessel lower head. Temperature of the highest temperature vessel nod is plotted as a function of time in Figure 13-37. The cases analyzed were:

<u>Case</u>	<u>Time of Initial Contact, minutes</u>	<u>List</u>	<u>Average Fuel Temperature at Time of Contact</u>
I	63	15°	2170 F
II	63	15°	2780 F
III	63	0°	2170 F
IV	63	0°	2780 F

In all cases, the maximum temperature peaks at approximately 600 minutes. Beyond this time, the heat transfer rate to the natural circulation cooling water exceeds the decay heat generation and the vessel temperature falls.

The peak vessel temperatures for the 0° list cases range from 940 to 955 F as the average fuel temperature at initial contact rises from 2170 to 2780 F. The peak temperature for the 15-degree list cases range from 1090 to 1108 F as initial contact temperature rises from 2170 to 2780 F.

The peak vessel temperature is relatively insensitive to variations in fuel temperature at time of contact. However, the peak temperature is about 150 F greater with a 15-degree list than with a 0-degree list. The 15-degree list causes the molten fuel to extend beyond the natural circulation cooling water exit nozzle as shown in Figure 13-35. Hence, this region is insufficiently cooled and becomes the hottest node. With 0-degree list, the cooling water entirely covers the vessel wall in contact with the fuel. For this arrangement, the hottest node is at the centerline of the vessel since the fuel depth is greater at the center and the conduction path to the vessel beyond the molten fuel is the longest from this point. Figures 13-38 and 13-39 are temperature profiles in the reactor vessel wall at the time the peak temperature occurs for the cases at 63-minute initial contact time and 2780 F average fuel temperature, and 0-degrees list and 15-degrees list, respectively.

The peak vessel temperatures are significantly below the maximum allowable temperatures for carbon steel. Therefore, it is concluded that the molten fuel will not melt through the reactor vessel. The 1000-hr creep rupture stress for carbon steel is 25,000 psi at 1000 F. The maximum stress in the vessel is caused by the weight of fuel plus the weight of all the reactor vessel internals and is less than 55 psi. Hence, the vessel stress level is very small compared to the stress required for failure.

### 13.5.1.7 Effect on Containment Pressure

#### 13.5.1.7.1 Description of Analytical Methods

Analysis of the containment vessel pressure and temperature as a function of time following the loss-of-coolant accident is accomplished by use of the digital computer program, PTH-1. This code simulates the pressure and temperature inside the containment vessel including mass addition, energy addition, and energy removal by storage in slabs representing the heat sinks and heat transfer to the surroundings. Pressure and temperature of the volume are determined by a search of the thermodynamic properties of steam, which are included in the program input. Heat storage in the slabs is calculated based on heat conduction into the slabs using the finite difference method of solving the Laplace conduction equation.

#### 13.5.1.7.2. Assumptions and Conditions

The following assumptions are made in analyzing the containment vessel pressure history:

1. Blowdown is completed 10 sec after the initiation of the accident. This is the blowdown time calculated by FLASH.
2. The condensing heat transfer coefficient for steel surfaces is 620 Btu/hr-ft<sup>2</sup>-F at the start of the accident, and decreases linearly to 50 Btu/hr-ft<sup>2</sup>-F at the end of blowdown.
3. The following energy inputs are taken at end of blowdown:

<u>Source</u>	<u>Mass, lb</u>	<u>Energy, Btu</u>
Primary coolant	65,945	$33.436 \times 10^6$
Secondary fluid (from one steam generator)	8,000	$3.485 \times 10^6$
Burning of hydrogen in primary coolant		$0.050 \times 10^6$
	<hr/>	<hr/>
	73,945 lb	$36.971 \times 10^6$ Btu

4. Hydrogen generated by the metal-water re-  
action combusts as it is formed. All of  
the heat of combustion of the hydrogen and  
the heat generated by the metal-water  
reaction (155 cal/g of stainless steel) is  
added to the containment volume. The total  
energy addition is  $1.70 \times 10^6$  Btu over the  
period from 10 to 2780 sec.
5. The decay heat from the core is added to  
the containment vessel over the period  
after the end of blowdown. Decay heat is  
based on operation for two years at 80  
MWt.
6. The containment vessel free volume is  
 $34,000 \text{ ft}^3$  including the primary system  
free volume and the volume of the secondary  
side of the failed steam generator. The  
temperature of the containment vessel and  
the internal heat sinks is 130 F.
7. The containment volume is initially filled  
with air at 14.7 psia and 130 F.
8. None of the Emergency Cooling Systems in  
the Containment System functions. The  
only heat by conduction in the sinks and  
convective cooling of the containment vessel  
insulated surface by natural convection  
air at an ambient temperature of 130 F.

#### 13.5.1.7.3 Results of Initial Release

Total pressure in the containment volume (steam pressure plus air pressure) vs time is shown in Figure 13-40. The pressure rises to a peak of 188.5 psig at 10 sec, the end of blowdown, and then decreases as the heat sinks absorb energy. At approximately 4-3/4 hr, the pressure begins to increase from a minimum of 51.1 psig because the decay heat rate plus the heat generated by the primary system components is greater than the heat transfer rate out of the containment vessel or to the internal heat sinks. The study was terminated at a time approximately 12-1/2 hr after the accident. At this time the containment pressure was 58.6 psig and increasing at a constant rate of 1.3 psi/hr.

#### 13.5.1.7.4 Pressure Suppression Systems

The post-MCA containment pressure can be reduced by the following four independent methods:

1. The normal fresh water containment-cooling coils.
2. The sea water emergency containment-cooling coil.
3. Water spray into the top of the containment.
4. Heat removal through the containment shell by partial flooding of the lower reactor compartment.

Although it is considered credible that one of these methods could be rendered partially or completely ineffective, it is not considered credible that all of them would be simultaneously incapacitated. Each of the methods is discussed to illustrate the potential pressure suppression capability. The expected long-term effects on the pressure transient are then described by assuming the availability of

a portion of the installed capacity. Analyses show that the necessary pressure suppression may be accomplished by any of the methods investigated.

These analyses indicated that one effective cooling coil will provide suppression of 34 psi at 2 hours, 100 psi at 12 hours, and 170 psi at 24 hours after the MCA.

Calculations indicate that less than half of one effective coil will limit the containment pressure to 600 psig after 2 hours, and that limiting the pressure to 35 psig after 2 hours requires from 1.25 (at 2 hours post-MCA) to 0.5 effective coils (at 14 hours after MCA).

A spray rate of 10 gpm provides 22 psi suppression at 2 hours, 92 psi at 12 hours and 170 psi at 24 hours. A spray rate that varies from 6.0 to 4.7 gpm will limit the containment pressure to 60 psig from 2 to 24 hours after the MCA. To maintain the pressure at 35 psig, the required spray rate varies from 19.0 gpm at 2 hours to 7.0 gpm at 24 hours after the MCA.

The data for pressure suppression as a function of the cooling water level outside the containment vessel shows that a cooling water height of 3 feet provides suppression of 50 psi at 8 hours, 84 psi at 12 hours and 161 psi at 24 hours after the MCA. A cooling water height of about 1.75 feet will limit the pressure to 60 psig between 8 and 24 hours after the MCA. To obtain a pressure of 35 psig over the same period, the water height would have to be greater than 5 feet at 8 hours, and about 2.9 feet at 24 hours.

Cooling by natural circulation of the containment atmosphere across one containment cooling coil limits the pressure to about 66 psia (51 psig) during the

interval from 4 to 24 hours after the MCA.

Spray cooling through the CO<sub>2</sub> lines and nozzles will reduce pressure to about 35 psig within 4 hours and to about 2.5 psig within 24 hours after the MCA.

Table 13- 6 summarizes the pressure suppression information by listing the containment pressures at 2, 8, and 24 hours after the accident.

Table 13- 6 Summary of Potential Pressure Suppression Effects

<u>Pressure suppression mode</u>	<u>Containment pressure, psig</u>		
	<u>2 hours</u>	<u>8 hours</u>	<u>24 hours</u>
Cooling with 1 coil	38	26	17
Cooling with 2 coils	25	13	7
Spray beings at 100 psig	48	18	2
Flooding to 4.97 ft. level	72	16	6

### 13.5.1.8 Environmental Analysis

#### 13.5.1.8.1 Shipboard Radiation Levels

A calculation was conducted to determine the dose rate vs. time following the MCA at various important locations throughout the ship. The following work was accomplished in order to produce realistic predictions:

1. The time-dependent fission product leakage to the containment vessel was obtained from the results of a NURLOC run used in the evaluation of the MCA.
2. The intensity of the fission product sources external to the primary shield and within the containment was determined by evaluation of the fission product leakage rate, isotopic decay rates, and ORNL test data relative to plate-out and washdown of high burnup UO<sub>2</sub> fission products.

3. The time-dependent source within the reactor compartment and filters was determined from the measured containment vessel leakage rate and filter efficiencies, and actual plate-out test data of high burnup  $UO_2$  fission products.
4. The dose rates at the specified ship's locations were calculated by attenuation of the time-dependent spatially uniform sources in the primary coolant at the bottom of the containment vessel.

The results of these calculations indicate that there will be no significant interference with the required post-MCA operations due to excessive radiation.

### Results

Figure 13-41 shows the dose rate versus time in the forward control area. This area would receive the maximum potential dose since it is close to the reactor containment and also contains the iodine filters. On the basis of Figure 13-41, periodic entry to the forward control area could be accomplished, if necessary, for the first two hours after the accident.

Figure 13-42 shows the dose rate versus time for the main control center. Figure 13-42 indicates a maximum dose rate of 90mr/hr. This would allow the necessary manning of the controls without excessive exposure.

Figure 13-43 shows the dose rate versus time in the emergency generator room, which contains the alternate engineering control console. The average dose rate for the first 10 hours is approximately 15 mr/hr. Thus, manning of this area by a single individual for 10 to 20 hours is feasible.

Figure 13-44 shows the dose rate for the main navigation bridge area. The integrated dosage for 2 hours is approximately 200 mr. It is apparent that there will be no excessive exposure to the personnel on the bridge during the removal of the ship to the remote anchorage.

Figure 13-45 shows the dose rate versus time at the forward bulkhead of the engine room. With an average dose rate of about 1 r/hr, periodic access to this area can be allowed, but under strict health physics control.

### Conclusions

It is concluded that the ship could be moved to a remote anchorage without excessive exposure to the necessary crew members. Thus, the proper execution of emergency ship removal plans to protect the general public in accordance with accepted port plans can be ensured.

#### 13.5.1.8.2. Basis for Evaluation of Public Exposure Following the MCA

The evaluation of doses external to the ship following the MCA are based on the following conservative assumptions.

#### Plate-out and Washdown Within the Containment Vessel

It is assumed that 50% of the halogens released to the containment plate-out within the vessel. Little data are available on this effect, but it has been estimated that the removal of airborne iodides by various physical phenomena such as absorption, adherence, and settling could reduce the effective concentration by a factor between 3 and 10. An additional reduction would be expected from the effects of washdown by steam condensing on the cooler surfaces and in the cooling coils of the Containment Cooling System, but this effect is neglected.

## Leakage From the Containment Vessel

It is assumed that the free fission products within the containment vessel leak out into the surrounding reactor void compartments at the rate of 1.5% per day. This assumed leak rate is more than the leak rate determined from current tests at 60 psig. In all probability, the containment vessel pressure will be maintained considerably below 60 psig after the initial pressure peak.

## Fission Product Depletion Within the Reactor Compartment

No plate-out or holdup is assumed outside the containment vessel. Leakage from the containment is expected to be in the form of a number of small leaks through fittings randomly distributed over the containment surface. Under these conditions the reactor compartment would act as a holdup chamber serving to reduce the activity of isotopes with relatively short half-lives (Kr-88, I-135). This factor is of particular importance in the early stages of the accident, when fission products contain a high proportion of short-lived isotopes.

## Filter Effects

All gases exhausted from the reactor compartment pass through one of the duplicate particulate and iodine filters before discharge to the atmosphere. The filters are arranged so that one of the filter systems is normally in use, and the other system in on standby. In the event of an MCA, procedures require the operator to switch to the standby filter system, thus ensuring that an unused filter is on the line.

Fission product removal by the filters is assumed to be 99% efficient for the halogens and 99.9% efficient for solid aerosols. The filters are routinely tested for aerosol removal capability before the ship enters port, and the required efficiency is easily maintained. The more important effect is the iodine removal efficiency, which is demonstrated to be better than 99.9% in tests at intervals of approximately 90 days. Thus, a factor of at least 10 exists between the expected iodine removal efficiency and the value used for environmental release calculations.

### 13.5.1.8.3 Atmospheric Dispersion

The activity passing through the filters discharges from the exhaust stack 90 feet above sea level and disperses downwind. Atmospheric dispersion is assumed to occur according to Sutton's ground-reflected diffusion equation. In using this relationship, it is assumed that fission product release occurs at ground level and that the meteorological parameters used correspond to an inversion condition with a slow dispersion rate. Wind meandering might result in a further reduction factor of approximately three when calculated over a period, but no credit is taken for this.

The form of Sutton's equation and the values of the various parameters used in calculations are as follows:

$$X_{d,y,z} = \frac{20 \exp - d^{n-2}}{C_y C_z U d^{2-n}}$$

where

- X = concentration, curies/m<sup>3</sup>
- d = downwind distance, meters
- Q = release rate from stack, curies/sec.
- n = stability parameter - 0.50
- C<sub>y</sub> = horizontal diffusion coefficient = 0.40  
(meter) n/2
- C<sub>z</sub> = vertical diffusion coefficient = 0.07  
(meter) n/2
- U = average windspeed - 1.0 meter/sec

No credit is taken for the time that elapses between release from the stack and arrival at the downwind point of consideration. Since the point of consideration is assumed to be on the plume centerline, y and z are both zero. At wind speeds greater than the assumed 1 meter per second, the cloud dilution is proportionately increased.

#### 13.5.1.8.4 Environmental Hazards Evaluation

##### Introduction

The dose that a member of the public could receive at some downwind location is calculated using the Sutton diffusion equation. Two types of dose are of prime interest. They are:

1. Gamma dose to the whole body due to submersion in the cloud containing the fission products.
2. Dose to the thyroid due to inhalation of radioactive iodine.

The gamma dose due to material on board the ship and the gamma dose due to particulate matter in the cloud are negligibly small for the general public. The whole-body beta exposure from submersion in a radioactive cloud does not contribute significantly to the emergency.

##### Whole Body Gamma Dose

Calculations of the whole body gamma dose are based on a summation of contributions from krypton and xenon isotopes. Previous calculations have shown that whole-body doses from other fission products are negligible. The concentration of gaseous fission products at any point downwind from the release point is determined by Sutton's diffusion equation. The

gamma source strength due to these isotopes is taken from Bloemke and Todd. Since an infinite cloud model is used, it is assumed that the observer absorbs the gamma energy generated in the volume he occupies and that this energy absorption is converted to whole-body gamma dose units.

#### Thyroid Dose

In calculation of the thyroid doses, it is assumed that the observer is breathing at a rate of 30 cubic meters per day for periods up to 12 hours per day, and 20 cubic meters per day for a whole-day average. Decay of individual iodine isotopes is considered to occur only up to the time of release of the isotope from the containment. The concentration of individual isotopes at some downwind distance is based on Sutton's diffusion equation. The calculated thyroid dose results from a summation of contributions from the isotopes I-131 through I-135.

#### Dose Limits

The dose limits adopted are 25 rem to the whole body and 300 rem to the thyroid. These limits correspond to the once-in-a-lifetime accidental or emergency dose for radiation workers. According to recommendations of the National Committee on Radiation Protection, these doses may be disregarded in the determination of the radiation exposure status of radiation workers. However, these numbers are not construed to be acceptable emergency doses to the public, but are taken as reference values for accidents having an exceedingly low probability of occurrence and are used in establishing controlled zones and acceptable evacuation capabilities.

### 13.5.1.8.5. Environmental Zoning

#### Zone Definition

In accordance with guidelines (Calculation of Distance Factors for Power and Test Reactors, U. S. Atomic Energy Commission report TID-14844) and requirements (Reactor Site Criteria, Part 100 of Title 10, Code of Federal Regulations) all ports at which the N.S. SAVANNAH calls are surveyed prior to entry to establish certain zones at the berth and the remote anchorage so that the health and safety of the public will be properly protected. These zones are defined as follows:

Controlled Zone is that area, defined by fences, ocean fronts, bays, or other barriers, either natural or man-made, in which all persons are under the direct control of ship's personnel and local authorities so that, in the event of the occurrence of the MCA to the N.S. SAVANNAH, evacuation could be effected in a graded fashion within 2 hours so that no member of the public inside the zone would receive an exposure exceeding a 25-rem-whole-body dose or a 300-rem-thyroid dose, and no individual member of the general public at the outer boundary of the zone for 2 hours would receive an exposure exceeding a 25-rem-whole-body dose or a 300-rem-thyroid dose.

Low-Population Zone is that area which is immediately adjacent to the outer boundary of the low-population zone and cannot be evacuated, controlled, or protected. In the event of the occurrence of the MCA, the total integrated population exposure to all persons in this zone plus the controlled zone and the low-population zone will not exceed 2,000,000 man-rem.

Remote Anchorage is that area to which the ship may be removed after the occurrence of the MCA. A remote anchorage shall be deemed acceptable only if the stricken vessel may be anchored there for 30 days and the following zones can be readily established around the stricken vessel:

1. An uninhabited controllable exclusion zone through which no ship or member of the general public must pass except under the strict control and monitoring of the emergency team.<sup>2</sup>
2. A zone that encompasses an area that can be evacuated within 24 hours. This zone has a sufficient radius so that a person on the perimeter for 30 days would not receive more than a 25-rem-whole-body dose or a 300-rem-thyroid dose.
3. To ensure appropriate limitations to long term effects on the population as a whole, a surrounding zone that has a limit of 2,000,000 man-rem-whole-body dose to total population assuming the duration of the radioactive release to continue for 30 days.

#### Power Inventory and Zone Size

In order for the berth to be accepted as a suitable reactor site, a maximum permissible fission product inventory must be established for the ship's reactor so that the following limitations will not be exceeded in the event of the MCA:

1. A series of maximum exposure zones must be considered. These zones are circular in shape and concentric with the nuclear reactor and have radii so that after the occurrence of the MCA no person at the outside boundary would receive more than a 25-rem-whole-body dose or a 300-rem-thyroid dose in the period of time associated with the exposure zone. The dose

considered in determining the radius is that associated with the centerline of the radioactive plume being discharged from the fore-topmast of the ship. The zones considered are the:

1-hour zone  
2-hour zone  
24-hour zone  
30-day zone

The radii of these zones vary with the actual fission product inventory of the reactor.

The 1-hour zone is established while the ship is either underway or moored and has two or more tugs under power in attendance at the ship. External conditions must not prevent movement of the ship.

The 2-hour zone is established while the ship is not attended by at least two tugs either at a mooring location or while underway. The 2-hour zone must always fall entirely within the confines of the controlled zone established at the berth or for the underway condition.

The 24-hour zone is established while the ship is in port at its berth. This zone must fall entirely within the confines of the low-population zone.

The 30-day zone is established around the ship at the remote anchorage. This zone is defined as the circular area that is concentric with the nuclear reactor and has a sufficient radius so that no person at the perimeter would receive more than a 25-rem-whole-body dose or a 300-rem-thyroid dose in a period of 30 days after the occurrence of the MCA. This zone must be evacuable within 24 hours.

2. The total integrated population dose shall not exceed 2,000,000 man-rem. This dose is calculated for the 30-degree dense population sector that would receive the highest integrated dose in 24 hours and also included an arbitrary 25-rem dose in 24 hours for the maximum number of persons allowed in the 24-hour zone.

The hazard to the public for both the fuel shuffling at Galveston, Texas and sea trial operations are summarized in Table 13-7. Sea trials environmental analysis calculation is based on 55% fission product inventory.

Table 13-7 Summary of Environmental Analysis

	<u>Thyroid Dose, Rem</u>	<u>Noble gas Dose, Rem</u>	<u>Total Integrated Populated Dose, Man-ReMs</u>
MCA, Fuel Shuffle	33.2	0.46	90,500
MCA, Loss-of-Coolant	3.0	0.43	84,980
10 CFR 100 Criteria	300	25	2,000,000

13.5.2. Effect of Shuffled Core on Loss-of-Coolant Accident

Core shuffling results in a power distributions from Core I. This section presents the results of analysis work performed to determine whether the conclusions of Section 13.5.1. are still valid for the shuffled core power distributions.

Two cases of power distribution were studied, 2000 EFPH (Case 1), and 7000 EFPH (Case 2).

In this section, the major results of Section 13.5.1 with Core I are listed and the changes in each result produced by the shuffled core and the reasons for these changes are presented.

1. The piping break which resulted in the highest fuel temperatures at the end of blowdown was the double-ended break of the primary inlet line. Blowdown of the pressure vessel was complete at 10 sec. The results of this blowdown analysis were used to continue the study of fuel element heat-up and slumping.
2. The piping break which caused the maximum hydraulic loading of the pressure vessel internal structures was the single-ended break of the primary inlet line. The results of this analysis were used to determine the mechanical integrity of the conical support ring and some distortion but no failure of the lower flow baffle. Failure of the conical support ring would result in little movement of the core structure due to the proximity of the flow baffle to the pressure vessel. The failure would not affect subsequent flow through the core or core reactivity.

The above results involve the blowdown phase of the accident and are either independent of core characteristics or are affected by core average behavior only. Since the average core power is not changed by the core shuffle, the above results are not affected.

3. The fuel heat-up and slumping study indicated slumping initiated at approximately 1180 sec following the start of the accident. Slumping proceeded in a linear manner until the end of the analysis, at 3995 sec, at which time approximately 25% of the core had melted.

Fuel slumping initiated approximately 576 seconds for Case 1 (2000 EFPH) and 703 seconds for Case 2 (7000 EFPH). Slumping was assumed to proceed at the same rate as in Core I.

The reduced slumping times for the shuffled core are due strictly to the higher peaking factors. (The differences in average core decay heat rates due to the differences in

irradiation time are significant and a conservative operating history of infinite time at 80 MW (t) was used for all cases). The radial power profiles for Cases 1 and 2 are shown in Figures 13-46 and 13-47. The axial peaking factors are 1.693, 1.4 and 1.66 for Cases 1, 2 and Core I, respectively.

The effect of the power distribution on the peak fuel node temperature and relative heat generation following blowdown (average core temperature and decay heat following blowdown is the same for all cases) are shown in Table 13-8:

Table 13-8

<u>Case</u>	<u>Peak Fuel Node Conditions</u>	
	<u>Temperature F</u>	<u>Relative Heat Generation</u>
1	2270	1.25
2	2060	1.11
Core I	1895	1

The higher peak temperatures and heat generation rates result in the reduced time for the node to reach the slumping temperature.

Assuming a slumping rate equal to that of Core I for further calculations as described under Item 4 below is conservative since a higher slumping rate causes more rapid boil-off of the residual water and therefore results in earlier baffle melting and earlier desposition of the core on the lower vessel head. The actual slumping rates for Cases 1 and 2 would be lower than for Core I since the central core regions slump sooner (due to higher power densities) and the peripheral regions slump later (due to lower power densities).

4. The maximum reactor pressure vessel temperature reached was 1108 F. This temperature was conservatively based on deposition of the entire core on the reactor vessel bottom head at the time of failure of the flow baffle. This occurs at approximately 3800 sec - a time at which the analysis indicates less than 25% of the core has slumped. The reactor vessel heat transfer analysis assumed a ship list of 15° - the maximum design list. The stress in the vessel due to the weight of the molten core and all vessel internals was less than 55 psi. The 1000-hr creep rupture stress for carbon steel at 1000 F is 25,000 psi.

The maximum reactor pressure vessel temperature reached was 1116 F (Case 1) and 1113 F (Case 2). These temperatures were based on the same conservative assumption of deposition of the entire core on the reactor vessel bottom head at the time of failure of the flow baffle. A ship list of 15° was used in the heat transfer analysis. The vessel stress resulting from the weight of molten core and internals is unaffected by core shuffling.

Figure 13-48 shows the peak pressure vessel temperature plotted as a function of time for Cases 1 and 2 and the comparable case from Core I. These curves indicate the relatively minor changes in vessel temperature history due to the power distribution and earlier melting of the shuffled core. These curves were generated with the TIGER code. The only changes in the code input were the times of core deposition in the lower vessel head. Figures 13-49 and 13-50 show the spatial temperature distributions existing at t=600 minutes for Case 1 and 2, respectively.

The time for core deposition is the sum of a) the initial slumping time, b) the time to boil-off the residual water and c) the time to melt the lower flow baffle.

The sum of a and b, shown in Figure 13-51, are 1640 seconds for Case 1 and 1975 seconds for Case 2 as compared with 2780 seconds for Core I.

The time to melt the lower flow baffle was 690 seconds for Case 1 and 780 seconds for Case 2, compared with 1020 seconds for Core I.

The time for core deposition is, therefore, 2330 seconds ( ~38 minutes) for Case 1 and 2755 seconds ( ~45 minutes) for Case 2 as compared with 3800 seconds ( ~63 minutes) for Core I.

5. The peak containment pressure immediately following the accident was 188.5 psig which occurs at the end of blowdown (10 sec after the rupture). A minimum containment pressure of 51.1 psig is reached in approximately 4-3/4 hr after the accident. At 12-1/2 hr after the accident, the containment pressure had increased to 58.6 and was increasing at a constant rate of approximately 1.3 psi/hr.

This result is unaffected by core peaking factors since it is the average core power and power history which established the decay heat contribution to the containment energy and resultant pressure transient. Since the average core power is unchanged and the Core I containment energy considered decay heat, based on a history of two years at 80 MW (t), the shuffled core will cause no change in containment pressure history following the accident.

Based on the changes to the results as discussed above, it can be stated that the major conclusions established in Section 13.5.1. are valid for the shuffled core, that is -

1. The pressure vessel will contain the molten fuel following the loss-of-coolant accident.
2. The conical support ring is subject to failure under the hydraulic loading forces imposed by the loss-of-coolant accident.

Figure 13-1. Startup Accident - Total Reactivity

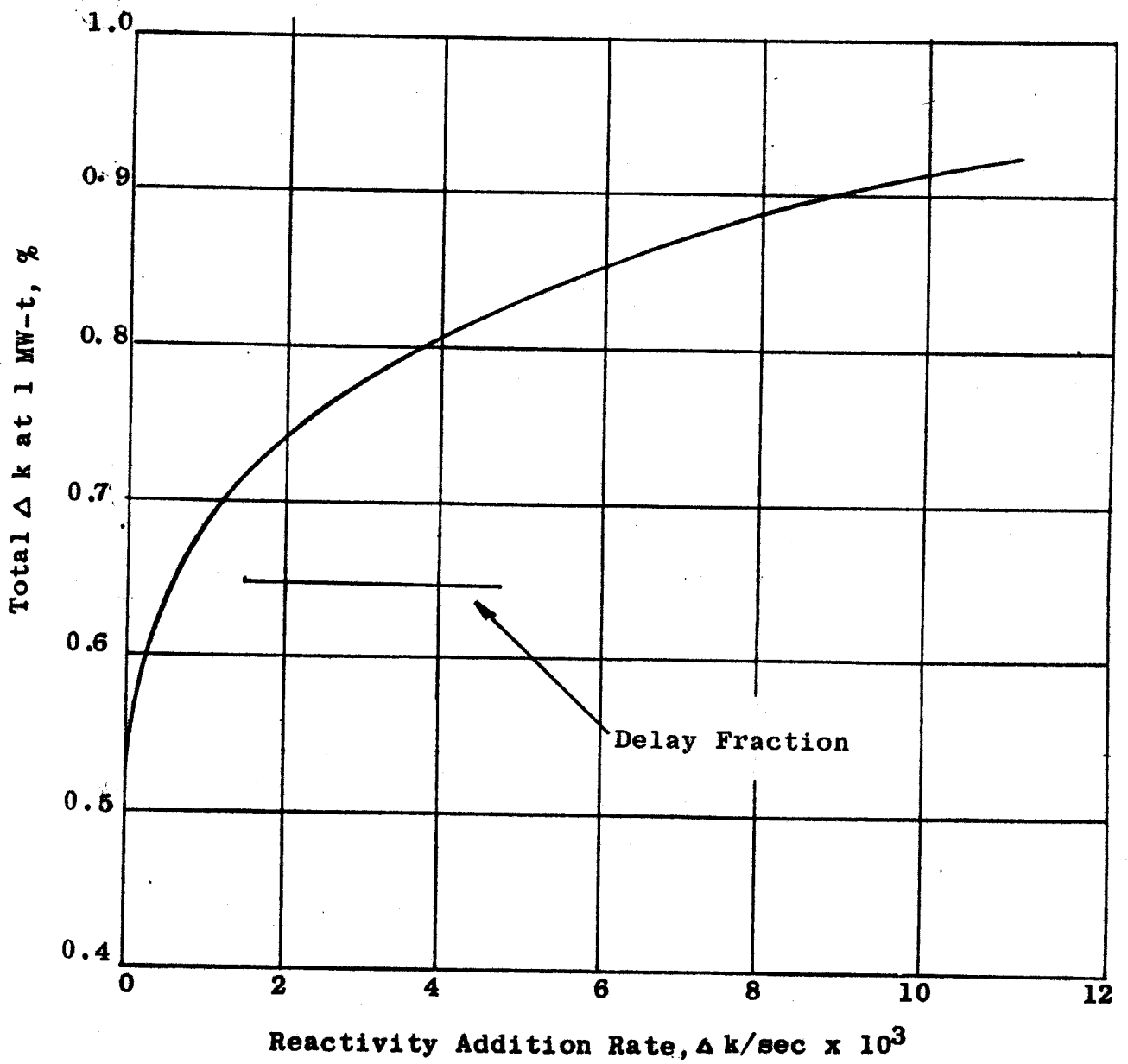


FIGURE 13-2. STARTUP ACCIDENT ( $4 \times 10^{-3} \Delta k/\text{SEC}$ )

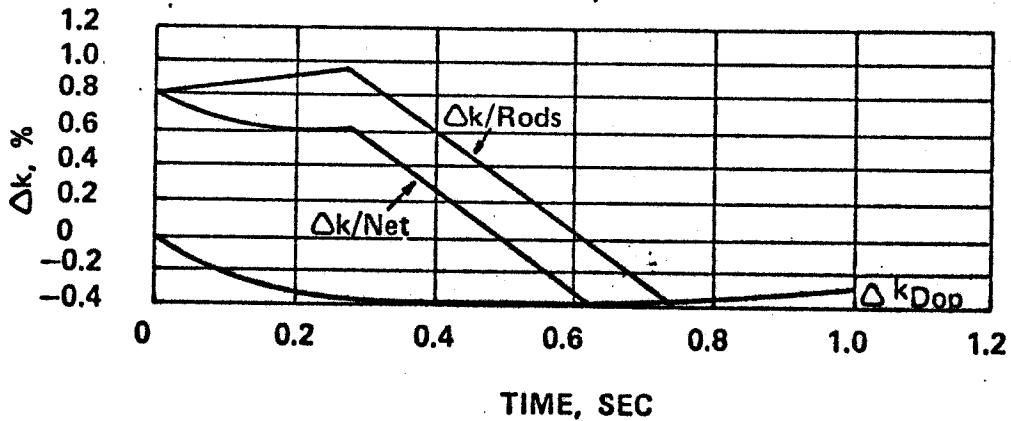
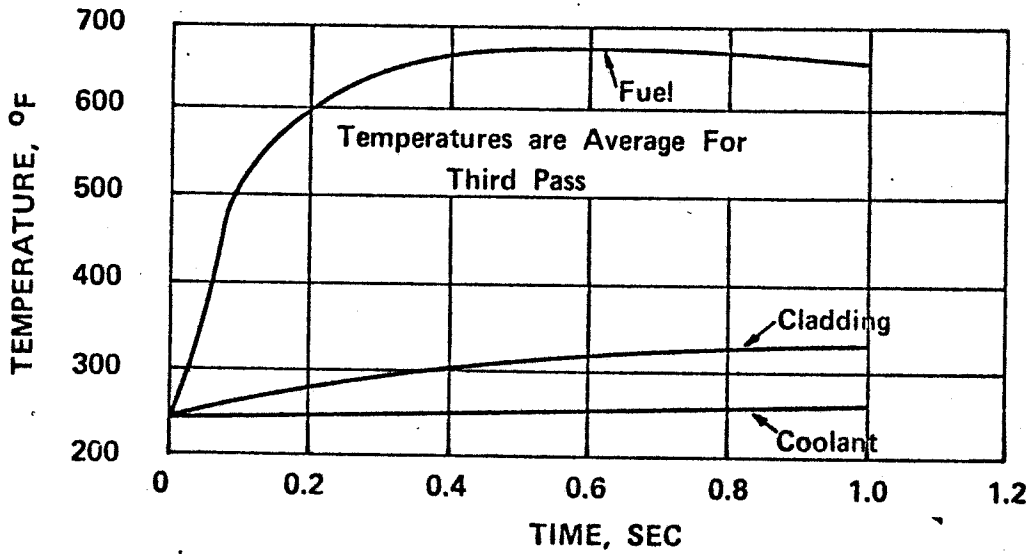
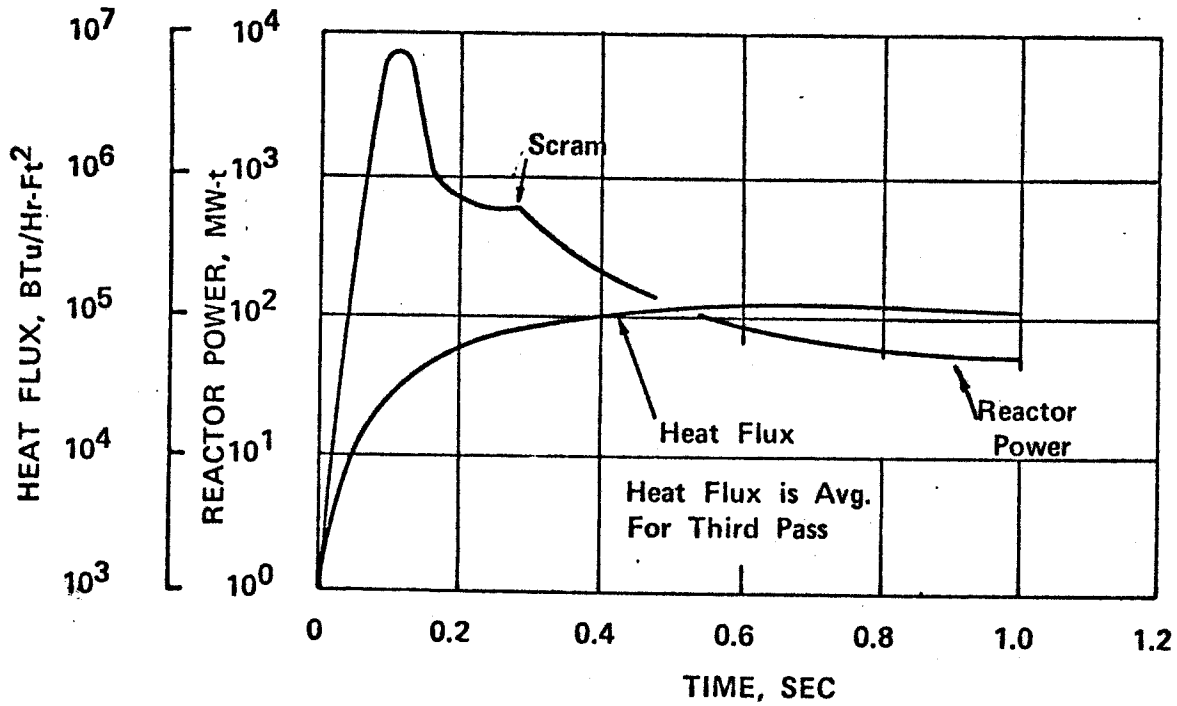


Figure 13-3 Startup Accident Peak Value Of Third-Pass Average Heat Flux

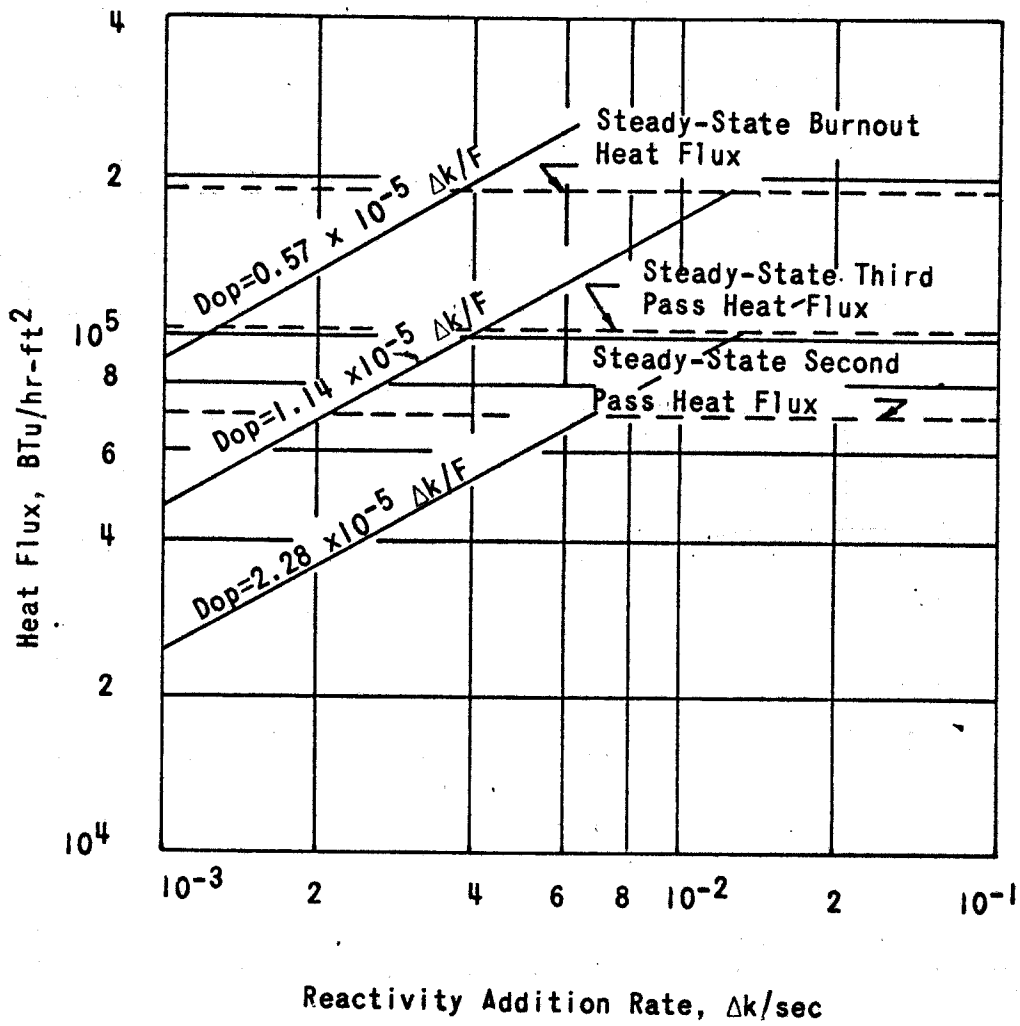


Figure 13-4 Startup Accident - Effect Of Control Rod Insertion Time On Third-Pass Avg. Heat Flux

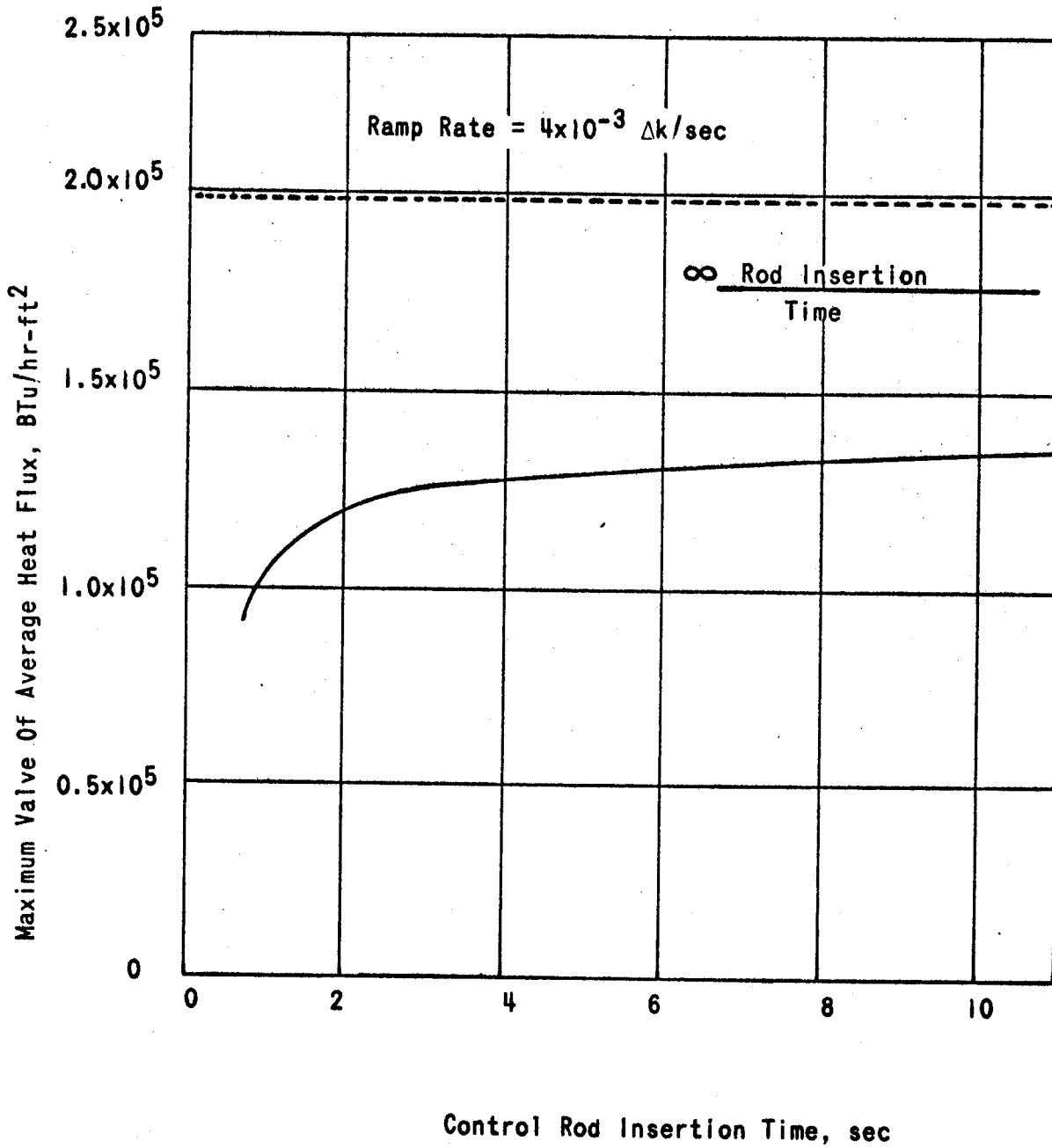


Figure 13-5. Rod Withdrawal Accident  
Peak Power Vs. Reactivity Addition Rate

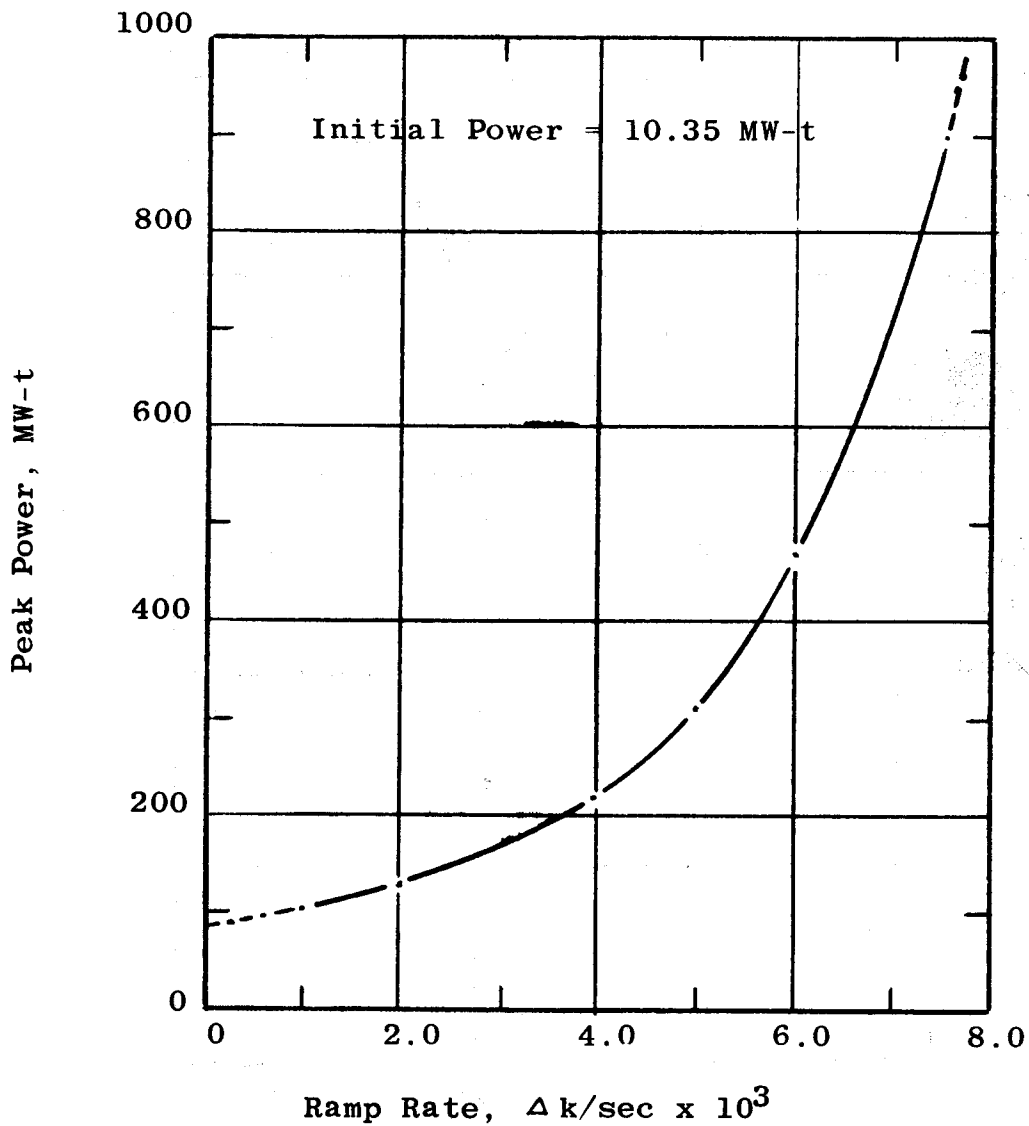


Figure 13-6 Rod Withdrawal Accident - Effect Of Initial Power Level On Third-Pass Avg. Heat Flux

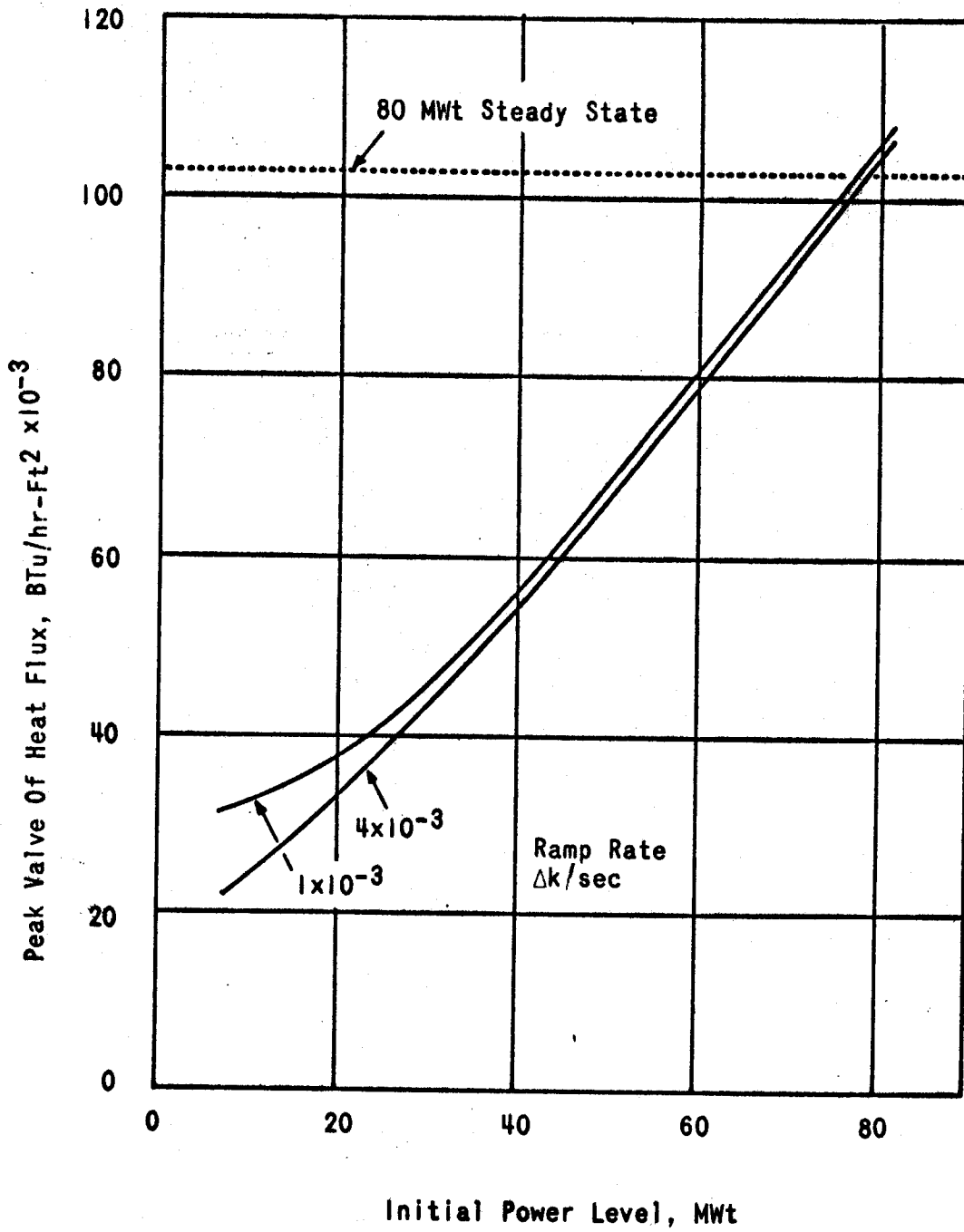


FIGURE 13-7 ROD WITHDRAWAL ACCIDENT EFFECT OF DOPPLER & MODERATOR TEMPERATURE COEFFICIENTS ON THIRD-PASS AVG. HEAT FLUX

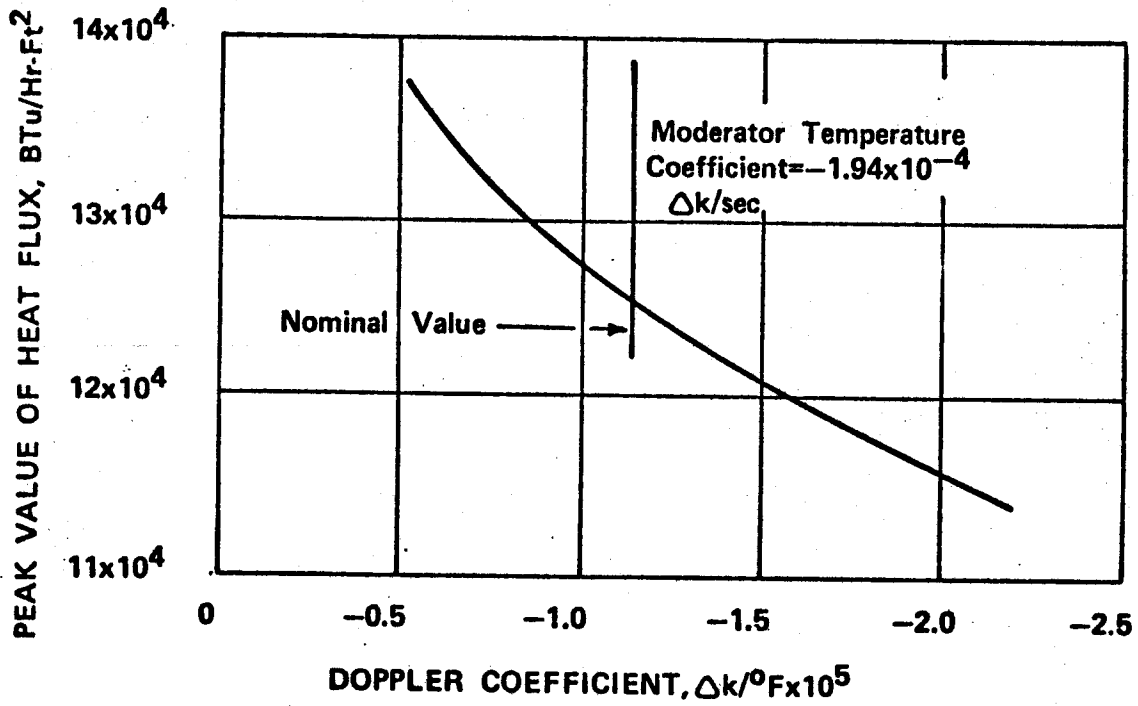
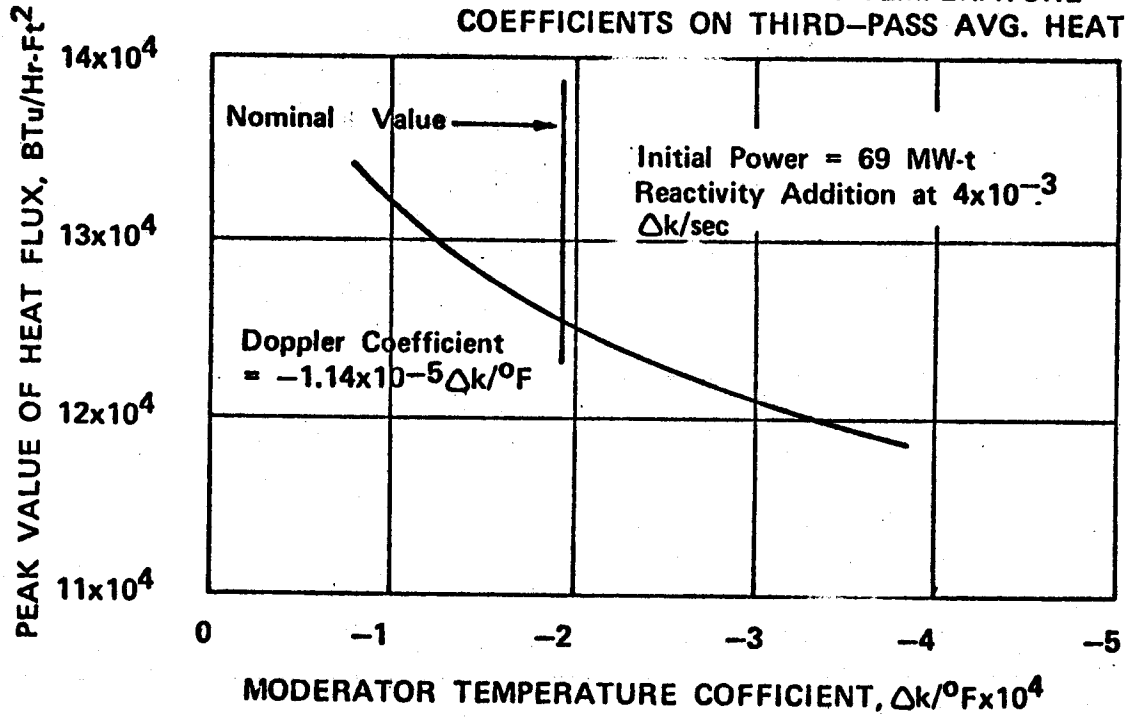


Figure 13-8. Rod Withdrawal Accident - Reactor Power Vs Time, 4 Pumps

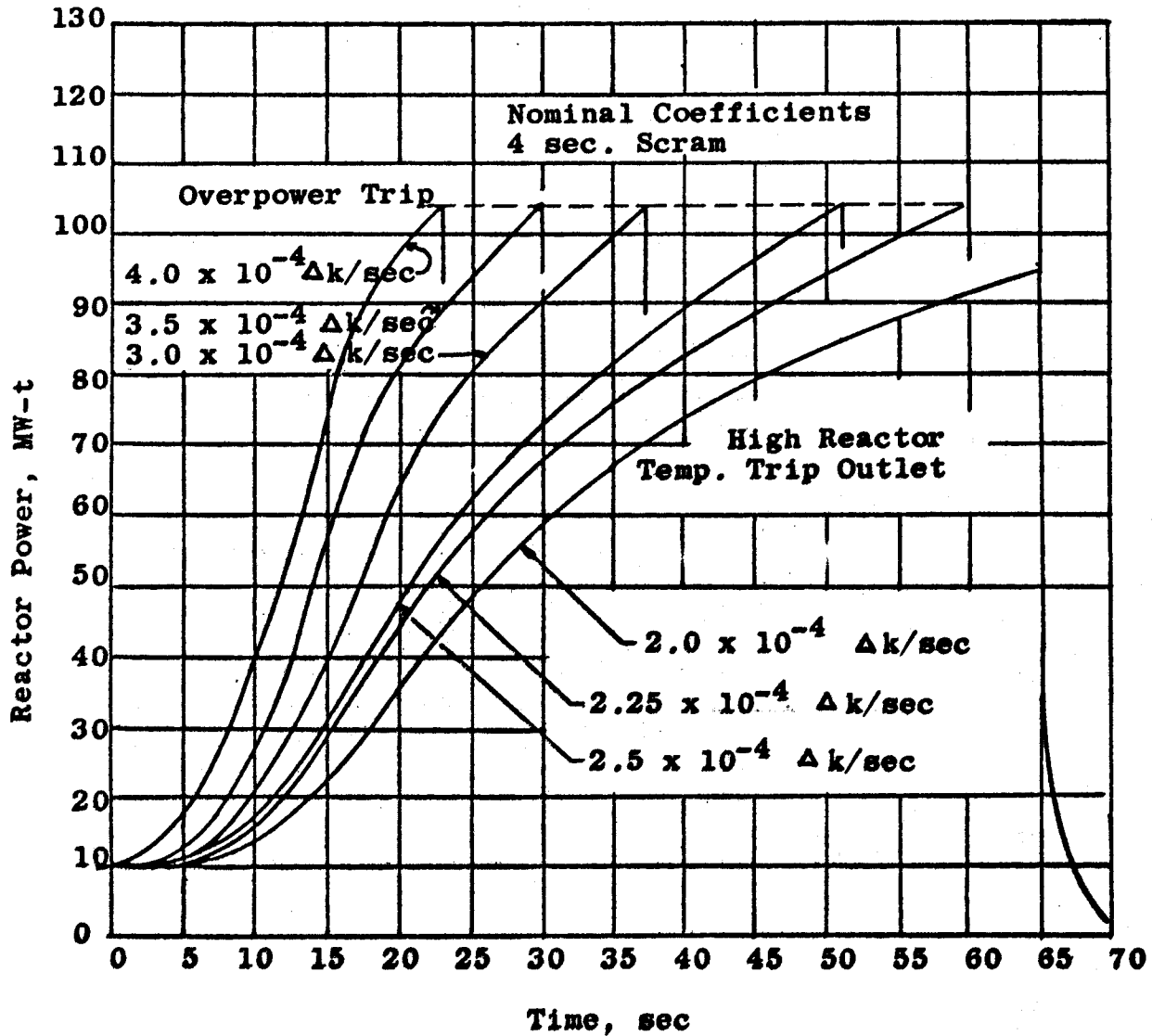


Figure 13-9. Rod Withdrawal Accident - Pressure Vs Reactivity Addition Rate, 2 Pumps

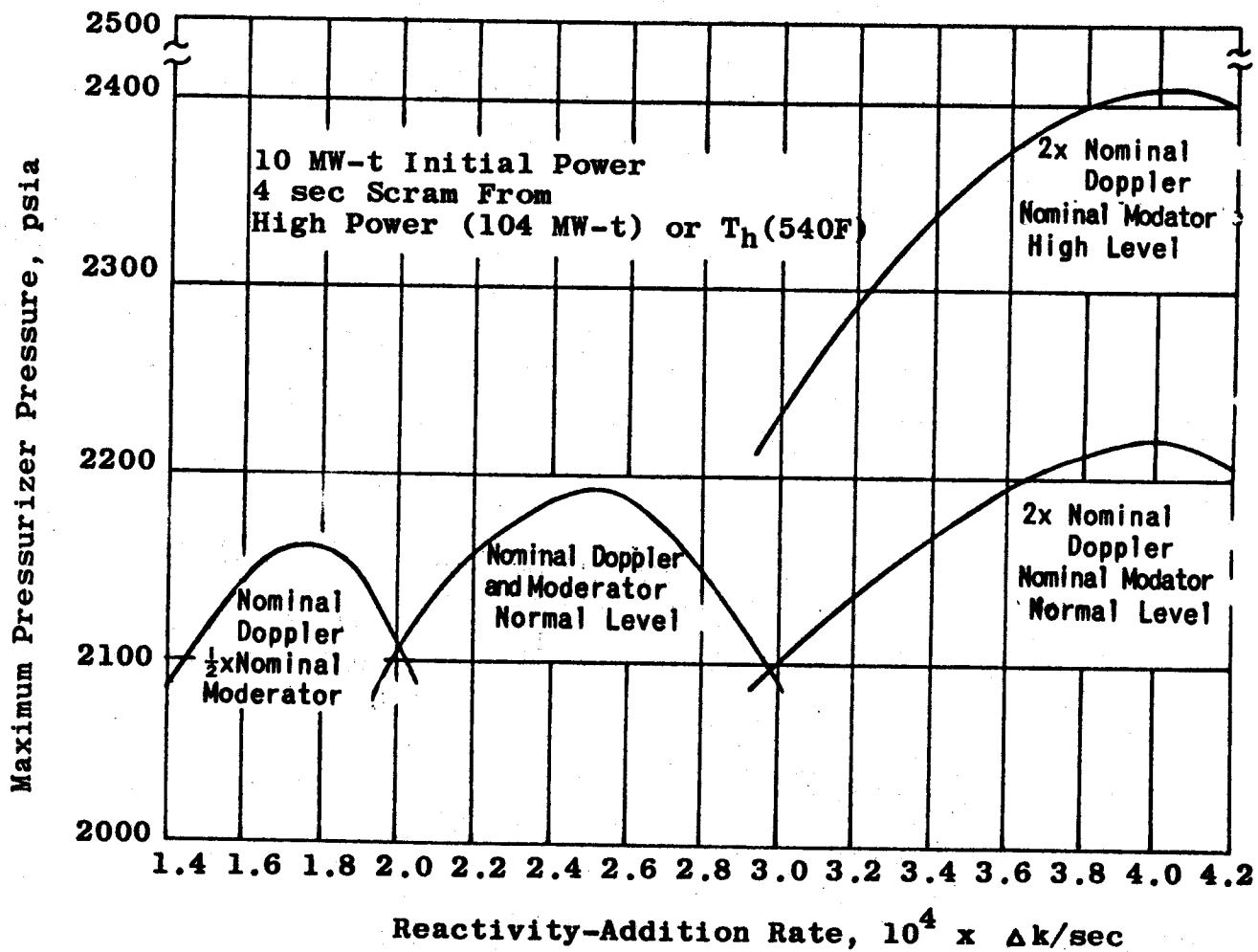


Figure 13-10. Rod Withdrawal Accident - Pressure Vs Time

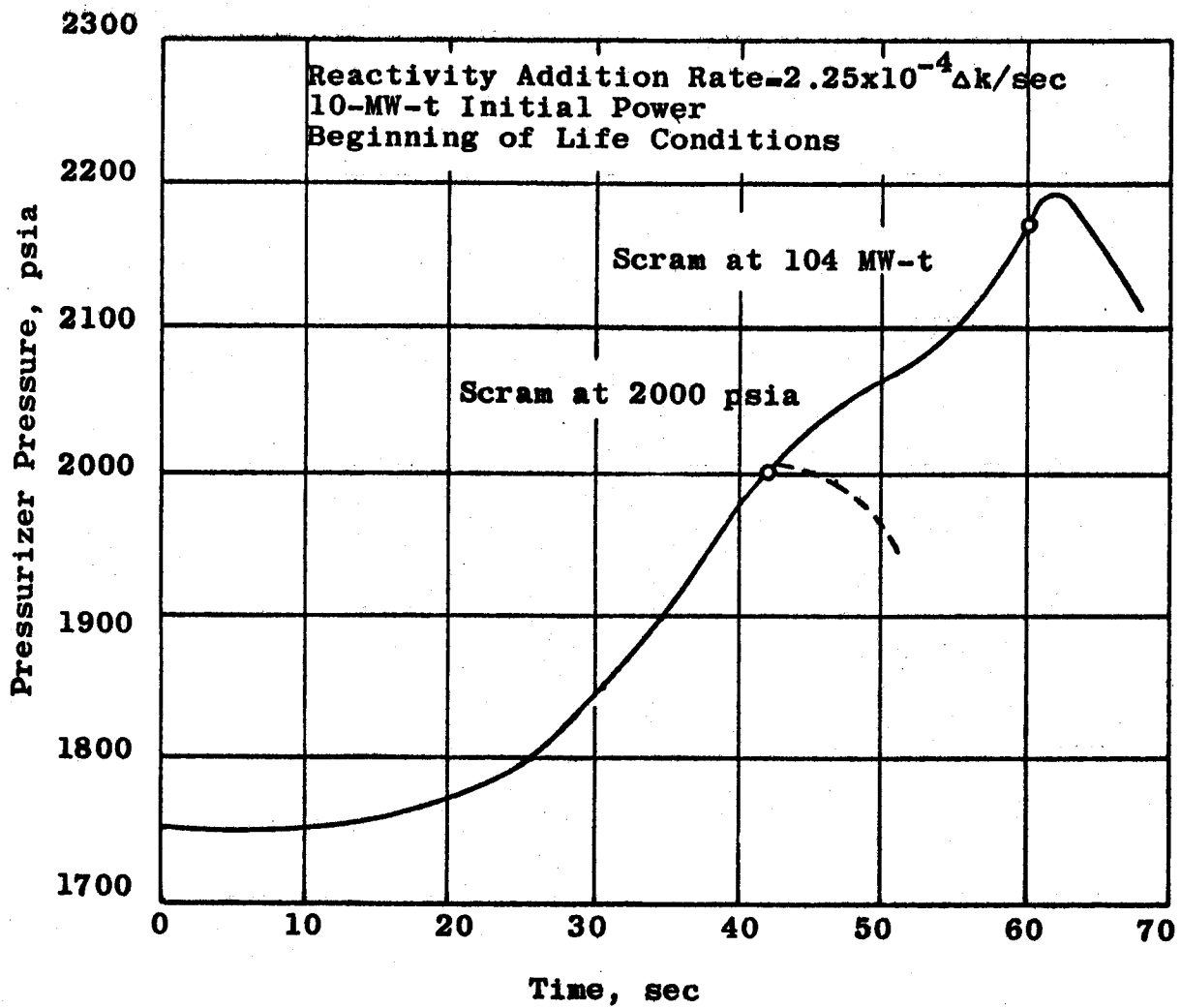


Figure 13-11. Reactivity Accident Verification

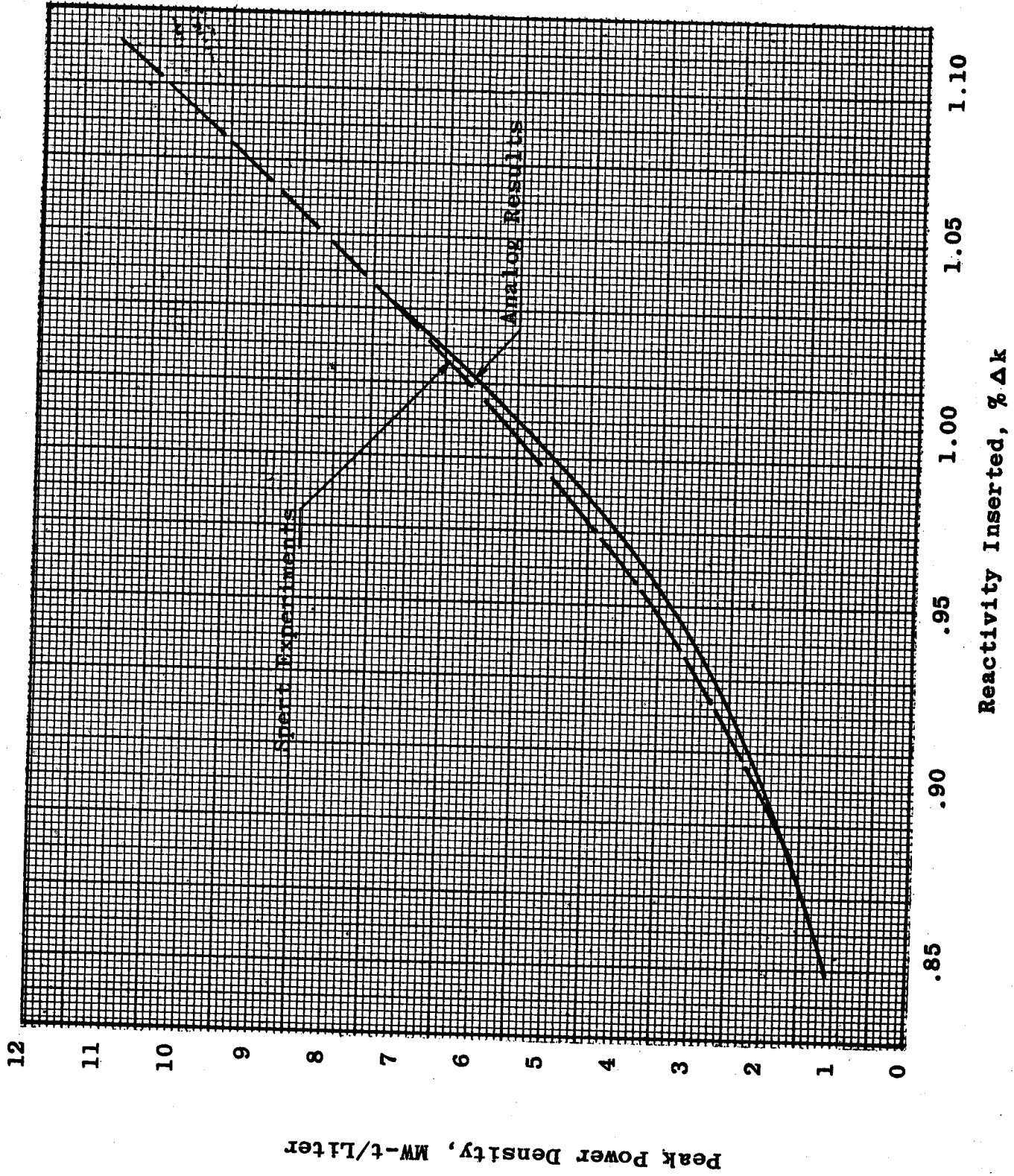


Figure 13-12. Reactivity Addition Accident -  
Experimental Vs Analytical Results

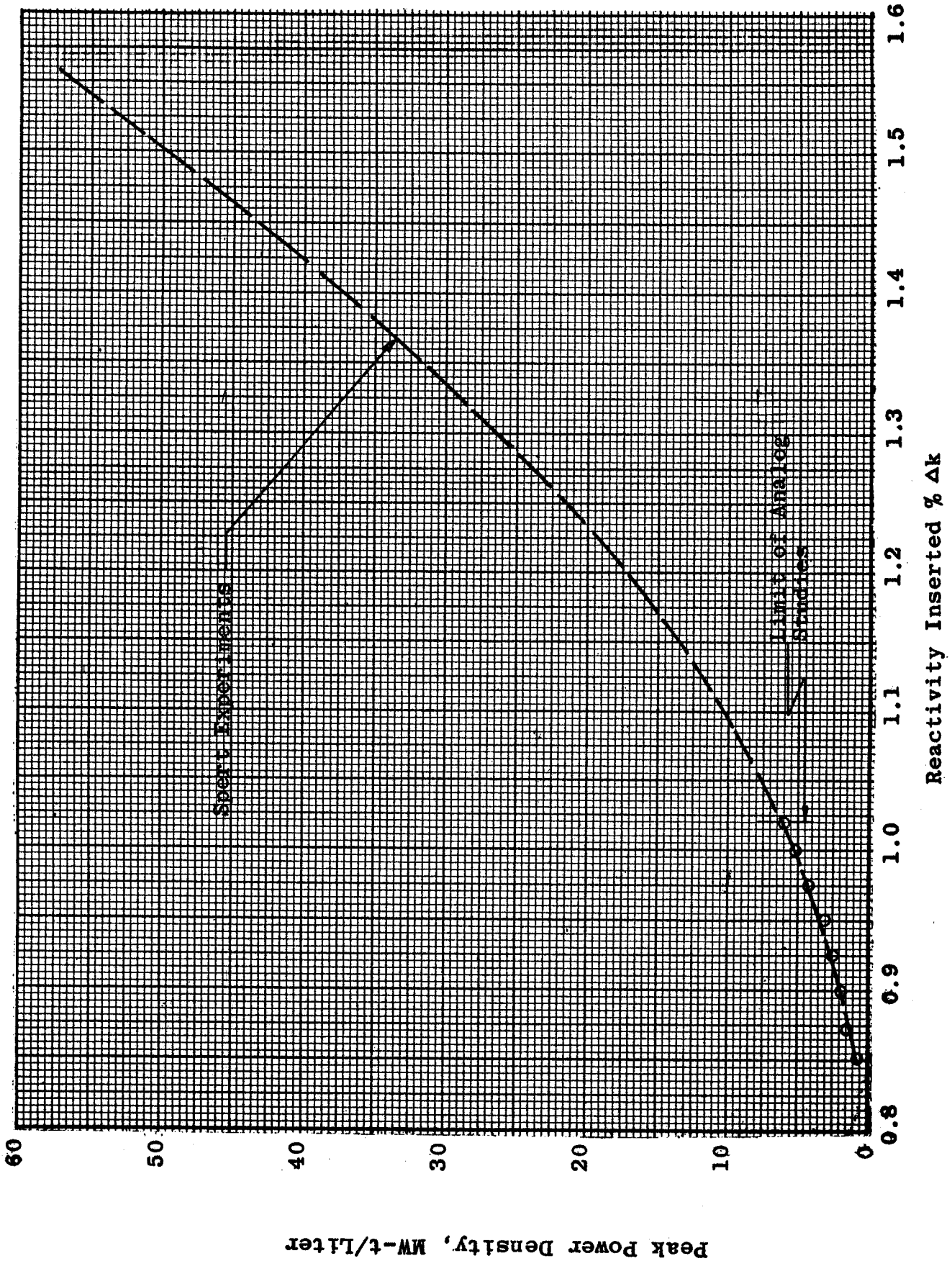


Figure 13-13. Cold Loop Startup Accident - Flow Transient Valve Limiting

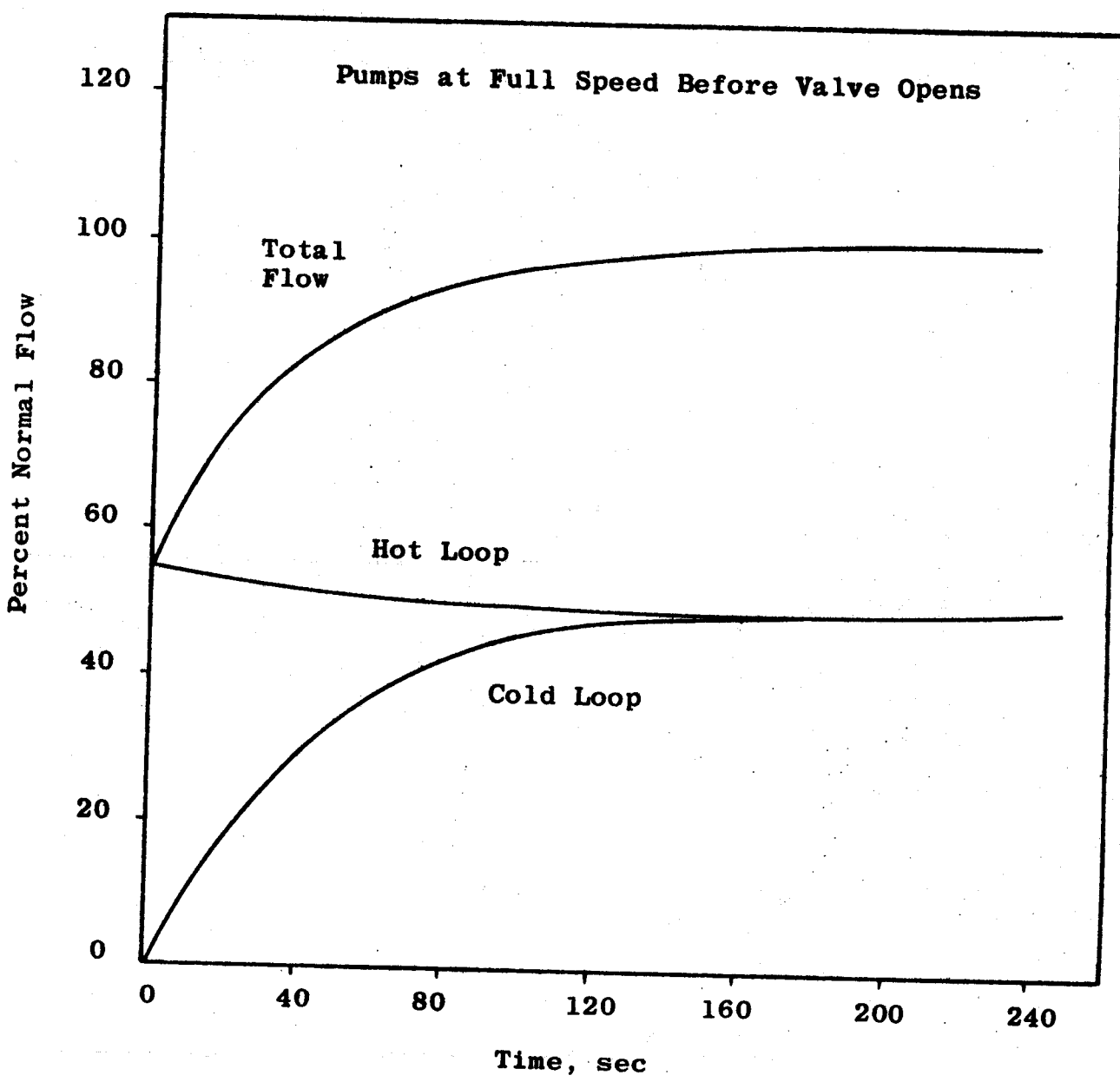


Figure 13-14. Cold Loop Startup Accident  
Flow Transient - Pump Limiting

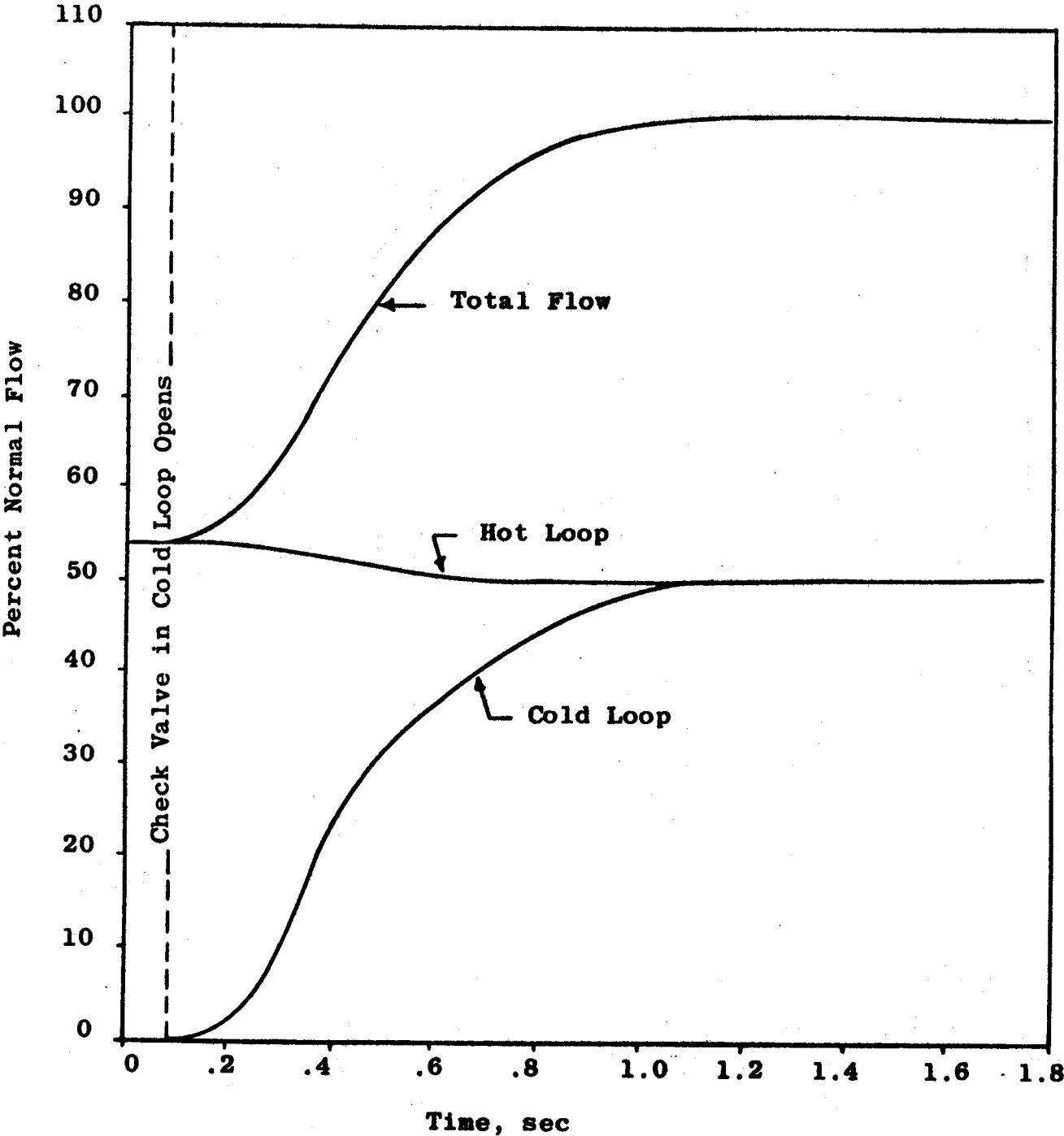


Figure 13-15. Cold Loop Startup Accident

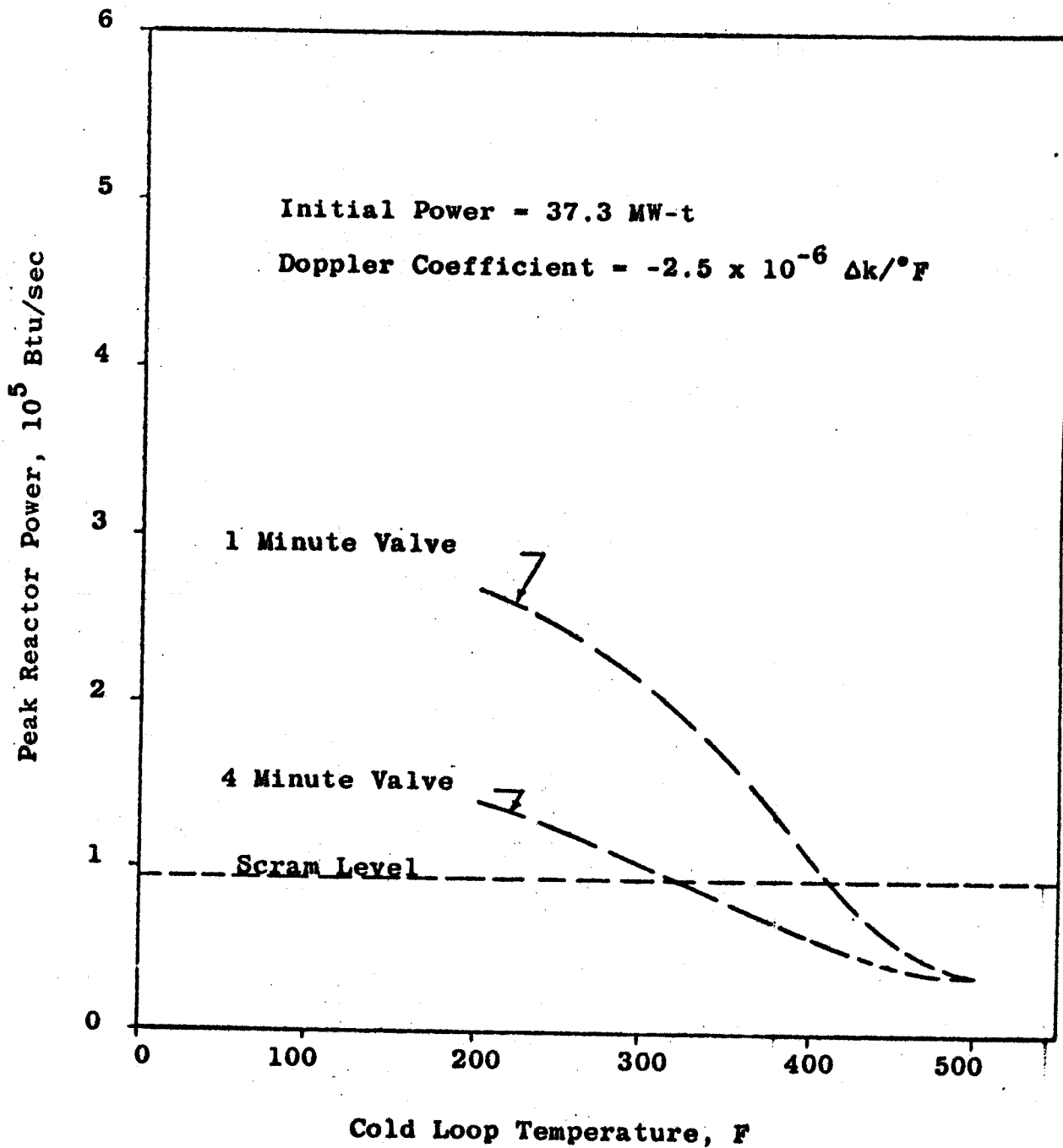
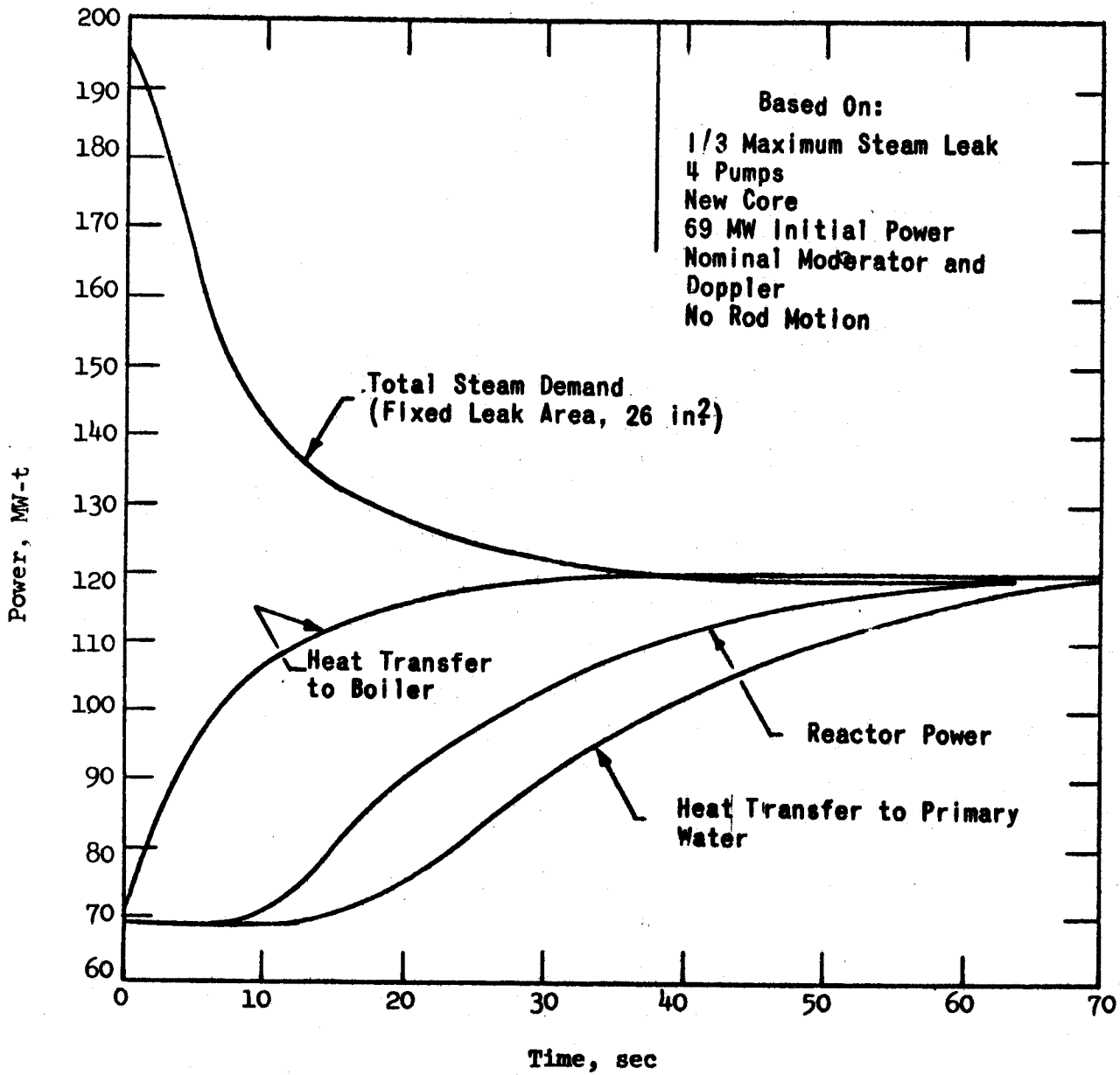


Figure 13-16. Steam Demand, Heat Transfer, and Reactor Power Vs. Time



**Figure 13-17. Primary and Secondary Temperature Vs. Time-  
Steam Leak**

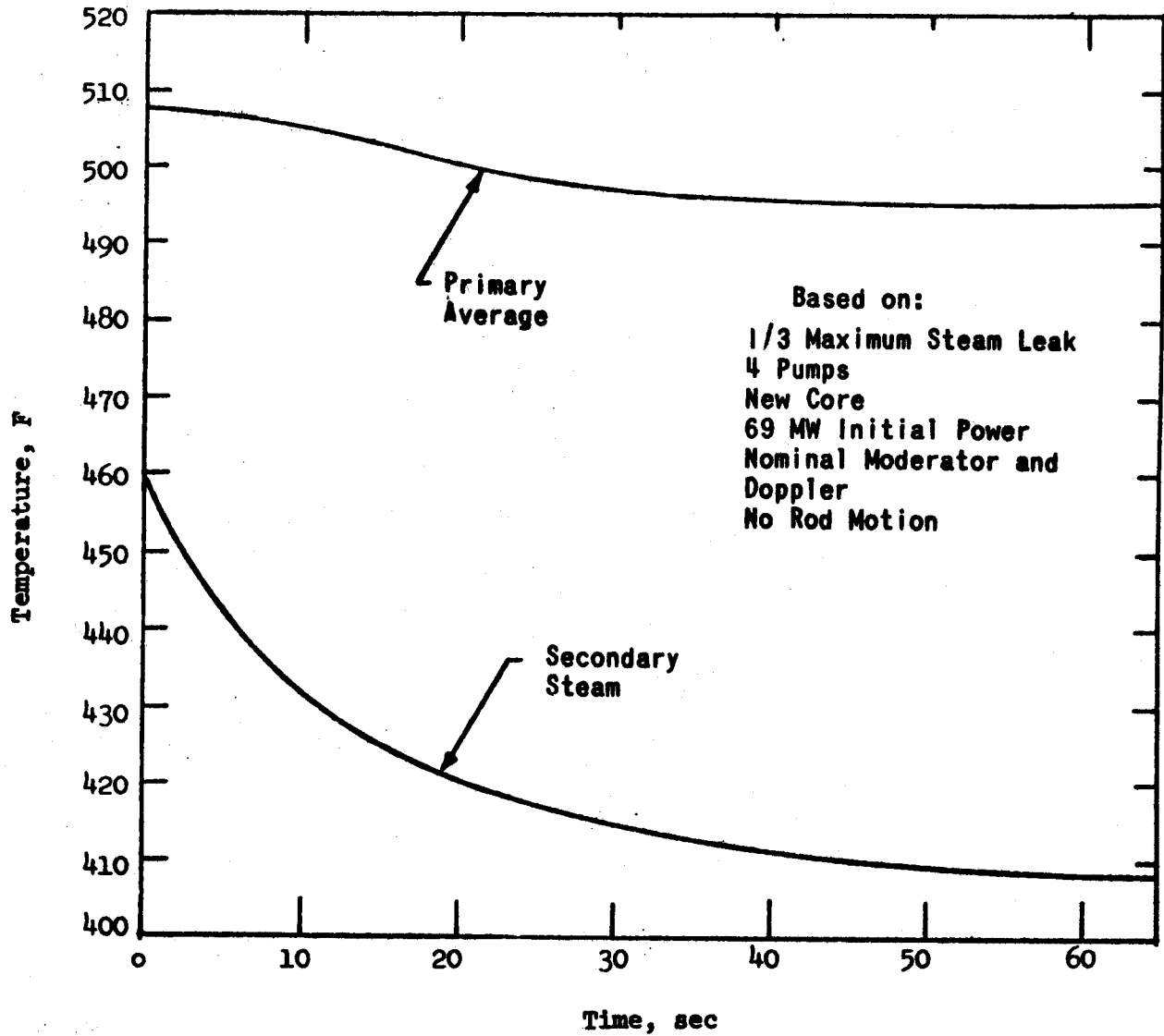


Figure 13-18 Maximum Reactor Power Vs Steam Leak Rate

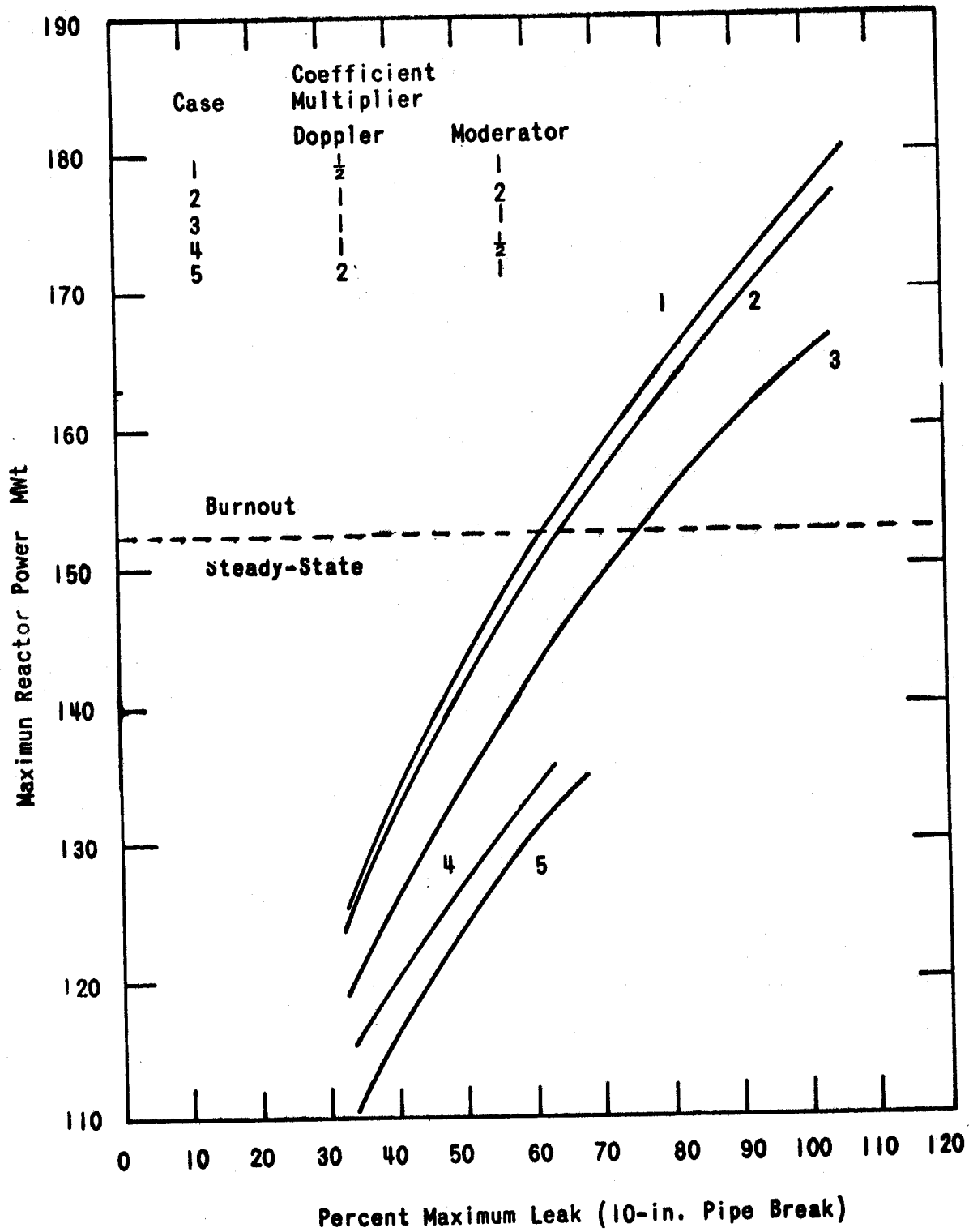


Figure 13-19. Maximum Steam Leak - Maximum Reactor Power Vs High Power Trip Point

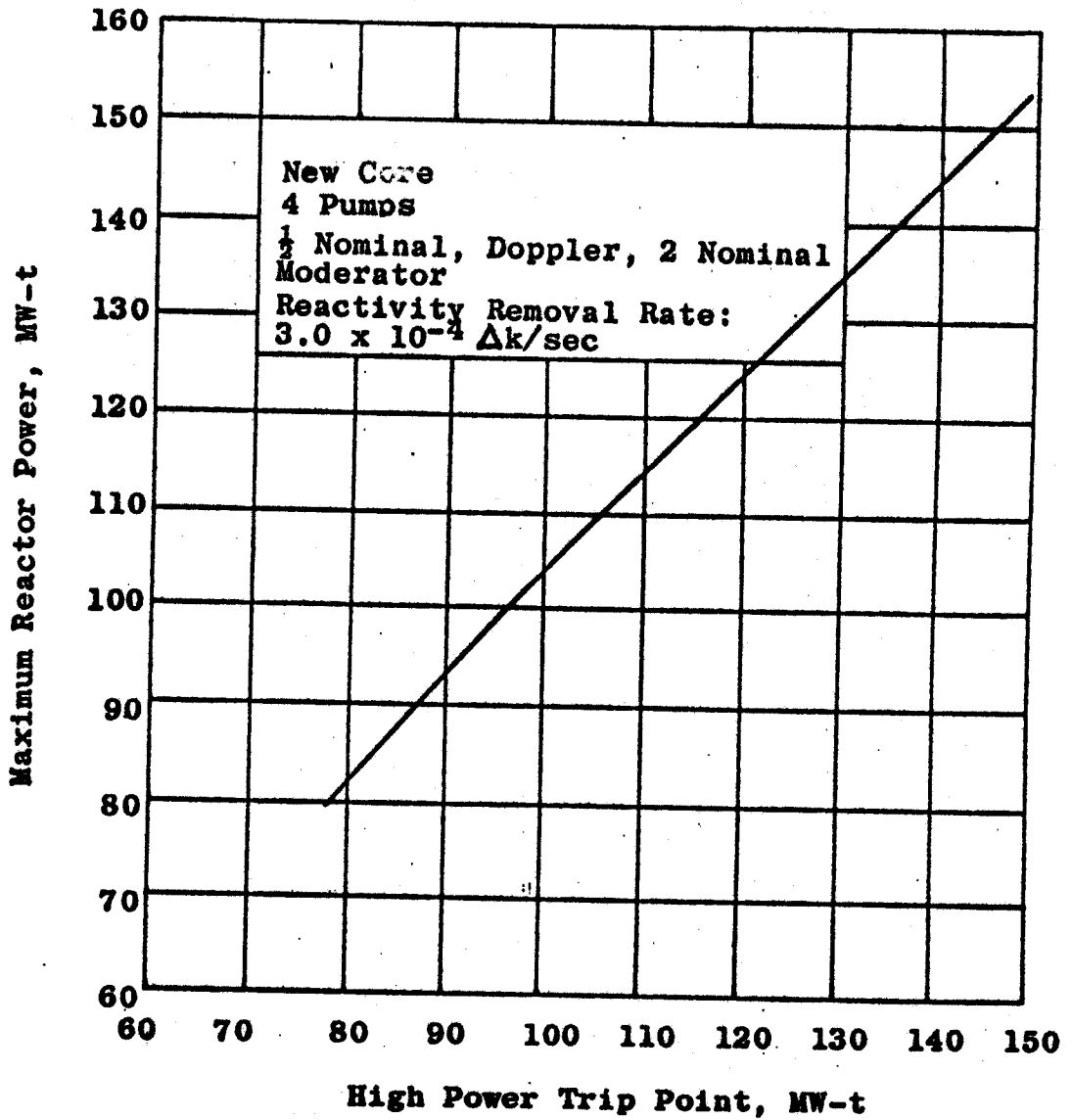


Figure 13-20. Reactivity Variations During Xenon Transient

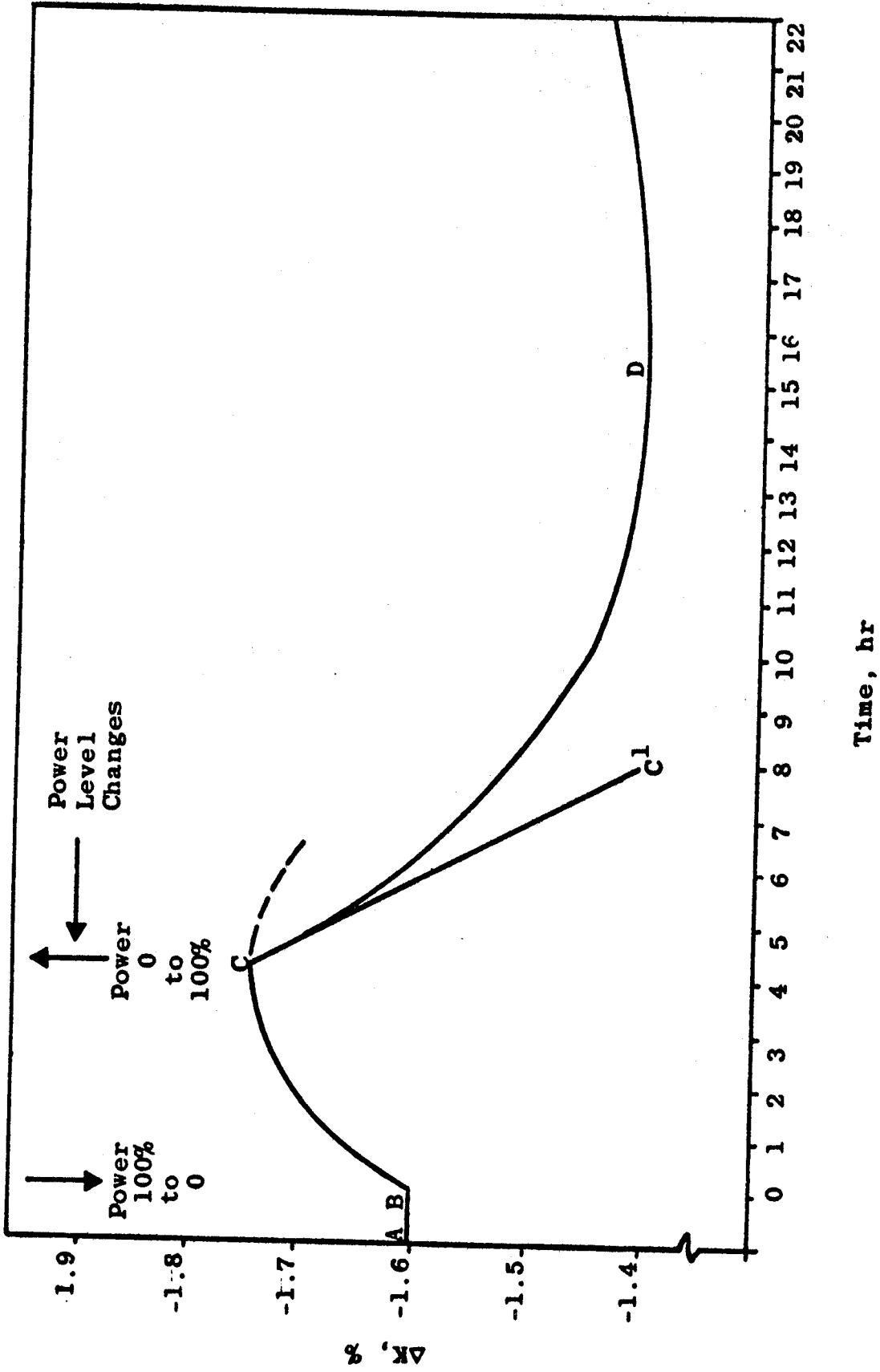


Figure 13-21. Power Increase Due to Xenon Burnout-  
No Control Action

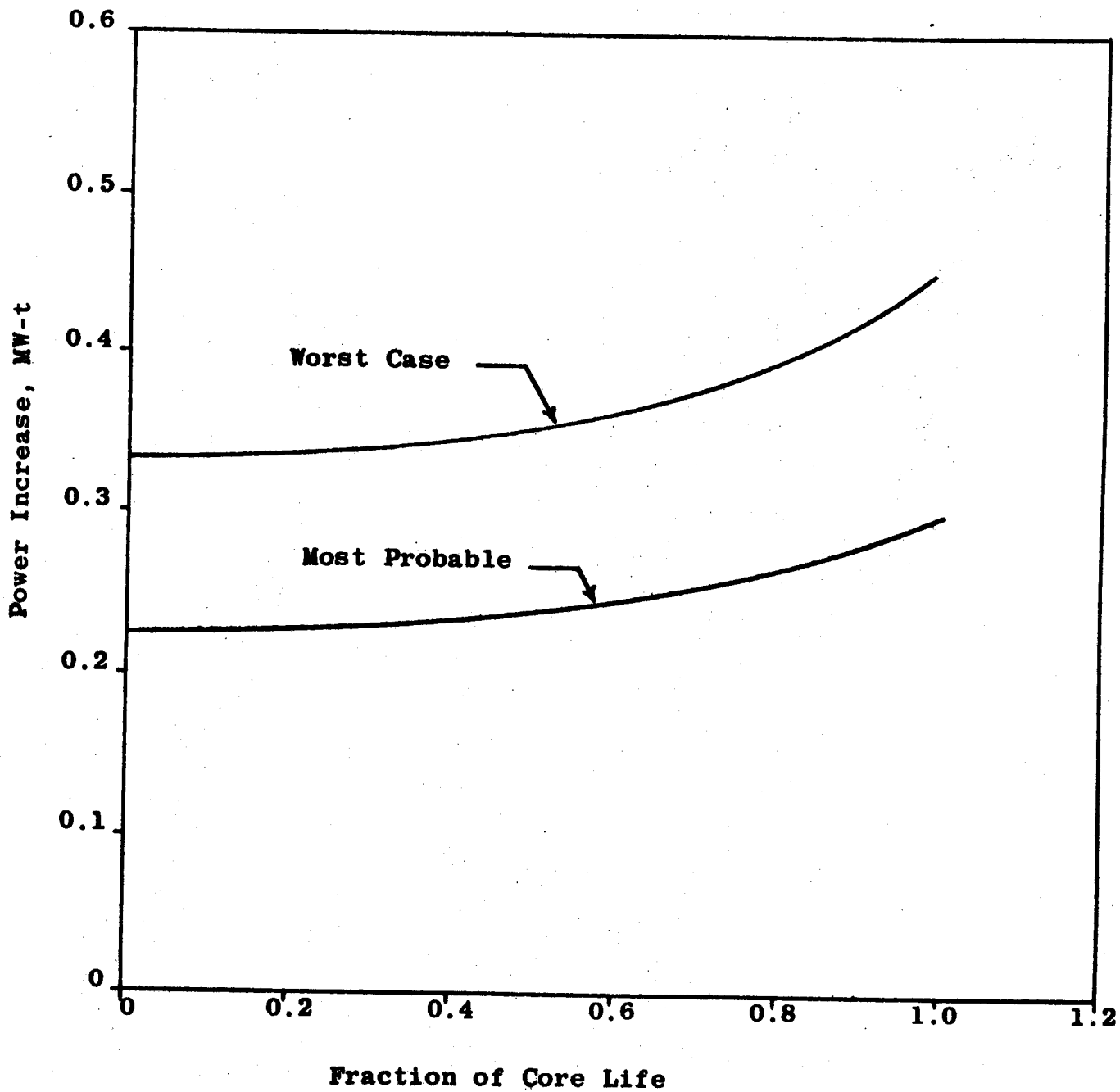


Figure 13-22. Reactor Power Following Sudden Closing Steam Stop Valves

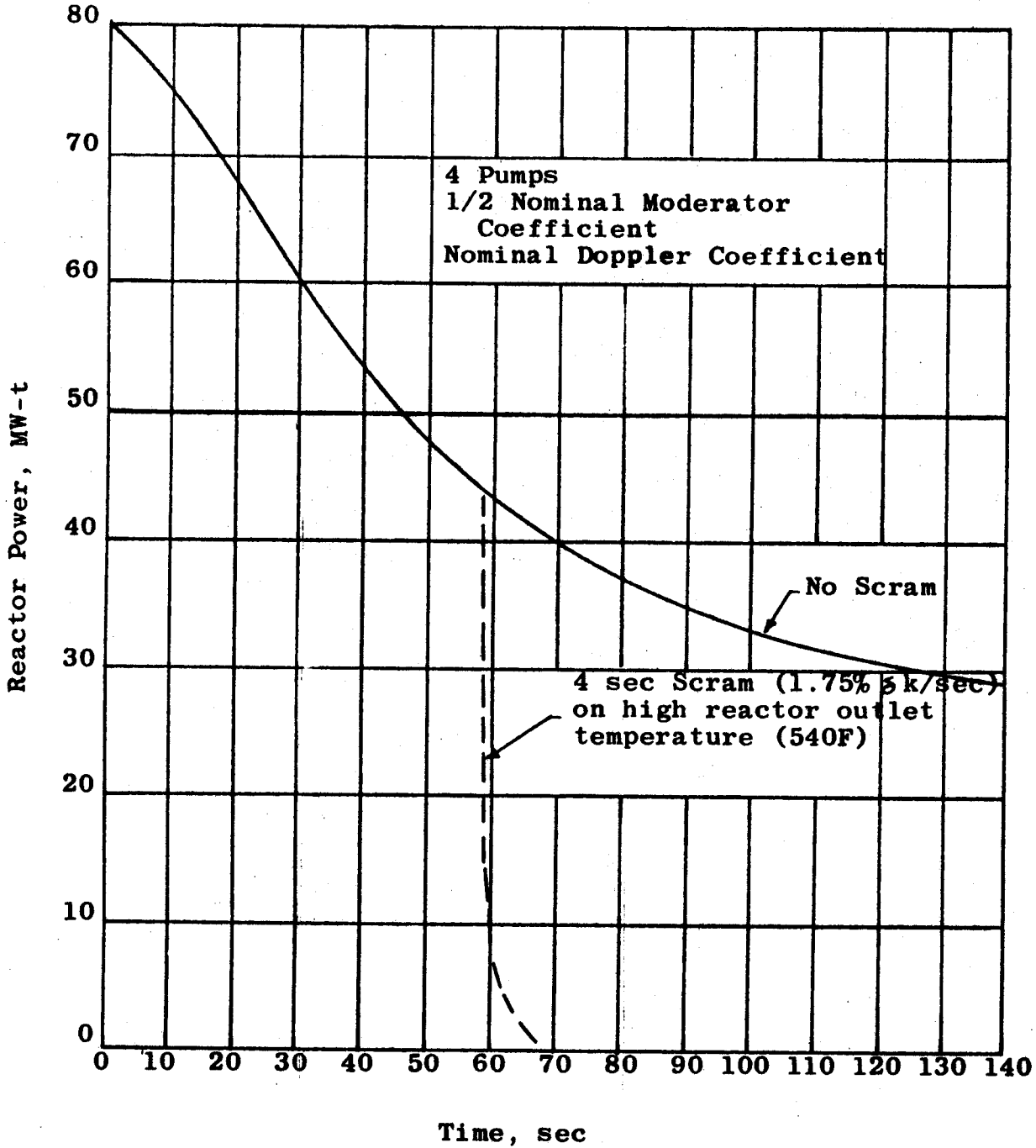


Figure 13-23. Primary Coolant Temperatures Following Sudden Closing of Steam Stop Valves

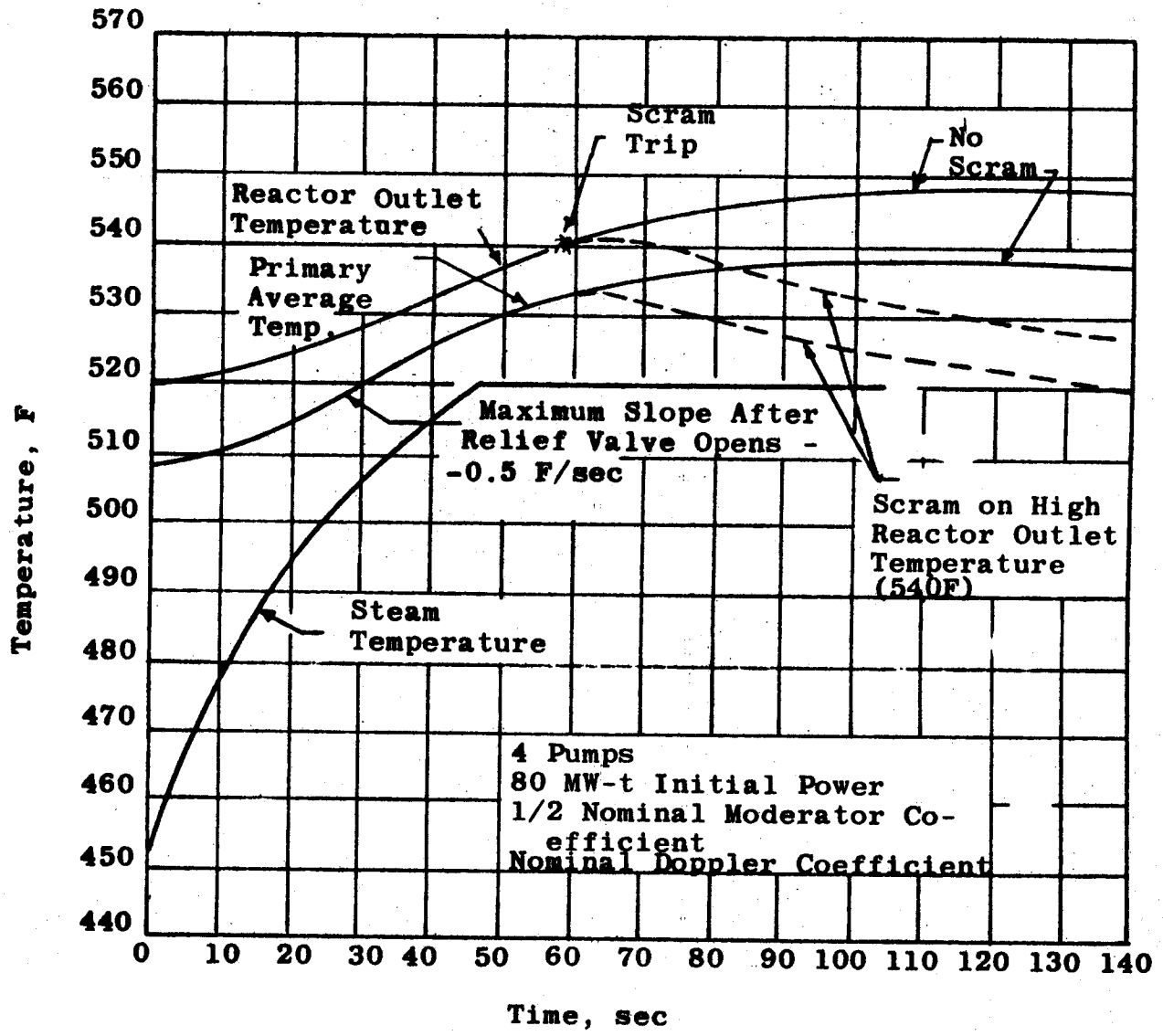
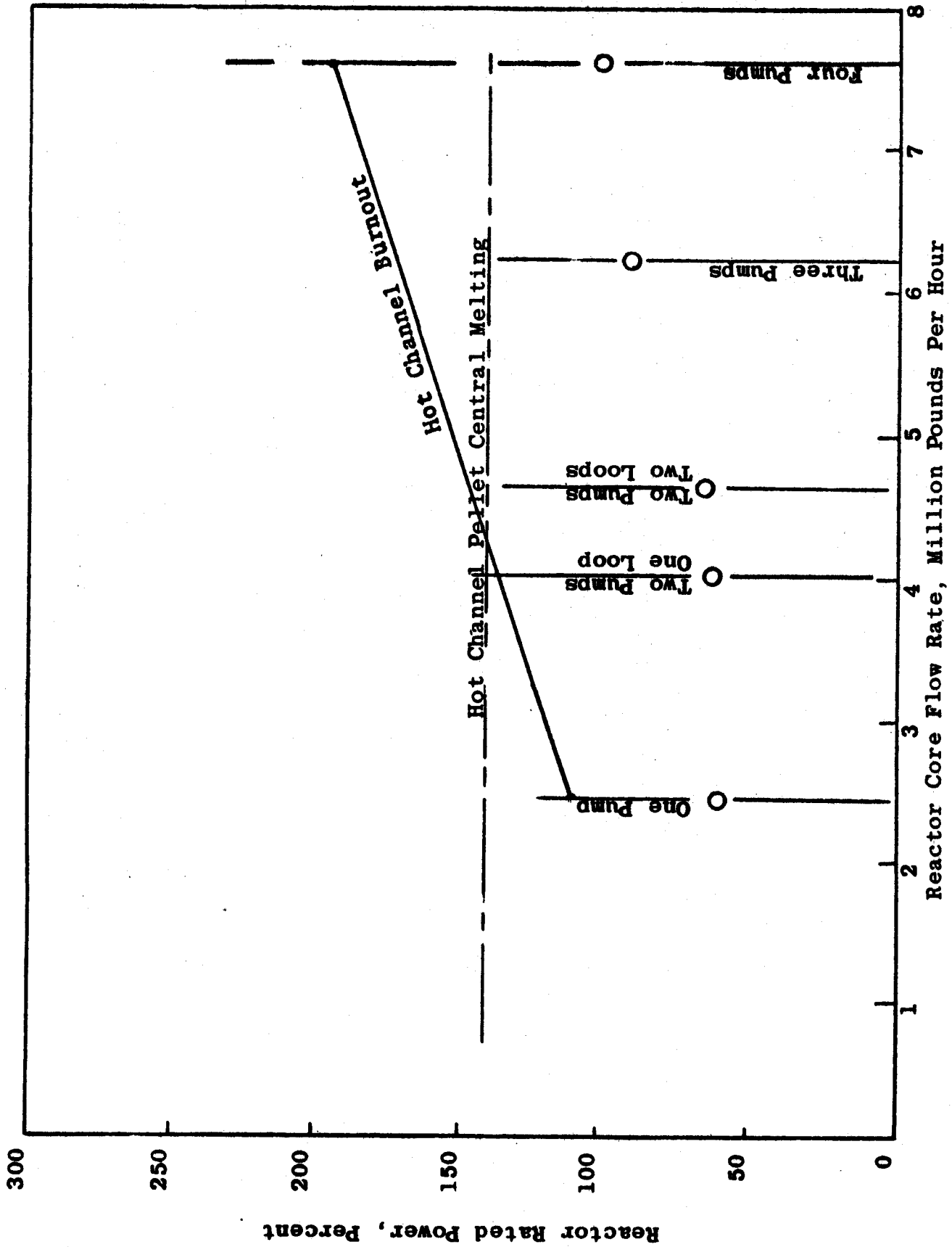
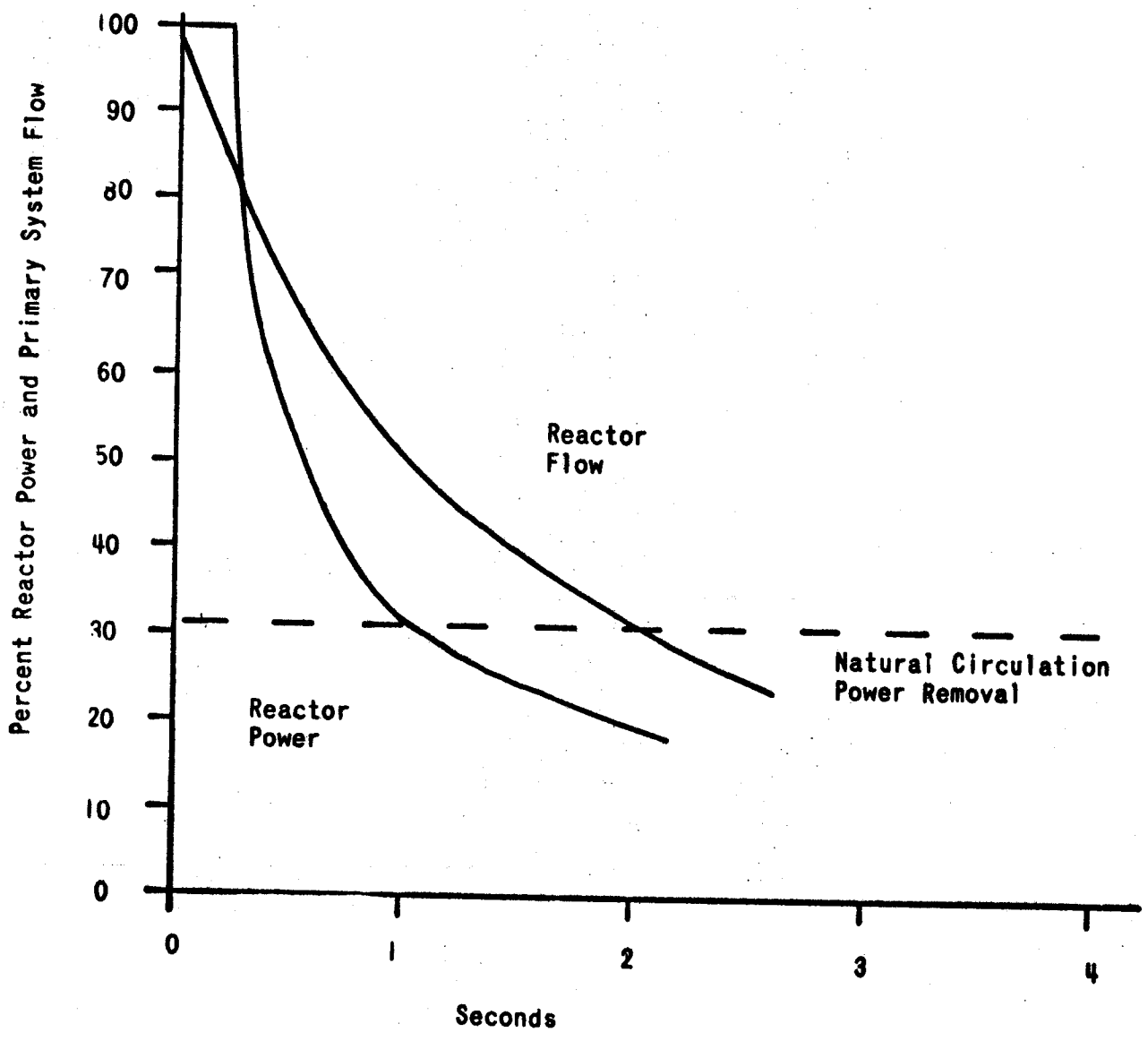


Figure 13-24. Flow Coastdown Limits on Reactor Operation

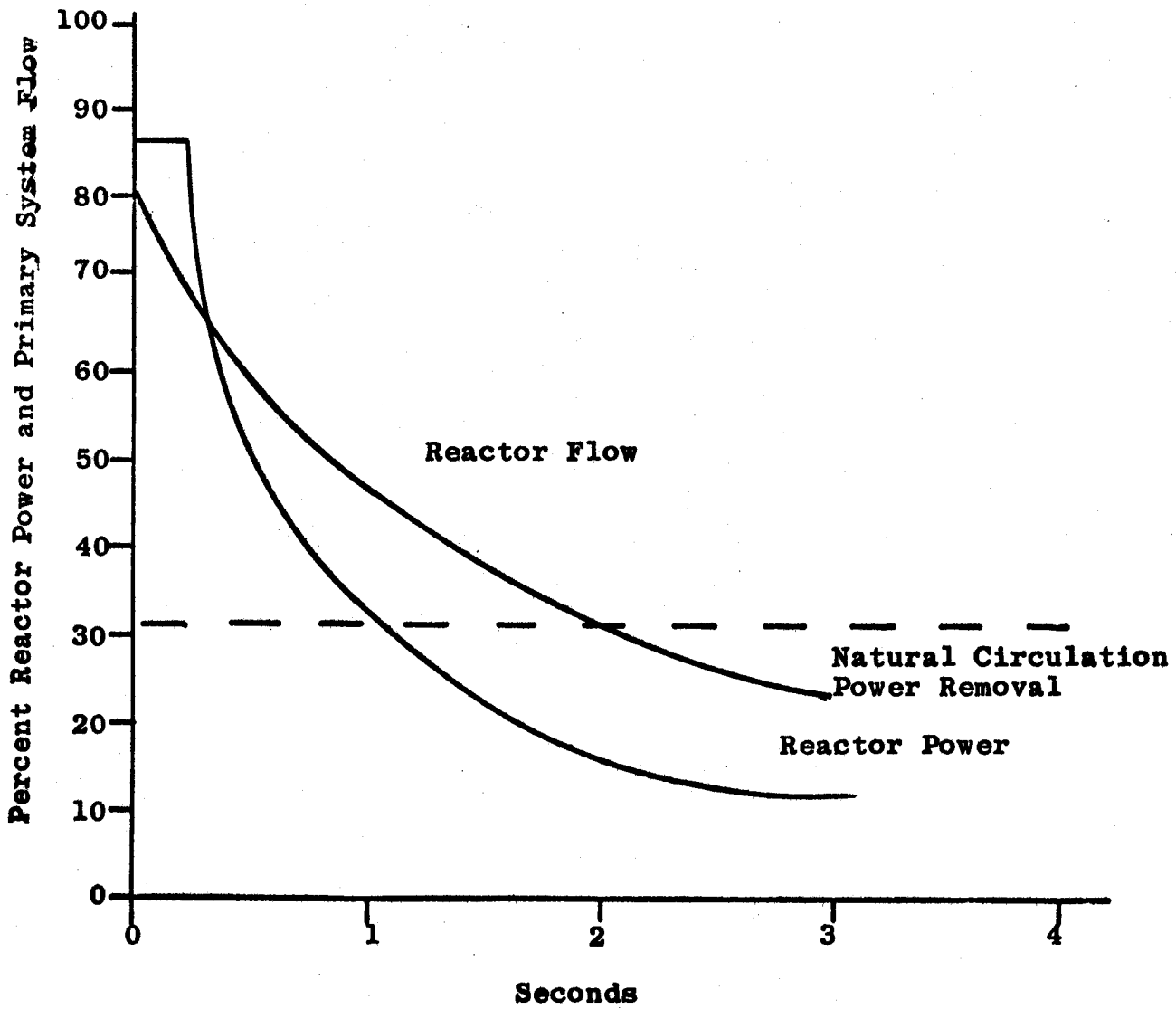


# LOSS OF FLOW - FOUR PUMPS

Figure 13-25

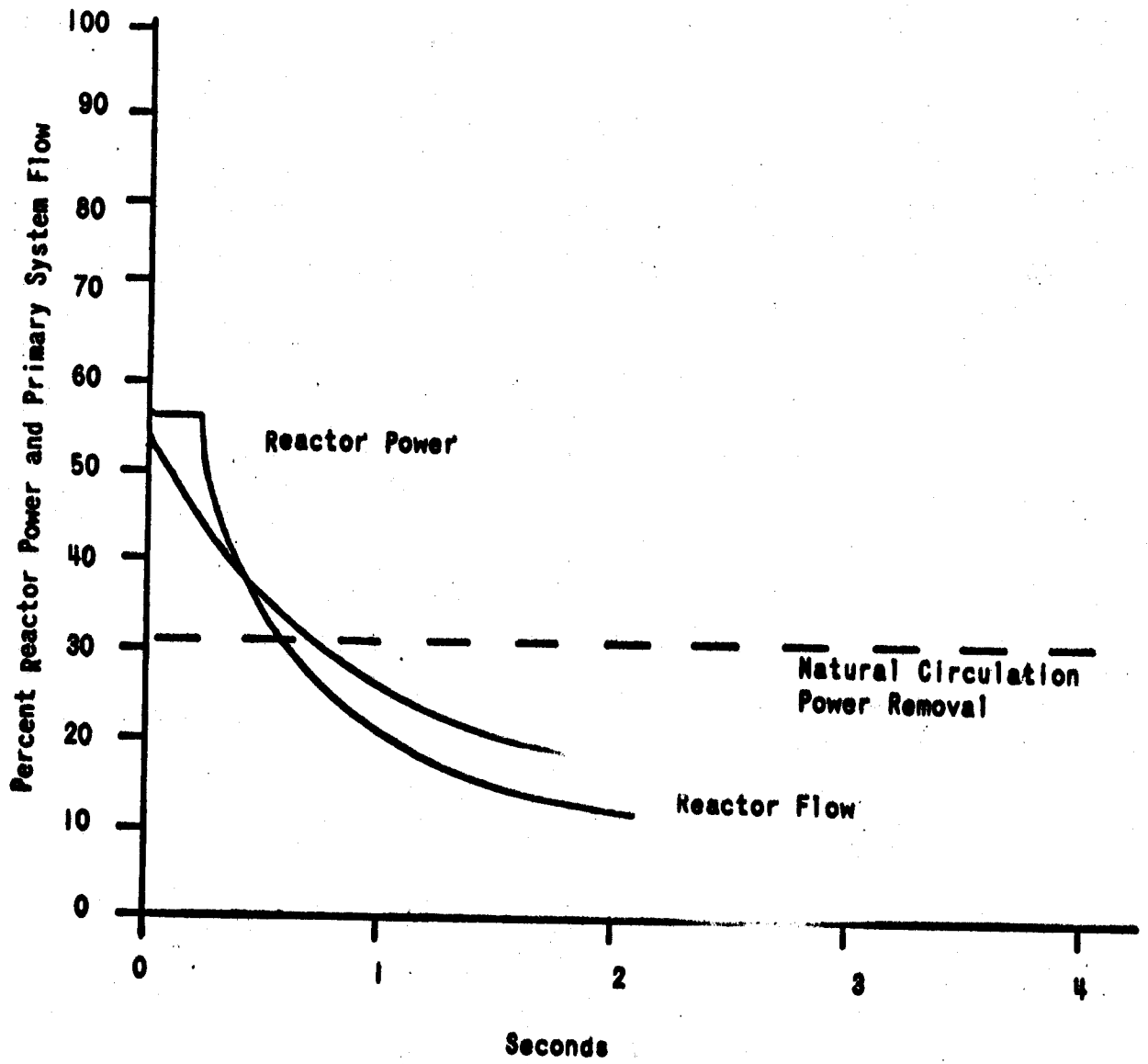


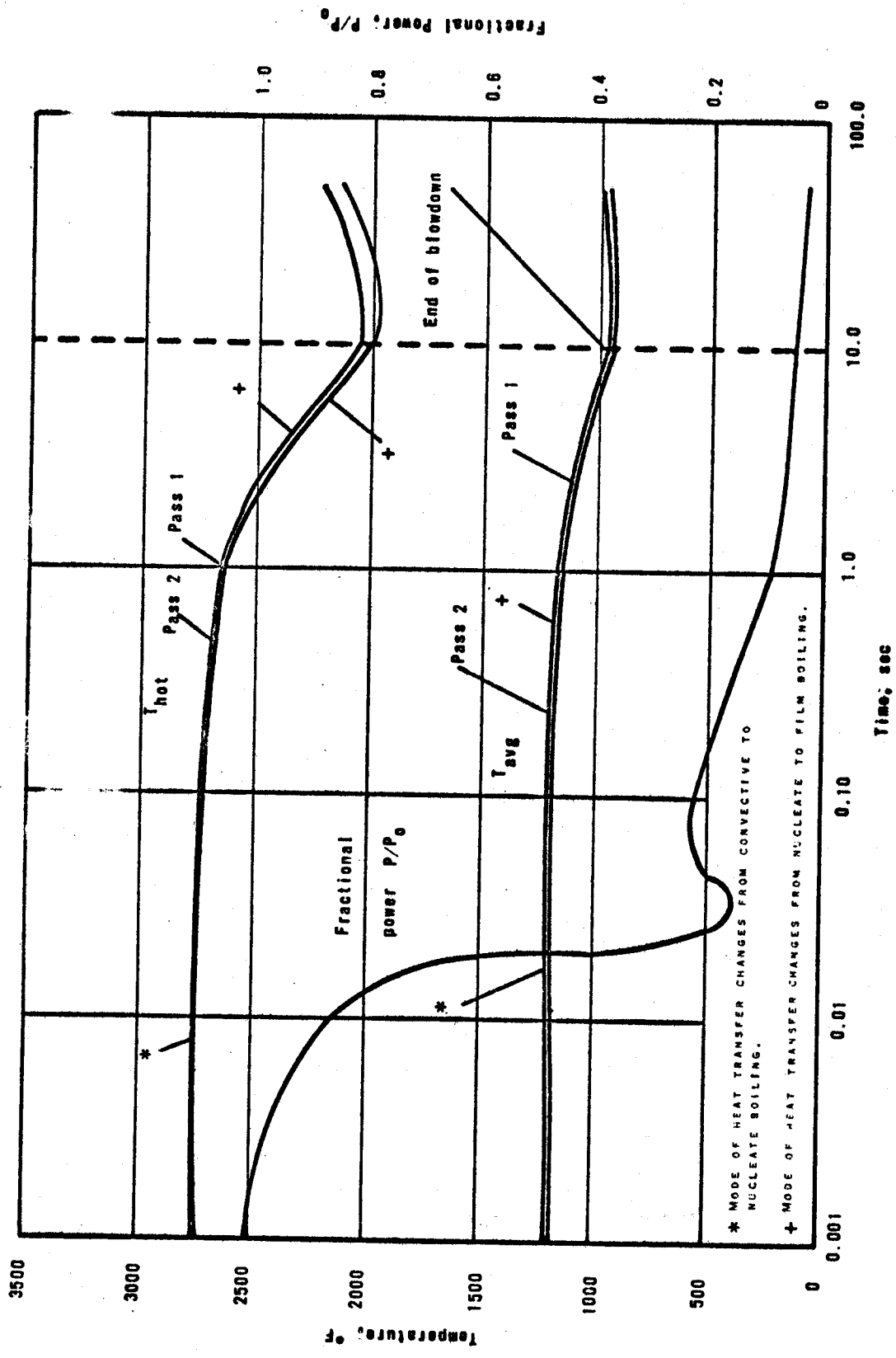
LOSS OF FLOW - THREE PUMPS  
Figure 13-26



LOSS OF FLOW - TWO PUMPS

Figure 13-27





Case 6 Bottom Break 12-9/15 in. Diameter Double Ended; Flow Baffle Intact

Figure 13-28

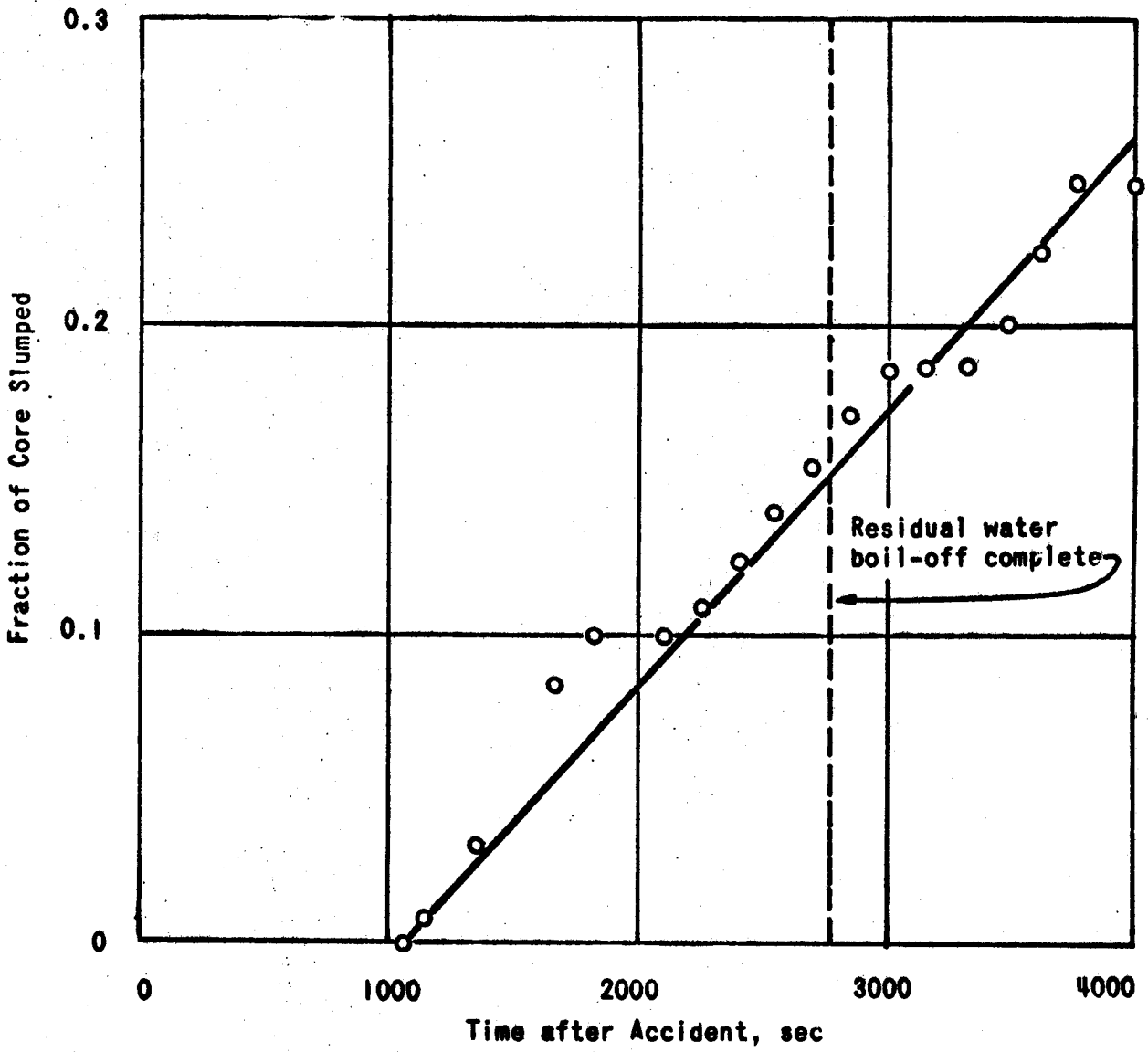


Fig. 13-29 Fraction of Core Slumped vs Time (to 3995 sec)

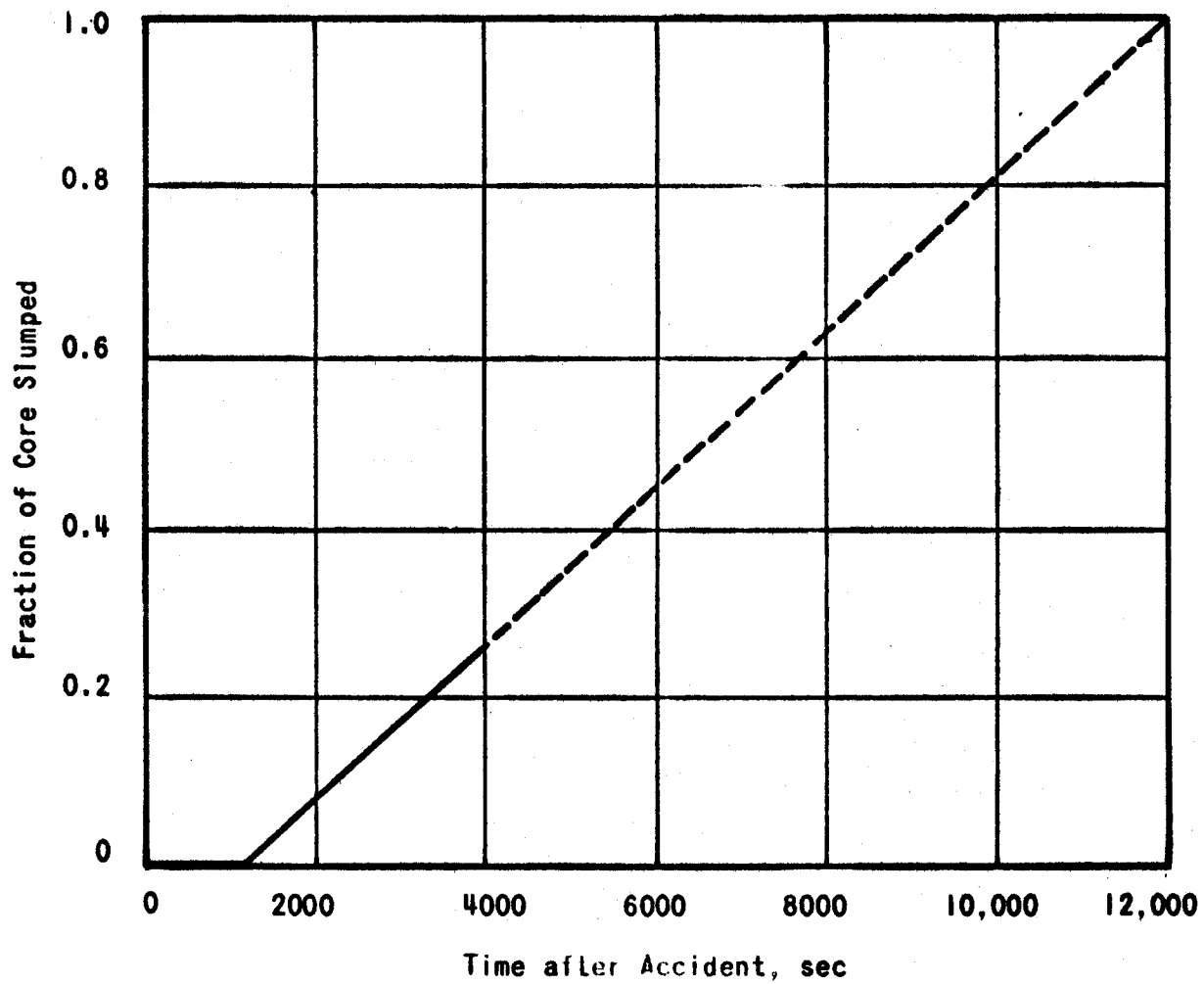


Fig. 13-30 Fraction of Core Slumped vs Time (to 12,200 sec.)

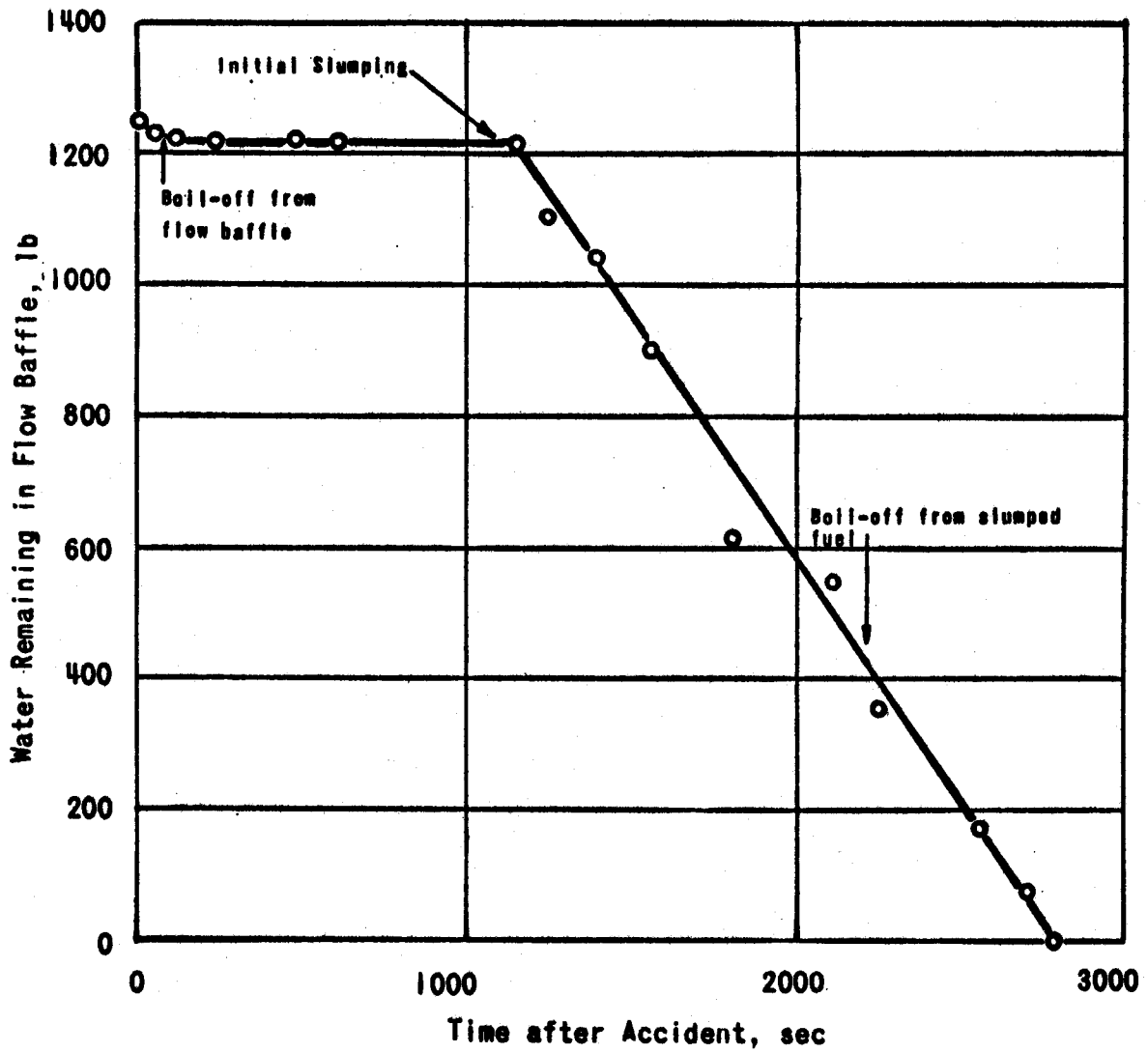


Fig. 13-31 Water Remaining in Flow Baffle vs Time

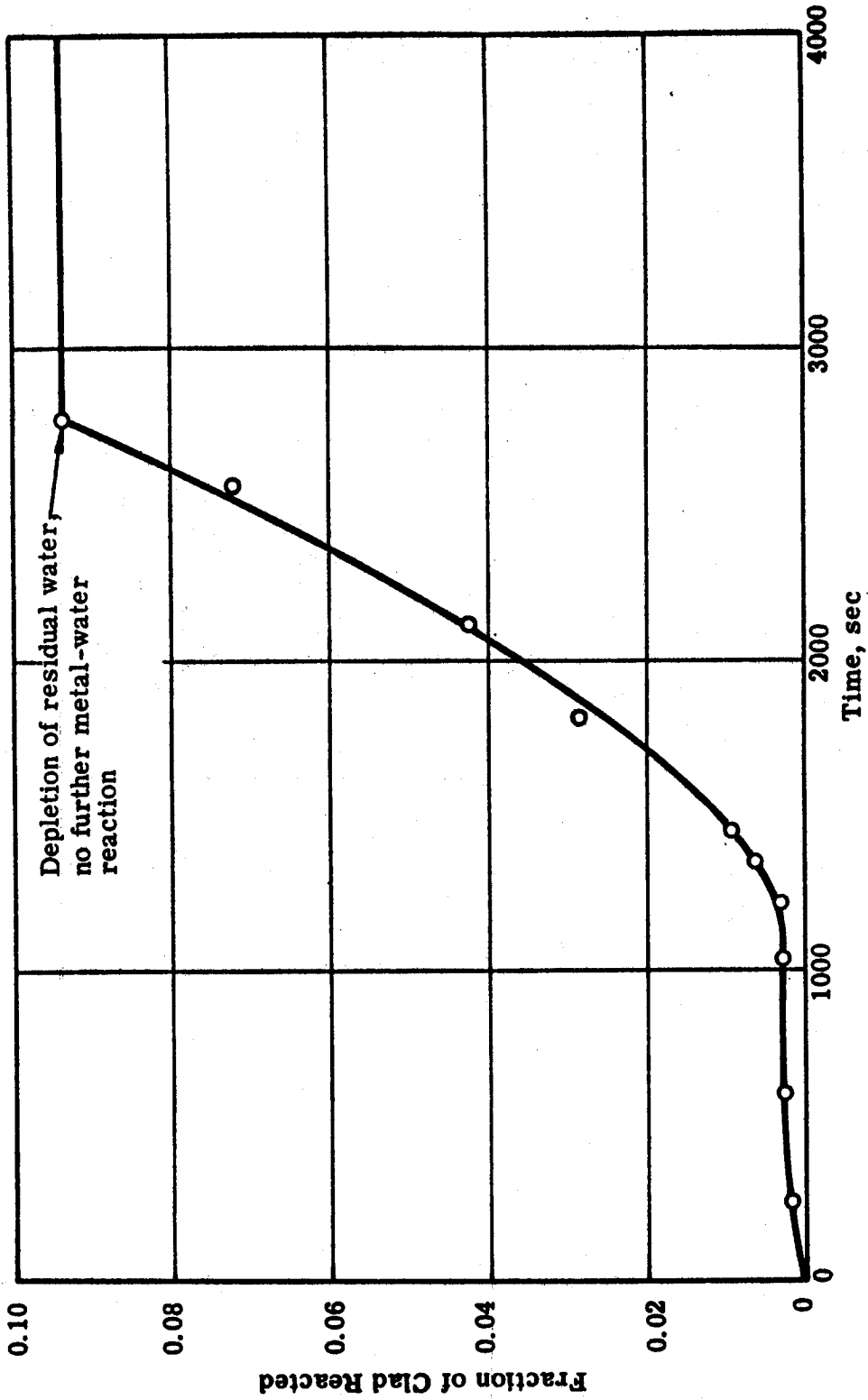


Figure 13-32. Fraction of Cladding Oxidized Vs. Time

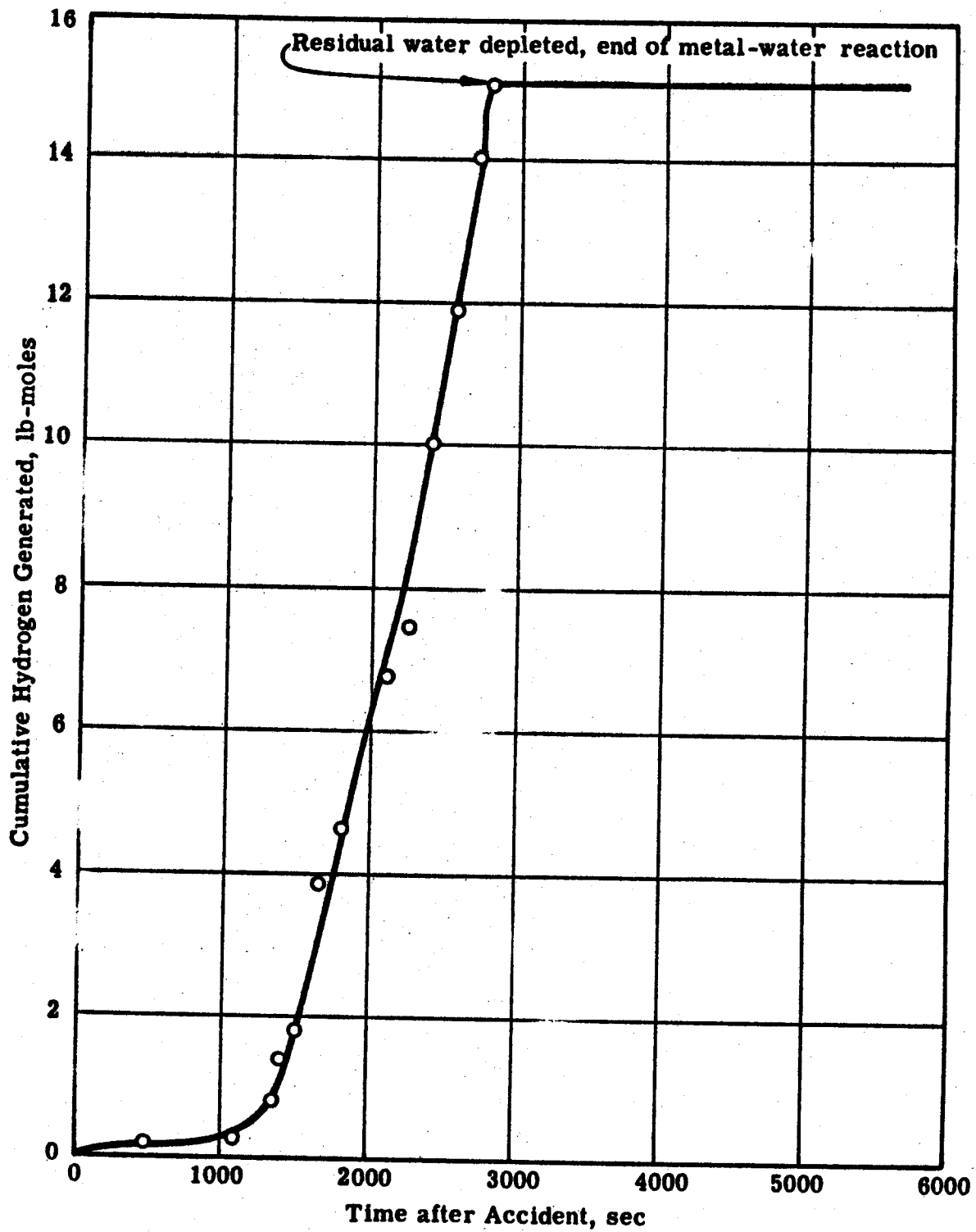
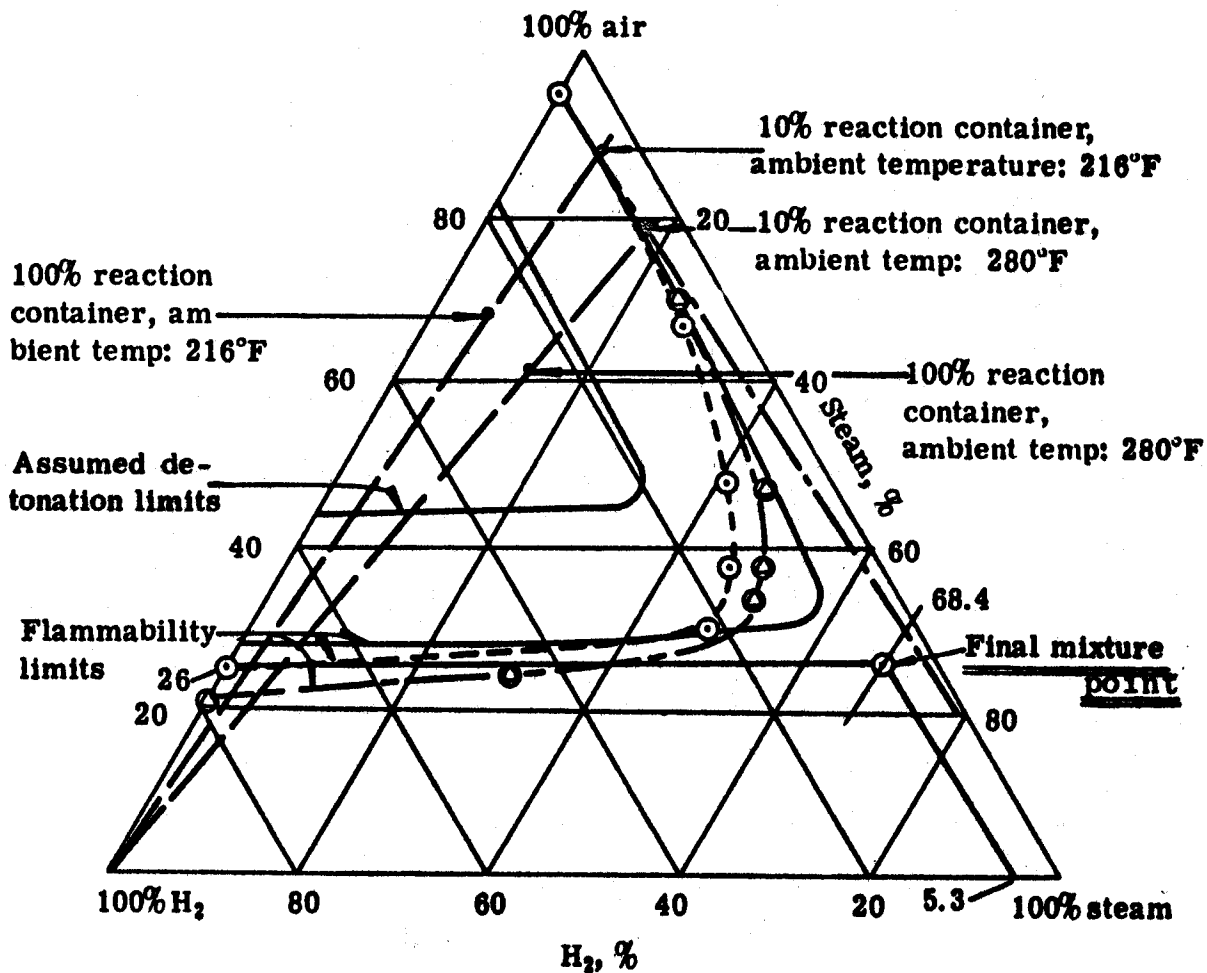


Figure 13-33. Cumulative Hydrogen Generated Vs. Time



**Flammability limits:**

- 75°F, 0 psig
- ⊙ — — — 300°F, 0 psig
- — · — 300°F, 100 psig

**Figure 13-34. Flammability Limits of Hydrogen - Air Steam Mixtures**

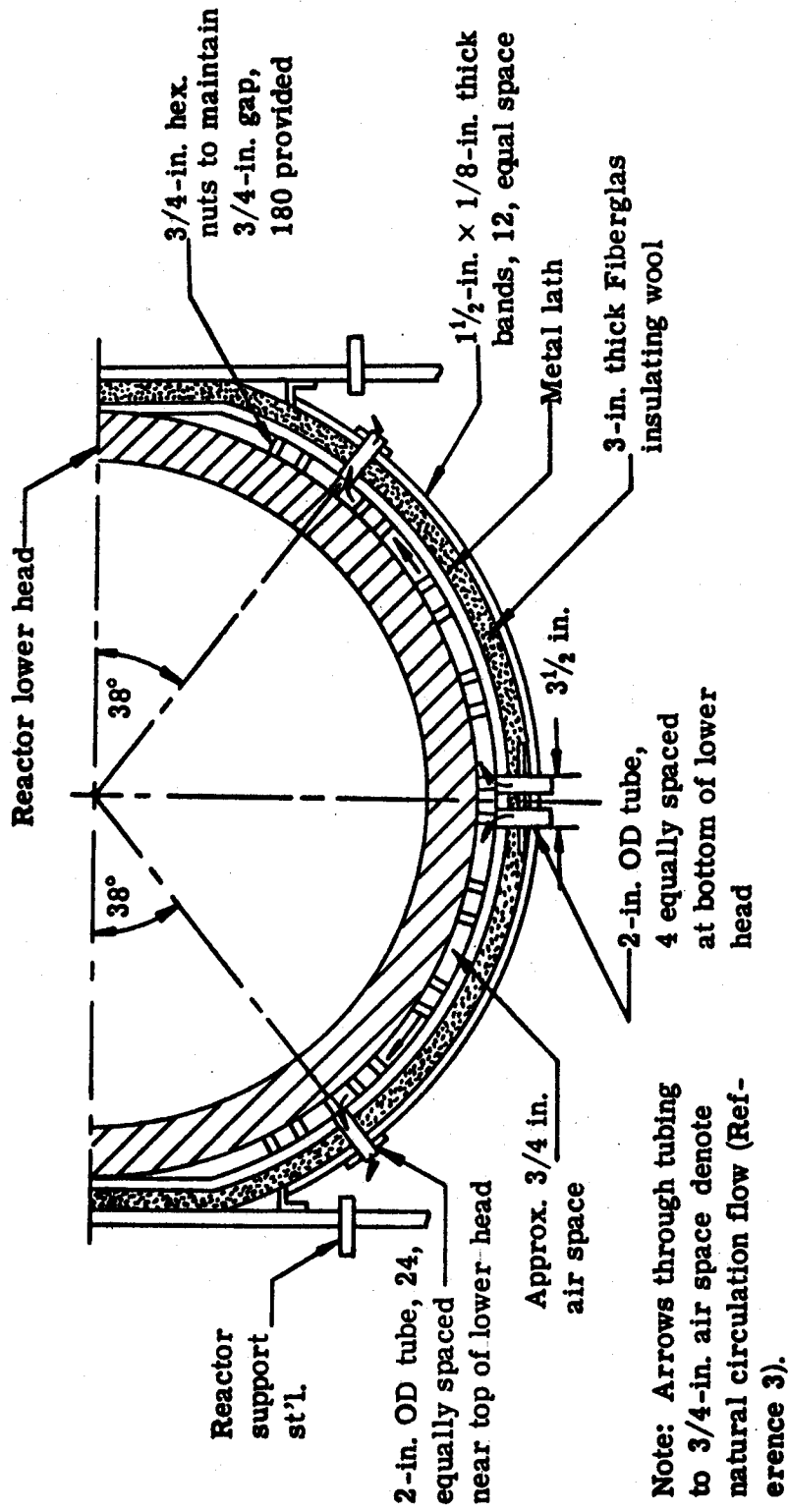


Figure 13-35. Arrangement of Reactor Vessel Lower Head and Insulation

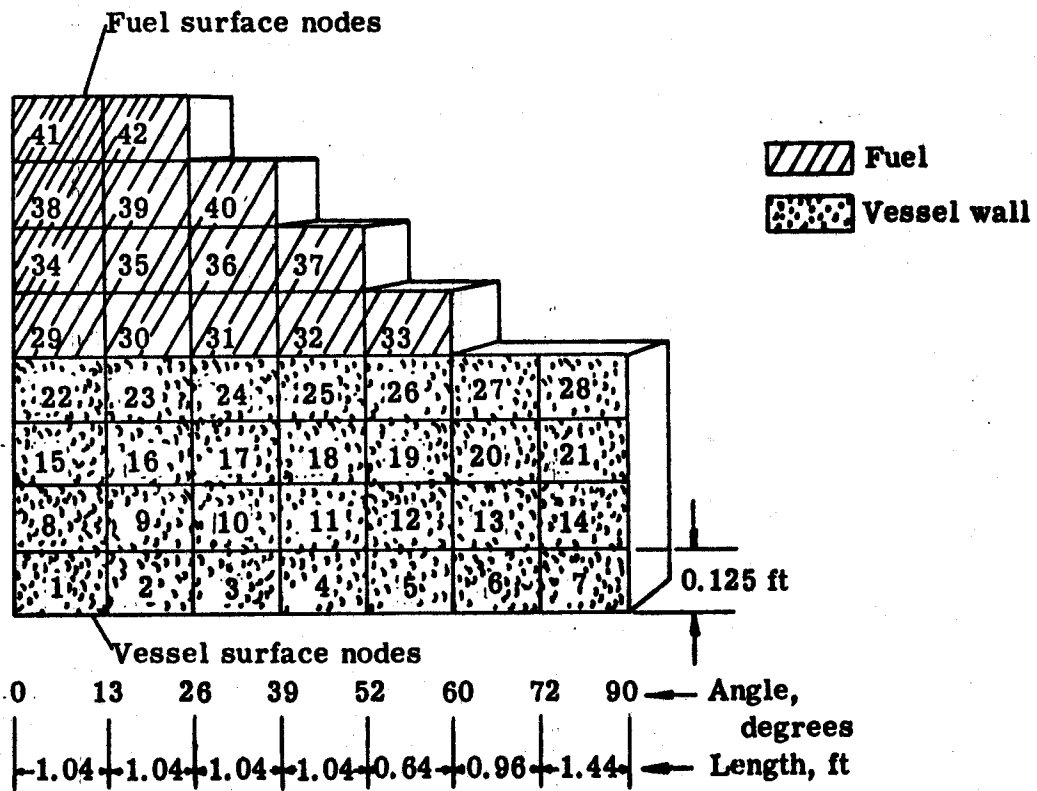
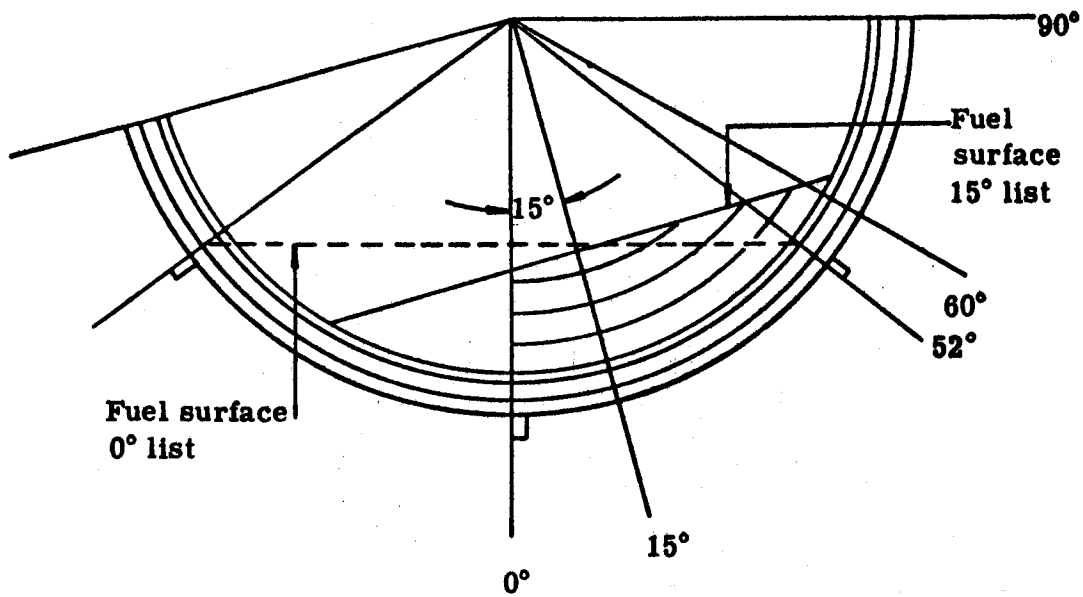


Fig. 13-36. Reactor Vessel Simulation for TIGER

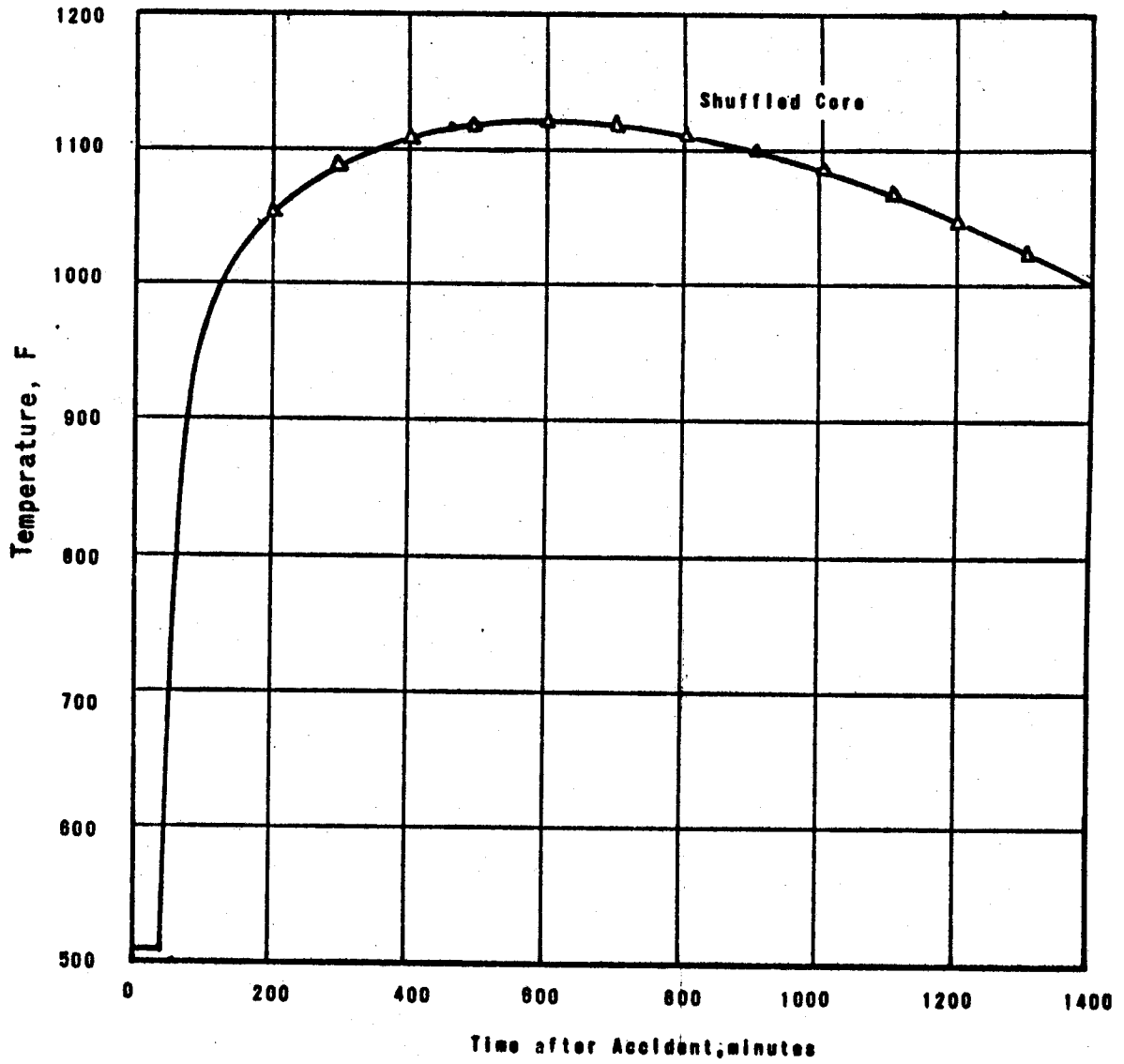


Fig. 13-37. Maximum Reactor Vessel Temperature Vs. Time

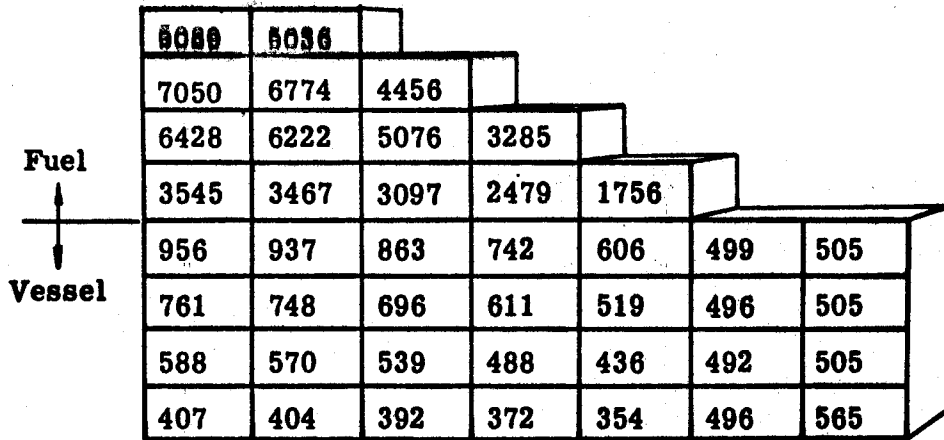


Figure 13-38. Temperature Distribution in Reactor Vessel Wall at 600 Minutes - 0° List, 2780°F Fuel Temperature, 63 Minutes Initial Contact Time

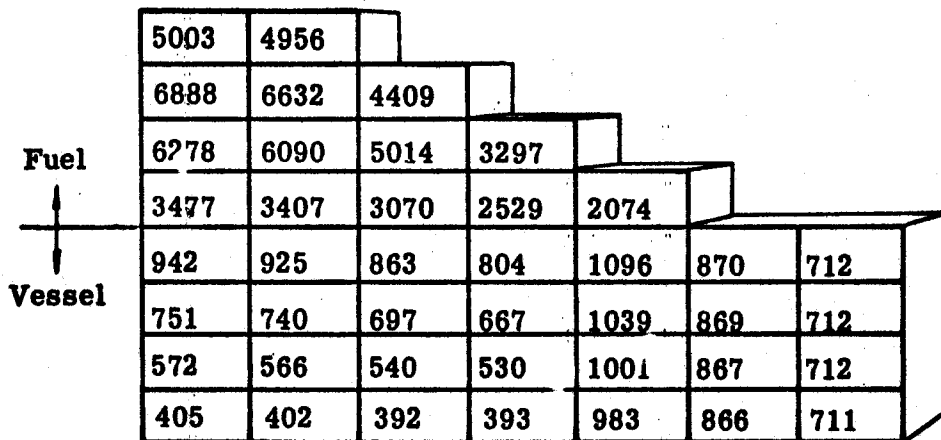


Figure 13-39. Temperature Distribution in Reactor Vessel Wall at 600 Minutes - 15° List, 2780°F Fuel Temperature, 63 Minutes Initial Contact Time

Fig. 13-40 Containment Pressure History

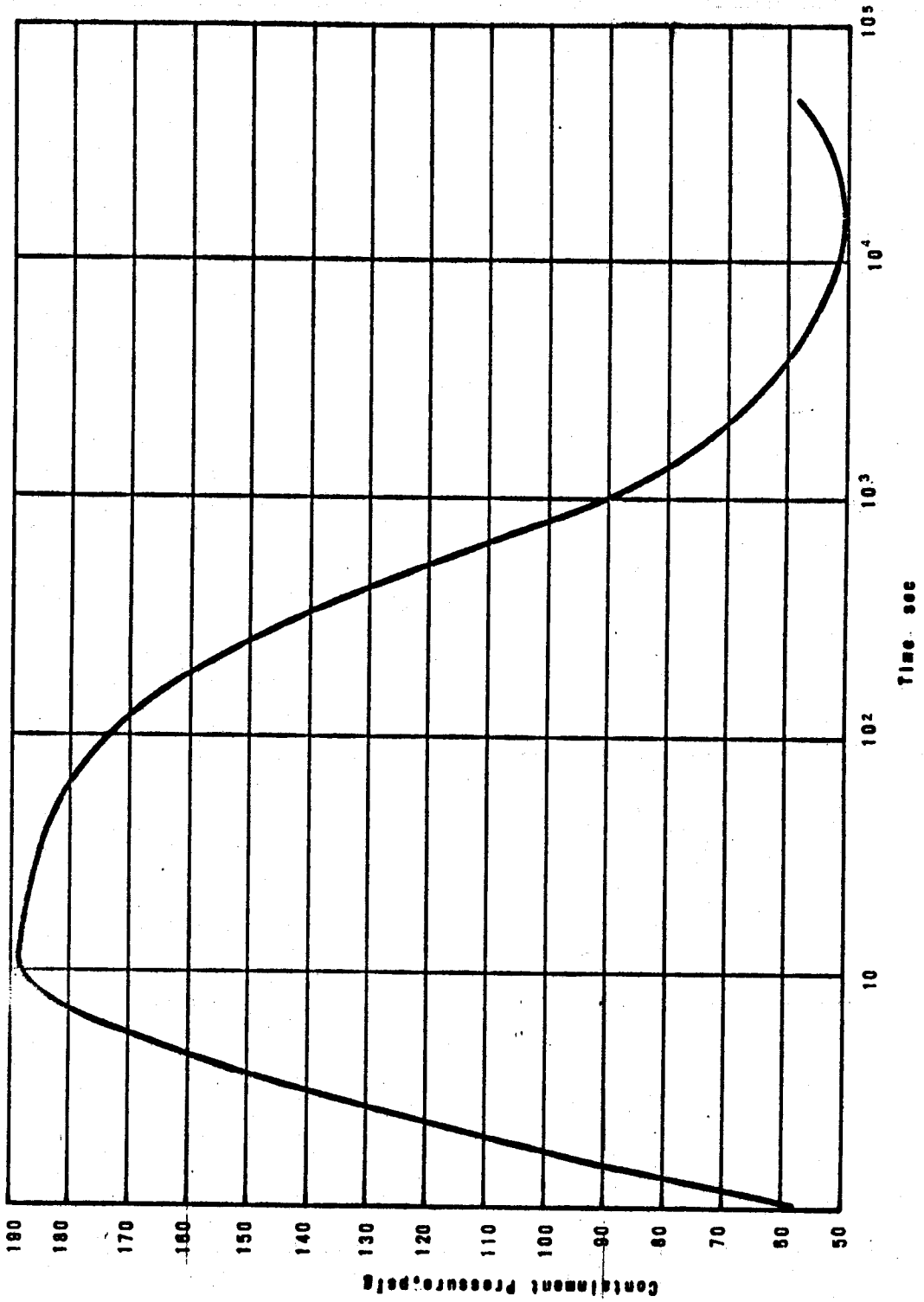


Figure 13-41 Dose Rate in the Forward Control Area

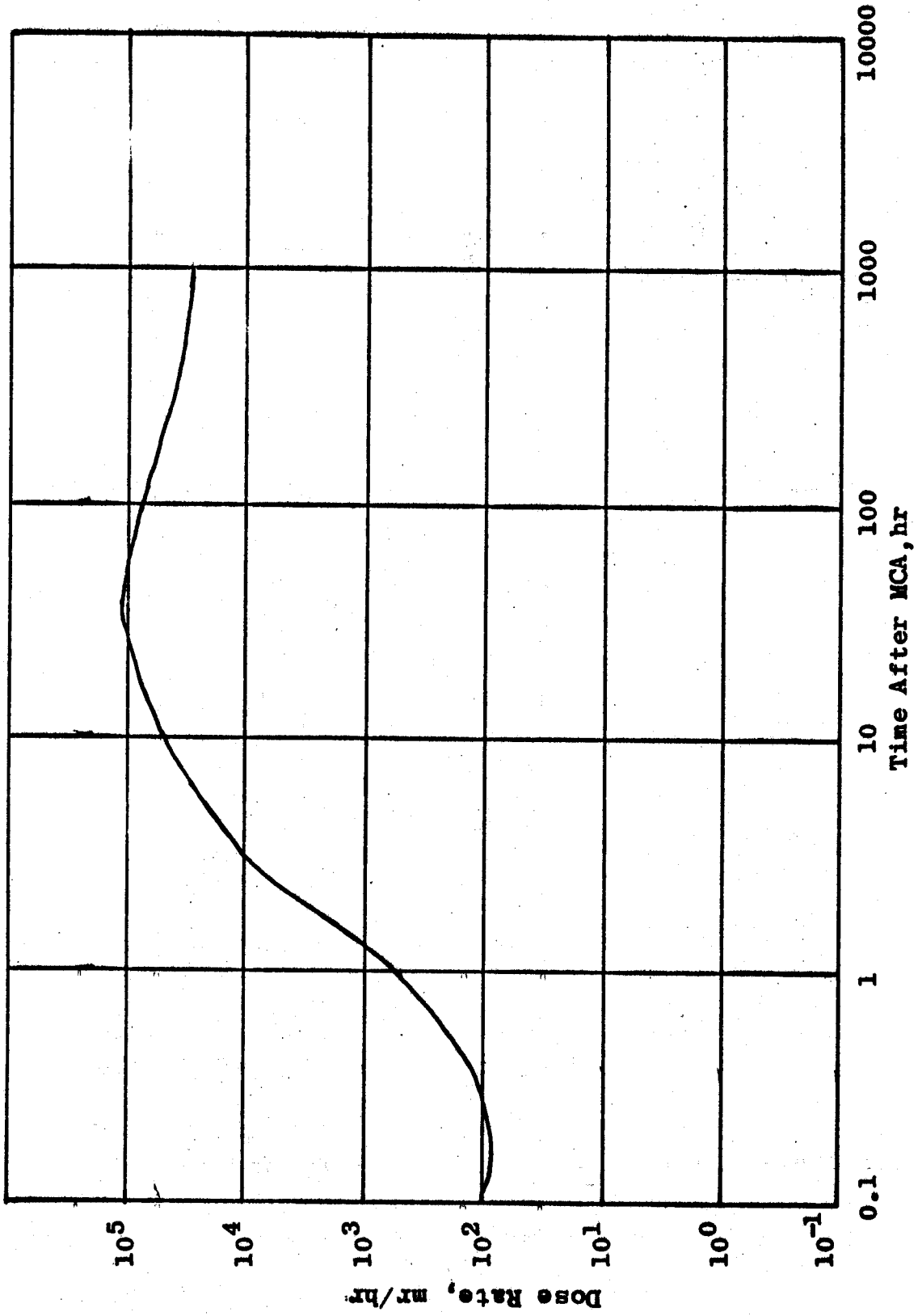


Figure 13-42 Dose Rate in the Control Center

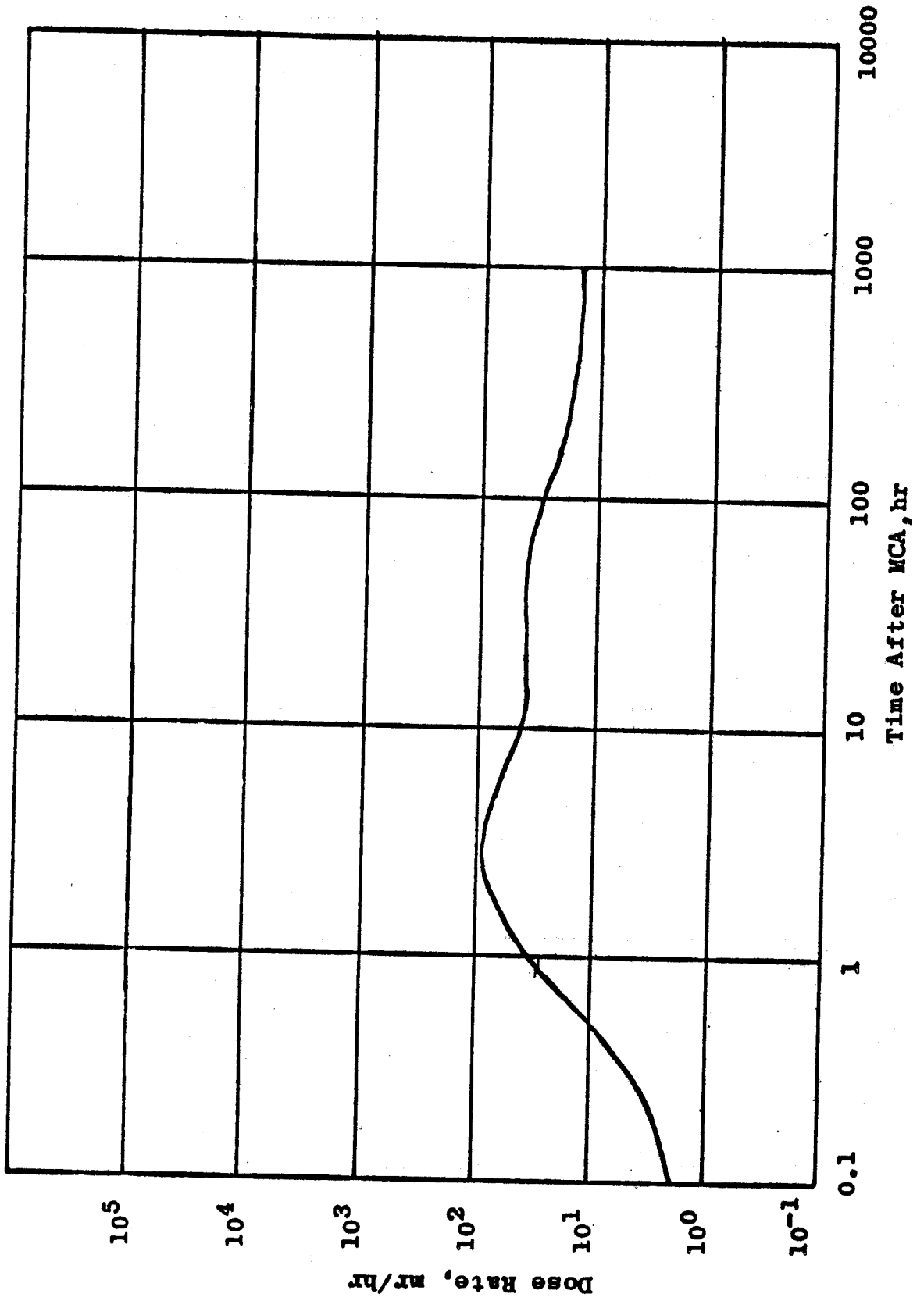


Figure 13-43 Dose Rate in the Emergency Diesel Generator Room

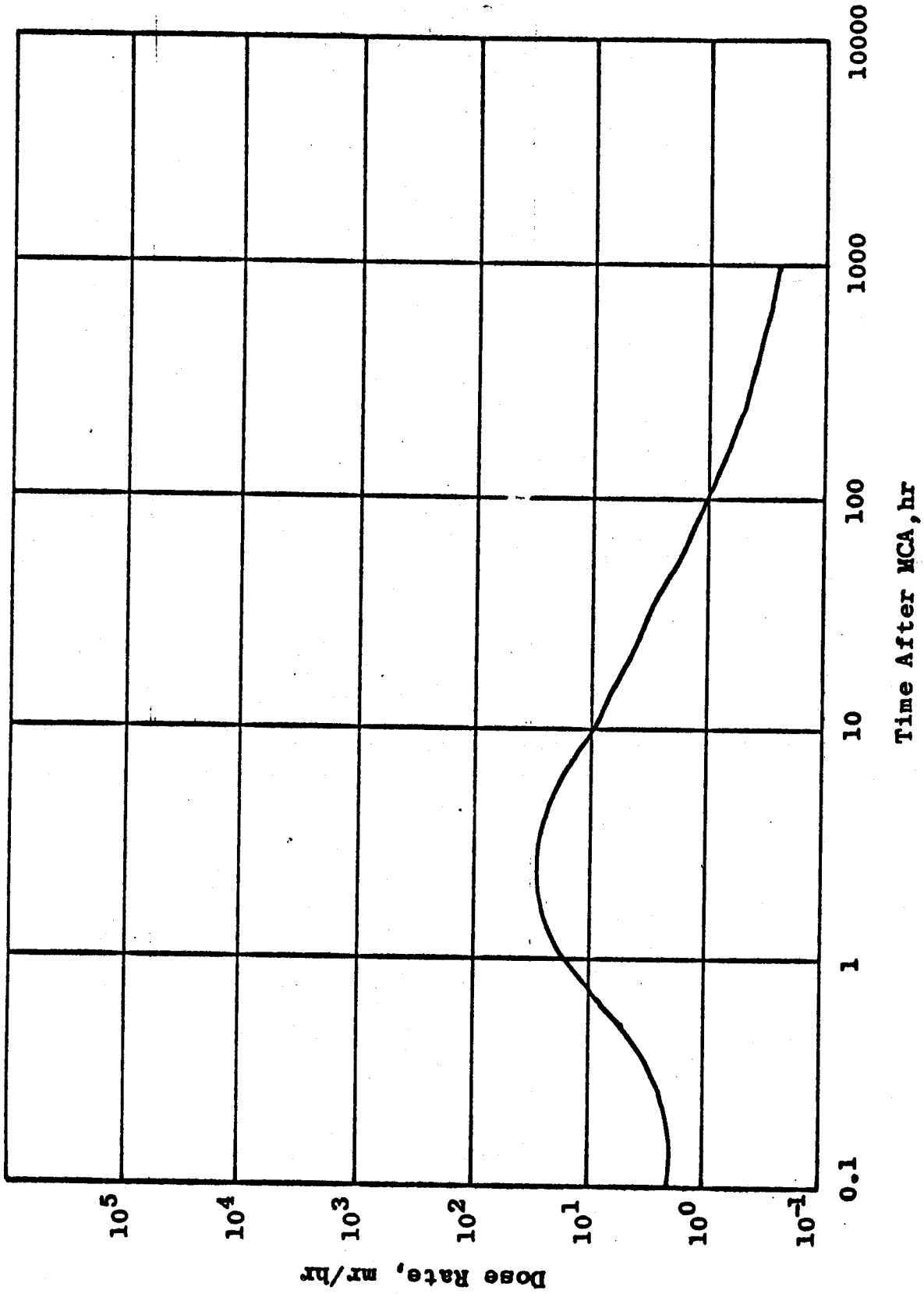


Figure 13-44 Dose Rate in the Bridge

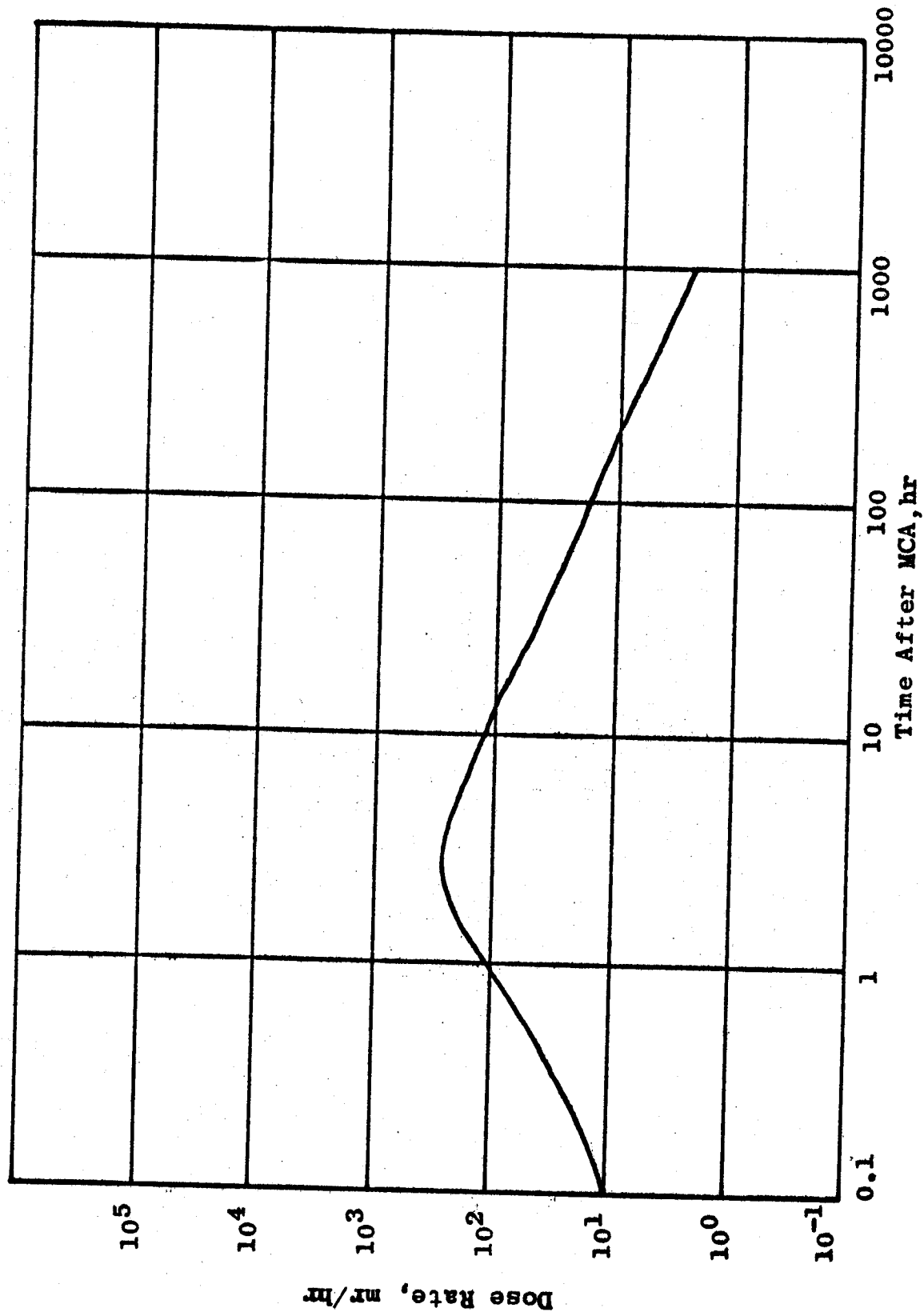


Figure 13-45 Dose Rate at the Engine Room Forward Bulkhead

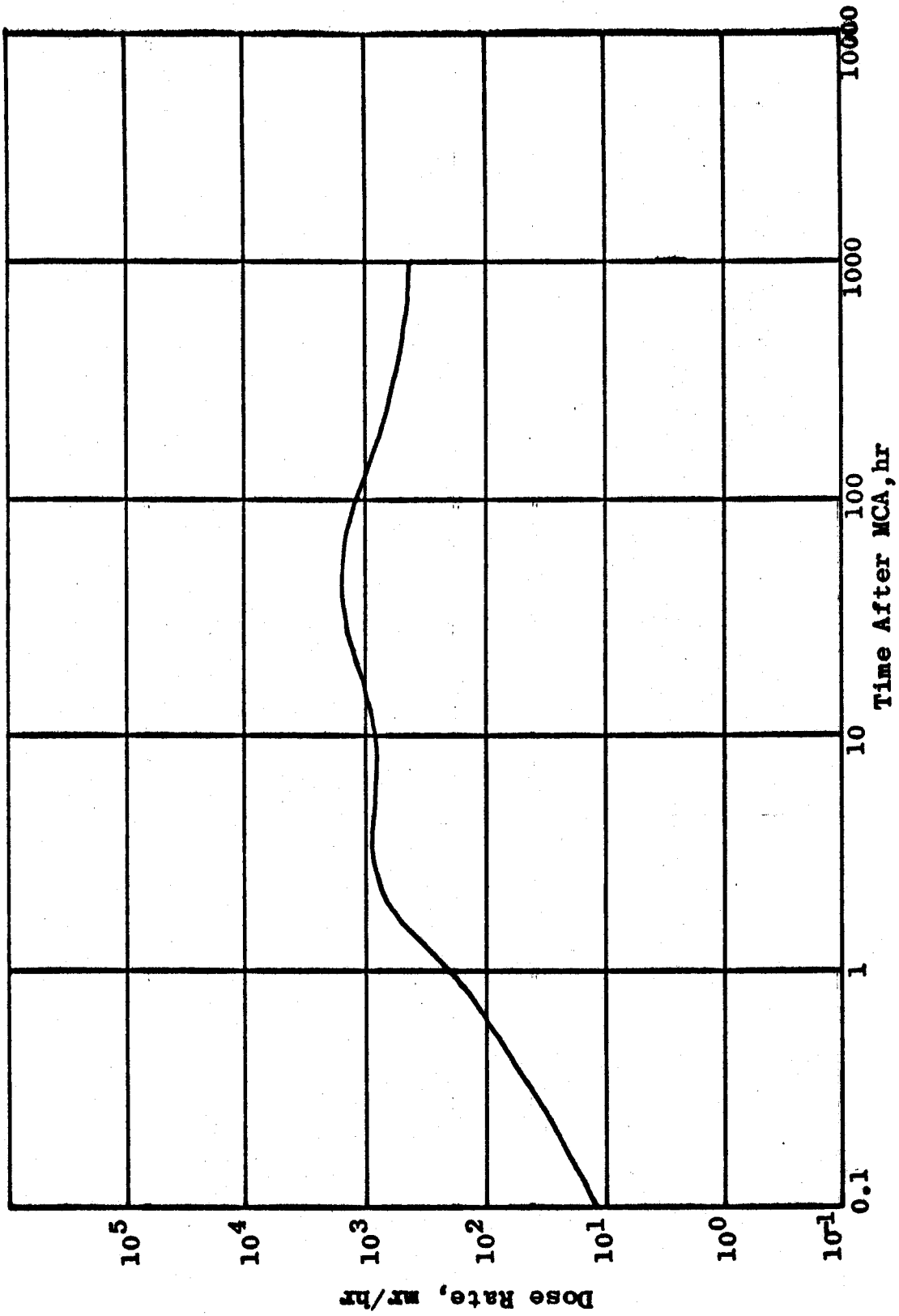


Fig. 13-46 Radial Power Profile 2000 EFPH

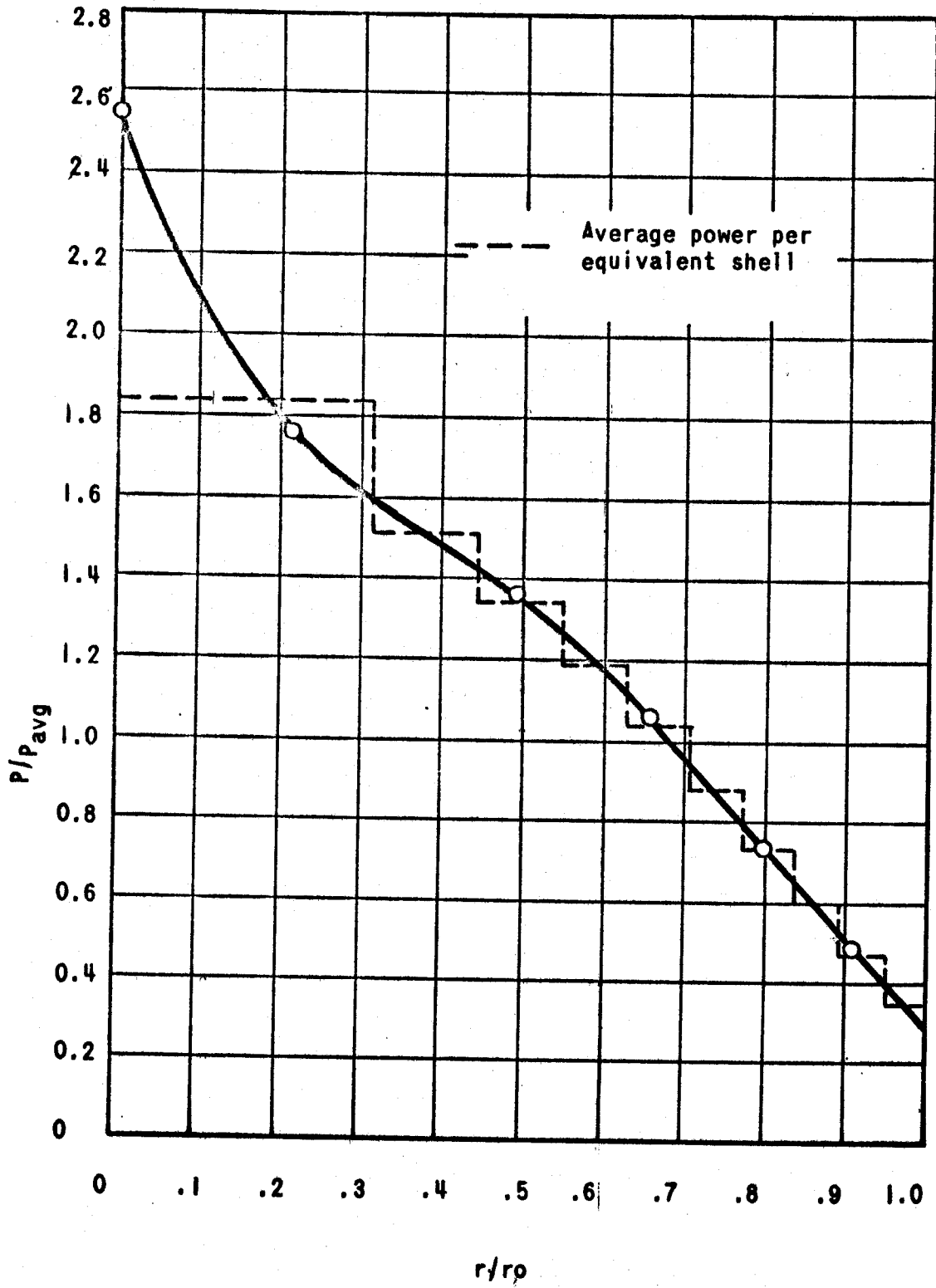


Fig. 13-47 Radial Power Profile 7000 EFPH

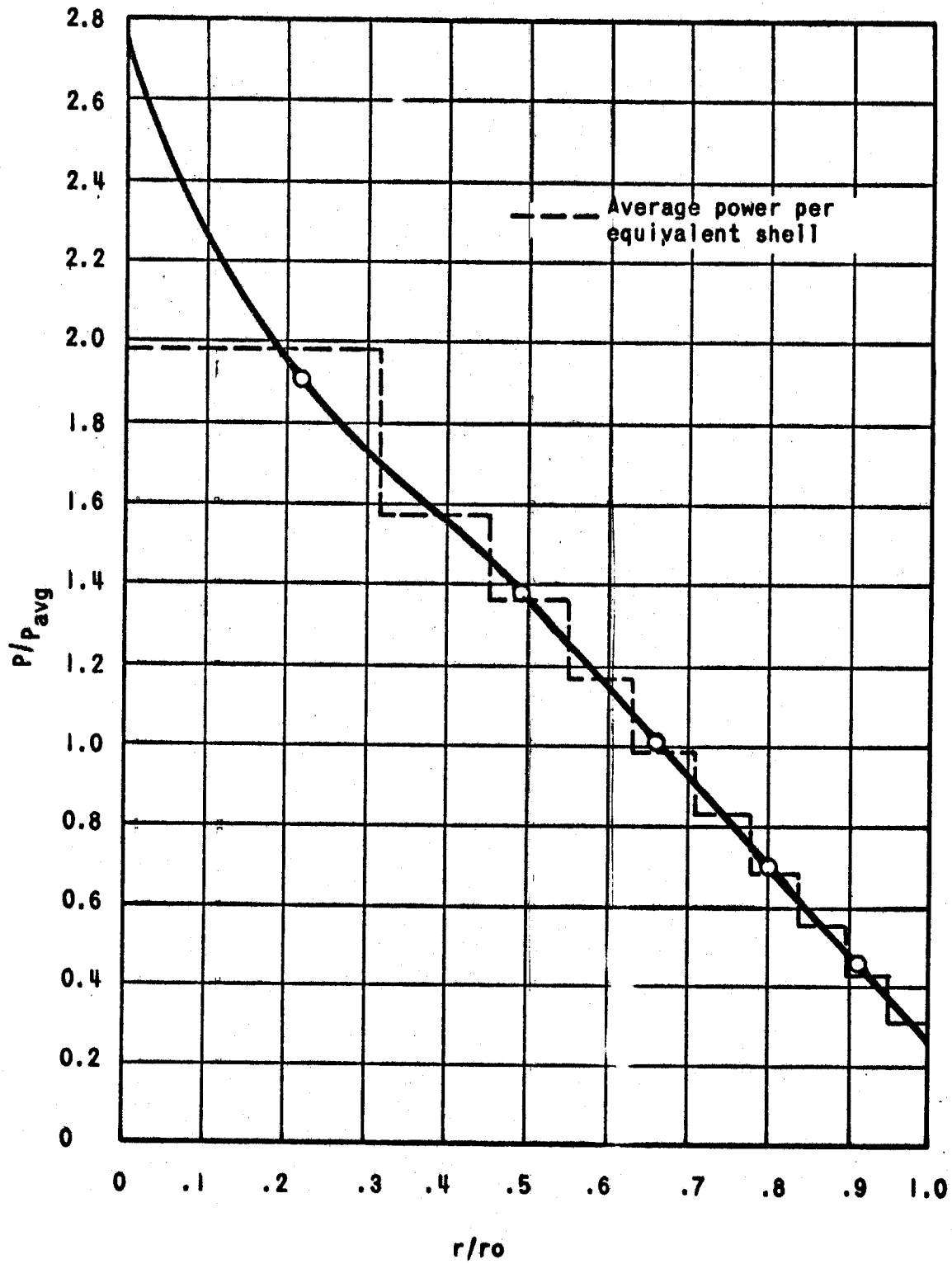
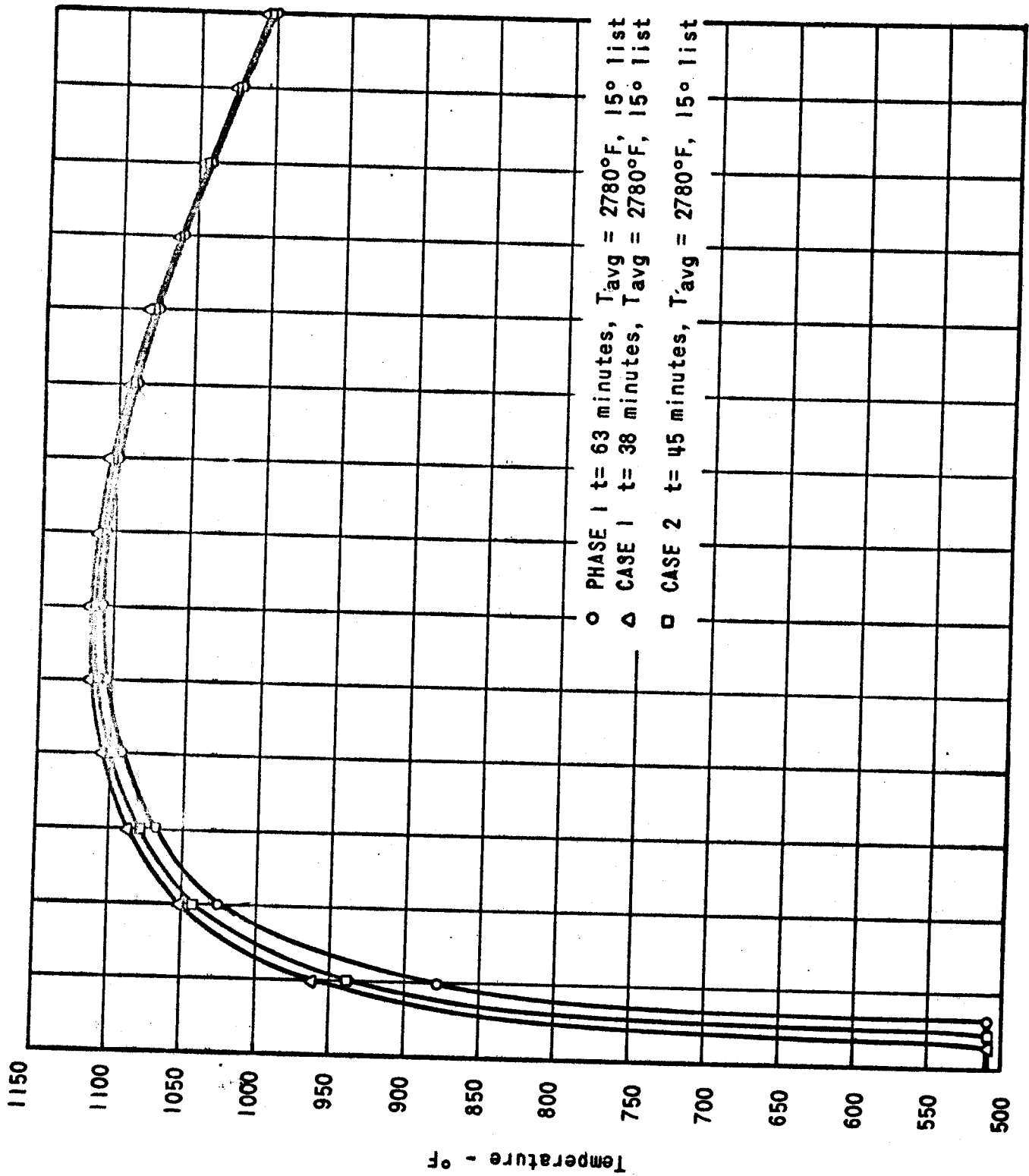


Fig. 13-48. Maximum Reactor Vessel Temperature vs Time (Shuffled Core)



Time After Accident - minutes

SHUFFLED CORE CASE 1

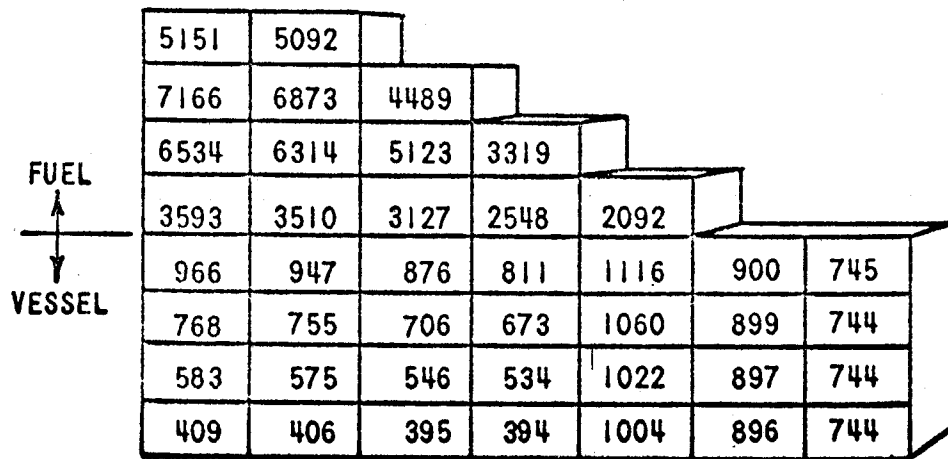


Fig. 13-49 Temperature Distribution In Reactor Vessel Wall  
At 600 Minutes - 15° List, 2780°F Fuel Temperature,  
38 Minutes Initial Contact Time (CASE 1)

SHUFFLED CORE CASE 2

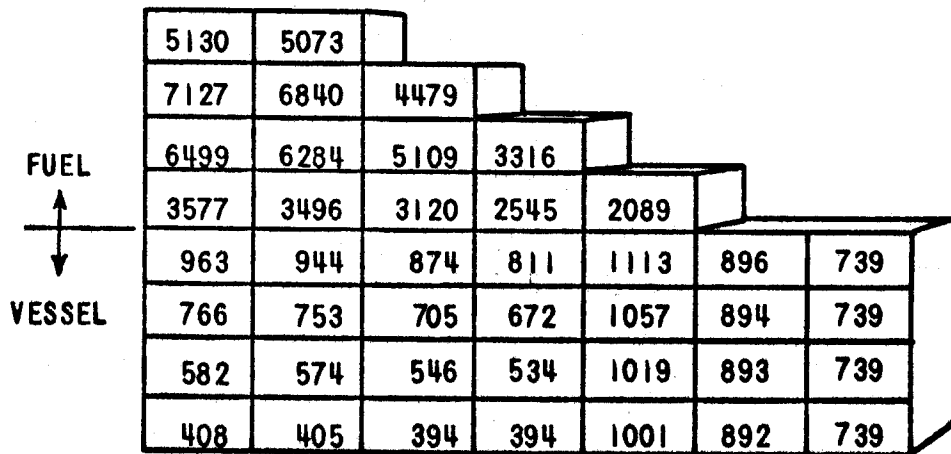


Fig. 13-50 Temperature Distribution in Reactor Vessel Wall  
 At 600 Minutes - 15° List, 2780°F Fuel Temperature,  
 45 Minutes Initial Contact Time (CASE. 2)

Fig. 13-51 Water Remaining In Flow Baffle  
vs Time (Shuffled Core)

